The heterogeneity of the RNA degradation exosome in Sulfolobus solfataricus

Dissertation for the degree for doctor of natural sciences
(Dr.rer.nat)

presented by

mphil.-biol. Chamindri Witharana

from Sri Lanka

Prepared at the Institute of Microbiology and Molecular Biology
Department of Biology and chemistry

Justus-Liebig-University Giessen

July 2013

First supervisor: Prof. Dr. Gabriele Klug

Second supervisor: Prof. Dr. Peter Friedhoff

I dedicate this thesis to
my mom
for her constant support and
unconditional love

Publications

Witharana, C., et al., *Heterogeneous complexes of the RNA exosome in Sulfolobus solfataricus.* 2012. Biochimie. **94** (7): p. 1578-87.

1. General introduction

RNA is necessary for protein synthesis and for gene regulation in all living organisms. Most RNA molecules are transcribed as precursors which are then maturated by ribonucleases (RNases) and RNA modification enzymes. Often large multi protein complexes are responsible for the maturation and for the degradation of various RNA molecules in the cell. The general mechanisms of RNA processing and degradation are highly conserved and include endonucleolytic cleavages, post transcriptional modification at the 3' end (RNA tailing) and exoribonucleolytic degradation or trimming in 3'-5' direction or in 5'-3' direction.

1.1. Archaea and extremophiles

Eukaryota, Bacteria and Archaea are the three domains of life [1]. Due to their 16S rRNA and other genetic, physiological, structural and biochemical properties, Archaea are fundamentally different from the Bacteria (Figure 1.1) [2]. There are two main phyla in Archaea; Euryrachaeota and Crenarchaeota. Another phylum was discovered which is known as the Nanoarchaea and a new phylum has been suggested as Korarchaeota [3]. Many Archaea live in extreme conditions such as very high temperatures (hyperthermophilic), highly concentrated salt solutions (halophilic) or strongly acidic (acidophilic) or alkaline environments (alkaliphilic) [4].

The structure of the cell wall and the plasma membrane of Archaea show significant differences to the other Domains. Most Archaea enclose a cell wall. Unlike Bacteria, Archaea lack peptidoglycan in their cell walls. Archaeal cell wall can consist of pseudo-murein (which is similar to murein), polysaccharides or glycoprotein, which gives them rigidity, strength and resistance against mechanical stresses and harsh environmental conditions. Archaeal cell membrane is significantly different from the membranes of the other domains. In Bacteria and Eukaryota, fatty acids are linked via an ester linkage to the glycerol molecules while in Archaea, simple fatty acids are replaced by branched isoprene units and those bind to the glycerol via diether bonds. Furthermore in some archaeal species lipid bi-layer is replaced by a monolayer [5]. These characteristics make the membranes more rigid.

Despite morphological similarities to Bacteria such as the cell size and lack of cell nucleus, Archaea possess genes and several metabolic pathways that are more closely-related to genes and pathways of eukaryotes, for example, the enzymes involved in transcription, translation and the processes such as replication, and repair mechanisms [6], [7], [8]. Archaea therefore can be taken as model organisms to study the complex eukaryotic systems.

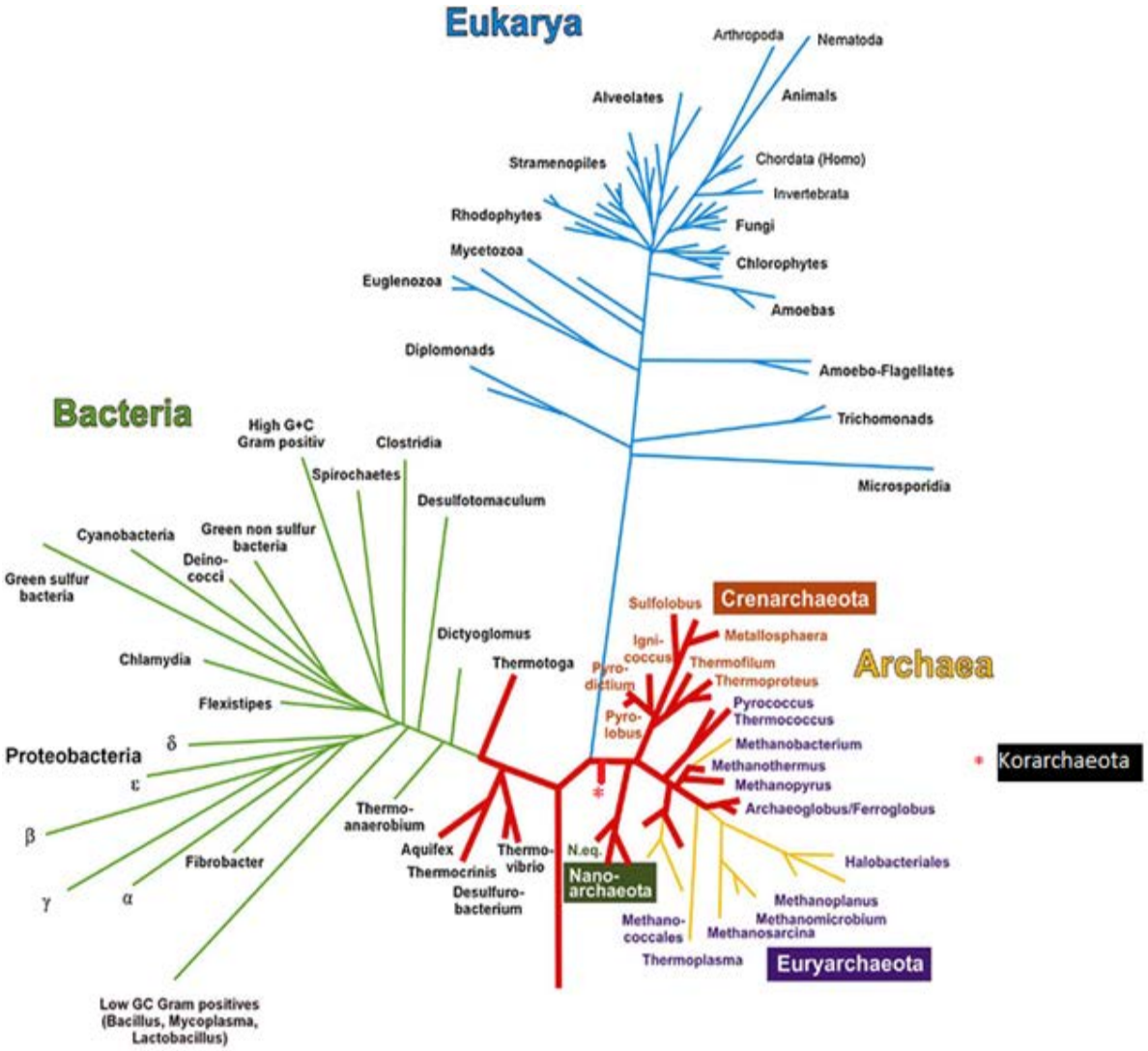

Figure 1.1 Phylogenetic tree of the three domains of life: Bacteria, Archaea and Eukarya. This was derived from comparative sequence analysis of 16S and 18S rRNA (adopted from [9]). Korarchaeota were not included in this analysis.

1.2. *Sulfolobus solfataricus*

Sulfolobus solfataricus is a hyperthermophilic archaeon which belongs to the phylum Crenarchaeota. *S. solfataricus* was first isolated from sulfur sources near Naples [10], [11]. In 2001 *S. solfataricus* genome was fully sequenced [12] and it is among the most commonly used and best-studied members of the Crenarchaeota due to its relatively straightforward growth requirements [13]. *Sulfolobus* optimum growth conditions are 75-80 °C and pH 3-4 [13]. The pH in the cells, however, lies within pH 7 neutral range [14]. Because of its growth conditions, thermo and acid-stable enzymes, *Sulfolobus* is getting more and more attention from biotechnology streams.

Sulfalobus has a versatile metabolic system. It can grow under aerobic or semi aerobic conditions. The main carbon source of *Sulfolobus* is CO_2 in nature [5], [15] but it may also grow using variety of carbon sources. In the lab conditions it relies on organic substances such as yeast extract and casamino acid. The dependency of the vast variety of energy sources makes it easy to grow under lab conditions.

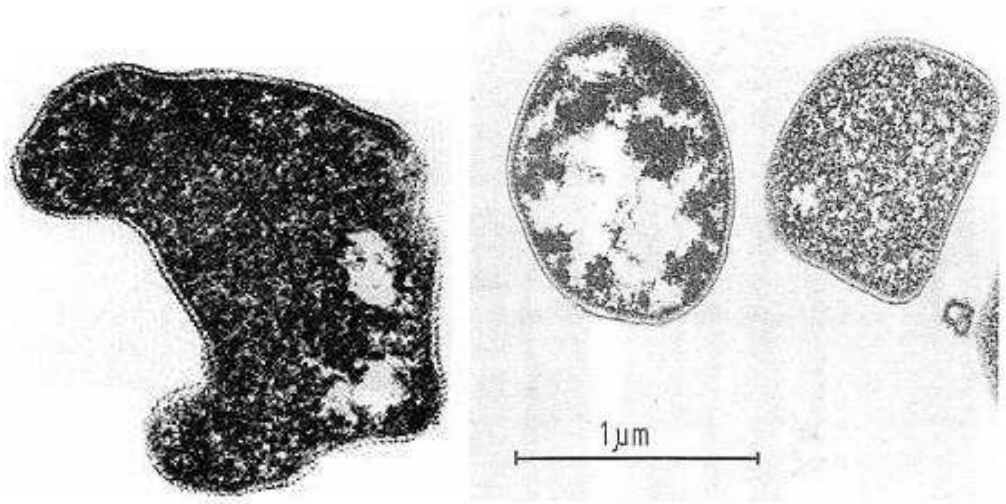

Figure 1.2 Electron micrographs of various *Sulfolobus* cells [11].

Sulfolobus cells are more or less spherical (Figure 1.2) [5], [11] which has a diameter of about 1 µm [16]. Like other hyperthermophilic Archaea, *Sulfolobus* also has a stable, bipolar single-layer cell membrane.

1.3. Processing and degradation of RNA in Bacteria

Particularly in prokaryotes, the RNA degradation plays an important role in gene regulation. For example, the degradation of the mRNAs affect RNA levels in the cell thus regulating gene expression [17]. RNA molecules can be divided into two classes: the structured, stable RNAs (rRNA, tRNA) and the short-lived mRNAs.

The stable rRNA and tRNA, which account for about 95% of total RNA, are hardly degraded during the exponential growth. Those are degraded only under certain stress conditions or when an RNA molecule is defective (i.e. quality control) [18]. The mRNA's fast degradation serves to continuously regulate the message population to the needs of the cell for precise proteins. Most bacterial mRNAs have rather short half-lives from a few seconds to a few minutes, so that the cell can respond quickly to changes in environmental conditions [18], [19], [20]. Small RNAs (sRNAs) are another distinctive group of RNA molecules. These are highly structured, typically characterized by their length (50-250) and play a key role in regulatory functions. They can bind to protein targets, and modify the function of the bound protein. Further they also can bind to mRNA targets and regulate gene expression [21], [22].

The RNA stability is determined by various factors such as the proteins to which the RNAs are bound and protected, the RNA secondary structures and/or the polyadenylation dependency of the RNAs [23]. Furthermore, the triphosphate at the 5' end of primary transcripts, RNA stem-loop structures at the 3' end or the 5' UTR (untranslated region) also contribute for the stability of the RNA.

However, attachment of poly (A) tail makes the bacterial RNA destabilized. The polyadenylation of mRNAs plays an important role not only in the degradation, but also in the quality control. At the 3' end of the RNA, the homogenous poly (A) tail is synthesized by poly (A) polymerase I (PAP I) in *Escherichia coli*. Additionally, heteropolymeric poly (A) rich tails are produced by the polynucleotide phosphorylase (PNPase). These RNA tails have a length of about 10-50 nucleotides. However, in *in vitro* PAP I could elongate RNA by approximately 500 adenyl residues [24]. The presence of such poly (A) - or (A)-rich attachments on the 3' end of bacterial mRNAs promotes their degradation due to the high affinity of the tails to the RNases, involved in the degradation [25], [26].

Previously it was considered that the degradation of mRNAs and stable RNAs is a very different process from the maturation of RNAs. It was assumed that there were certain enzymes that were responsible for the degradation of different classes of RNA. However it became clear that the specificity of the RNases is rather determined by the accessibility of the substrate. Thus, many RNases are involved in both the RNA degradation as well as the processing [18].

1.3.1. Bacterial endo- and exoribonucleases

The degradation of the mRNA basically begins with the cleavage by endoribonucleases. Endoribonucleases cleave phosphodiester bonds within the RNA at specific cleavage sites. They contribute both to the processing and to degradation of RNA molecules. The resulting products are then further degraded to mononucleotides by exoribonucleases. Secondary structure of the mRNA can slow the degradation by 3'-5' exoribonucleases. The best-studied model organism for RNA degradation in Bacteria is *E. coli* (Figure 1.3).

In many cases, the degradation of RNA is initiated by the removal of the stabilizing 5' triphosphate pyrophosphatase by RppH [27]. Then endoribonucleases come in to play. In *E. coli* the main endoribonucleases are RNase E, RNase G and RNase III. The key enzyme for the initiation of mRNA degradation is endoribonuclease E (RNase E). The RNase E interacts with the monophosphorylated 5' end of the RNA molecule before the endonucleolytic cleaving [28], [29]. RNase E recognizes specific cleavage sites, usually in single-stranded A/U-rich regions, and makes endonucleolytic cuts [30], [31]. RNase E is also an important component of a RNA degrading multi-enzyme complex, the degradosome (Chapter 1.3.2). RNase E also can interact with the RNA chaperone, Hfq, and multiple small RNAs to form ribonucleoproteins [32].

Another endoribonuclease which exist in *E. coli* is RNase G. It has a high sequence identity with the N terminus of RNase E. Both these endoribonucleases have similar sequence specificities and it has been shown that RNase E mutant cells were not viable, but can be complemented by overproduction of RNase G. However, RNase G complemented cells accumulate RNAs such as the precursors of 5S ribosomal RNA (rRNA) indicating that normal processing of these RNase E-cleaved RNAs were not completely restored by RNase

G. Furthermore RNase G cannot take over the task of RNase E in degradosome, because it lacks the crucial C terminal part of RNase E [33].

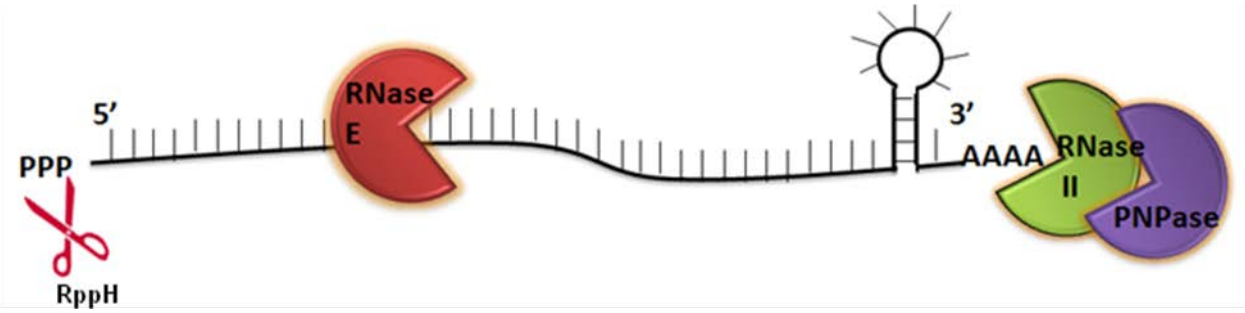

Figure 1.3 The mRNA degradation in prokaryotes (eg, *E. coli*). Bacterial mRNAs begin with a 5'-triphosphate and end with a stem-loop structure. RNA decay is initiated by removing the stabilizing 5' triphosphate pyrophosphatase by RppH. The preferred substrate for RNase E is RNA with a 5'-monophosphate. In the presence of the poly (A) tails, the attack at the 3' end by PNPase and RNase II is facilitated. However the 3′-stem-loop structures block the processive activities of these two RNases. Other RNases are also involved but these are omitted for simplicity.

RNase III degrades specifically double-stranded RNA regions and participates in the processing of 30S rRNA precursors to 16S rRNA and 23S rRNA [34]. In some Bacteria further RNase III dependent processing of the 23S rRNA occurs [35]. Conversely, deletion of the RNase III structural gene (*rnc*) does not lead to any considerable alteration in the decay of total pulse-labelled RNA or specific transcripts [34], [36]. Perhaps it is not a major player in mRNA degradation.

The RNA fragments resulting from the cleavage of endoribonucleases are usually unstable and are degraded further by endo or exoribonucleases. The 3'-5' exoribonucleases, polynucleotide phosphorylase (PNPase), RNase R, RNase II and the Oligoribonuclease in *E. coli* play a decisive role in degradation of these resulting RNA fragments.

The PNPase catalyzes the reversible phosphorolysis of polyribonucleotides with the liberation of nucleoside diphosphates. PNPase is composed of three identical subunits with a

molecular mass of 77.1 kDa and each has two RNase PH-like domains (RPD1 and RPD2) [37]. Crystallographic analysis of PNPase from *Streptomyces antibioticus* have shown that these three subunits form a hexameric ring, which contains catalytic sites in the central channel [38]. This trimeric ring structure of the PNPase has structural similarities to the eukaryotic and archaeal exosome (Chapter 1.4.1 and 1.5.1).

The RPD1 and RPD2 domains are linked by α helical domain. At the C terminus of each subunit there are two RNA binding domains, which are positioned on the hexameric ring: S1 (S1 protein homology) and KH (K homology protein). Deletion of the S1 and KH domain leads to the loss of activity and the loss of ability to bind RNA substrates [39].

The hydrolytic 3'-5' exoribonucleases RNase R and RNase II, have both catalytic and structural similarities [40]. However, RNase R is the only exoribonuclease that is capable of degrading highly structured RNA. This implies that RNase R is playing a significant role in the degradation of highly structured mRNA [41] and in the quality control of rRNA and tRNA [42] *in vivo*. Furthermore it also has a helicase activity [40], [43]. It is also known that the quantity of *E. coli* RNase R increases under various conditions, such as under cold shock and upon the occurrence of the bacterial culture in the stationary phase [41], [44]. Thus, the enzyme has an important regulatory role in different stress conditions. RNase II is an exoribonuclease which degrades single-stranded RNA in a processive manner. It preferentially degrades poly (A) attachments [45].

The double mutant *E. coli* K-12 strains (lacking PNPase and RNase R) having been not viable suggests that these enzymes carry out an essential function in RNA metabolism that cannot be taken over by any of the other cellular exoribonucleases, even the closely related RNase II [46]. Both PNPase and RNase R remove defective rRNA molecules as soon as they are generated [42]. PNPase is also involved in the degradation of damaged tRNAs. However, degradation is largely reliant on polyadenylation of the precursor by poly (A) polymerase [47] and PNPase [48].

All three mentioned exoribonucleases cannot degrade RNA molecules to a mononucleotide. The final degradation products have a length of about 2-5 nucleotides. The Oligoribonuclease catalyzes the final step in the degradation of these 2-5 nucleotide substrates to mononucleotides. Free 3' OH ends are required for the activity of this enzyme [49], [50].

Though the gram-negative model organism *E. coli* was used for the analysis of bacterial 3’-5’ exoribonuclease activity, 5’-3’ exoribonuclease activity was first found in gram positive bacterium *Bacillus subtilis.* In contrast to *E. coli*, *B. subtilis* lacks the essential RNase E and RNase II homologs and Oligoribonuclease. Instead, it harbors two paralogs of a novel RNase (RNase J1 and RNase J2) with both endo and 5’-3’ exo ribonucleolytic activity. Although these enzymes have no sequence homology to RNase E, they have similar substrate requirements [51], [52]. More homologues of the RNase J were found in other Bacteria and Archaea including the organisms that also possess an RNase E ortholog. For example, RNase J is in *Sinorhizobium meliloti* involved in the maturation of the 5' ends of the 16S and 23S rRNA [53]. Furthermore, RNase Y plays a major role in endolytic cleavages of RNA in the RNase E lacking, gram positive, *B. subtilis*. This endoribonuclease has functional similarities to *E. coli* RNase E although it is completely lacking the sequence homology to RNase E [33].

1.3.2 Bacterial mRNA degradation by multi protein complexes

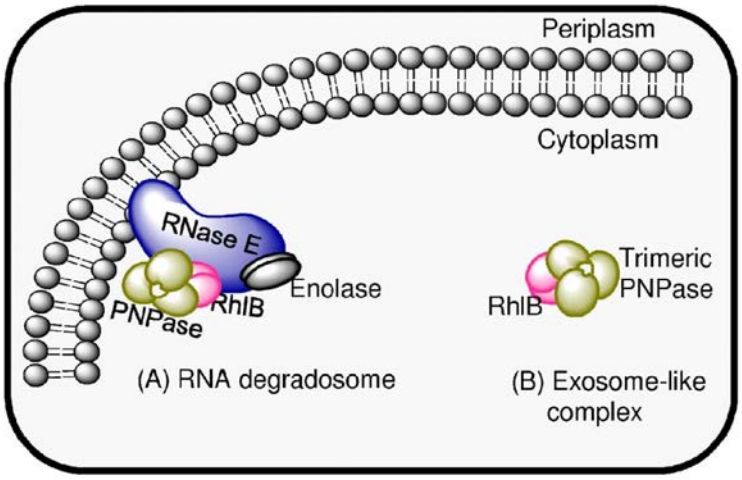

Figure 1.4 Bacterial mRNA decay machineries. (A) The degradosome: It is a multi-protein complex which includes an endoribonuclease (RNase E), a 3'-5' exoribonuclease (polynucleotide phosphorylase (PNPase), the glycolytic enzyme enolase and a DEAD-box RNA helicase (RhlB helicase). (B) The bacterial exosome: It is composed of PNPase and RhlB. It is independent of the RNA degradosome. RhlB is used as cofactor to unwind structured RNA in an ATP-dependent manner. This complex was shown to catalyze the 3'-5' exonucleolytic degradation of RNA. Taken from [54] .

The degradosome in *E. coli* is a multi-enzyme complex which is involved in the degradation of mRNA (Figure 1.4A). The central unit in the complex is the endoribonuclease RNase E. the N terminus contains the active site of the enzyme while the C terminus is critical for the formation of the complex [55], [56]. The object of the helicase RhlB is to unwind the stable secondary structures. Then the RNA can pass into the active site in the central channel of the PNPase [57].

It has been demonstrated that RhlB and PNPase can also form a complex independent of the degradosome *in vitro* and *in vivo* [58] (Figure 1.4B). Bacterial cells, in which the helicase RhlB was inactivated, show strong deficits in the mRNA degradation.

The glycolytic enzyme enolase is very abundant in *E. coli* and only a small amount is bound to the RNase E in the degradosome [58], [59]. The function of the enolase in relation to the

mRNA degradation is not fully revealed. It is only known that the enolase plays a role in regulating the stability of specific mRNA in the response to phosphosugar stress [32].

The degradosome was of great interest in the recent research. Lot is known about the protein-protein interactions of its subunits and its role in RNA degradation. However, the detailed structure and organization of the protein complex was recently discovered. *In vitro* experiments with phospholipids have shown that it binds to the membrane by RNase E [60]. The association with the cytoplasmic membrane occurs with the aid of an amphipathic helix, which is referred to as the A segment. Changes of the localization pattern of RNase E have been observed as a result of the deletion of segment A or replacements of hydrophobic residues of the amphipathic helix. It has appeared to clump in the peripheral region of the cytoplasm or it has completely loss the localization [61]. Since, the degradosome subunits bind to the C terminus of the RNase E, the whole degradosome is localized at the cytoplasmic membrane. The role of the membrane localization of the degradosome on the RNA degradation is still unknown. Studies on *B. subtilis* using fluorescent tagged RNA polymerase and ribosomes have shown that RNA polymerase is associated principally with the nucleoid and the ribosomes which are localized almost exclusively to the cytoplasmic space outside of the nucleoid [62]. RNase Y, which is functionally similar to RNase E, localizes at the membrane, and in *in vitro* experiments it can form a ’degradosome’ with PNPase and other glycolytic enzymes. These results have been interpreted as witness for a compartmentalization of transcription and translation despite the lack of a nuclear membrane in Bacteria. The localization of RNase E and other enzymes to the inner cytoplasmic membrane suggests that RNA processing and degradation is also compartmentalized and group of transcripts, which remains to be identified, is processed or degraded on the inner cytoplasmic membrane.

1.4. The RNA processing and degradation in Eukarya

In Eukaryotes the RNA processing is much more complex than in Bacteria and in the following, only selected aspects of RNA processing of Eukaryotes are addressed.

The mature monocistronic mRNAs of Eukaryotes contains a 7 methyl guanosine cap at the 5’ end and a long poly (A) Attachment (200- 500 nt) at its 3' end (Figure 1.5). The 5' cap is involved in the initiation of translation and the operation of splicing of the pre mRNA, to

form the mature, functional mRNA [63], [64]. In Eukaryotes, transcription and translation takes place in the nucleus and in the cytoplasm respectively. Thus, the mature mRNA has to be transported from the nucleus to the cytoplasm. It was demonstrated that the 5' cap of the RNA confers a higher stability [65]. The polyadenylation of the RNA takes place by different enzymes, both in the nucleus and in the cytoplasm.

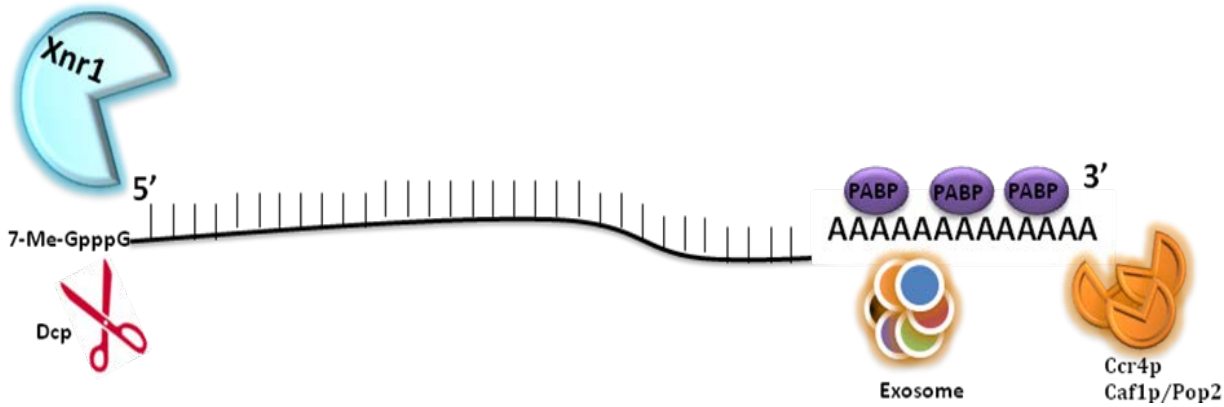

Figure 1.5 The mRNA degradation in Eukaryotes. Eukaryotic mRNAs begin with a 7-Me-GpppG cap structure on the 5' end and end with a 150–200-residue poly (A) tail. Degradation generally begins with shortening of the poly (A) tail to <30 residues by one or more deadenylases. Dcp2 is involved in cleaving the 7-Me-GpppG cap which generates a 5'-monophosphate end and subsequently degraded in 5'-3' direction by Xrn1 and in 3'-5' direction by the exosome.

The TRAMP complex (Trf4/Air2/Mtr4p Polyadenylation complex) is a multi-protein complex consisting of the RNA helicase *Mtr4*, a poly(A) polymerase (PAP) (either *Trf4* or *Trf5*) and a zinc finger protein (either *Air1* or *Air2*). It assist the nuclear exosomes by the synthesis of short poly (A) tails at the 3' end of RNA, which causes destabilization [66], [67]. However in the cytoplasm, poly (A) polymerase I (PAP I), forms much longer poly (A) tail to stabilize the RNA molecules. In comparison to the half life of the mRNA of Bacteria, eukaryotic mRNA has a longer half life which range from several minutes to hours which basically depends on the deadenylation [68], [69].

The poly (A) tail plays an important role in the degradation of the 3' end of the mRNA. The long poly (A) tails are protected by the poly (A)-binding protein (PABP), thereby preventing the degradation of the mRNA. The key steps in the degradation of mRNAs are the removal of PABP and the poly (A) tail by a complex which contains the proteins, Ccr4p Caf1p/Pop2.

This process occurs in the cytoplasm [70]. Thus, PABP is removed and the cap structure at the 5' end of the mRNA can be attacked.

In the cytoplasm, there are two pathways of mRNA degradation. In both cases, the degradation begins with the removal of the 3' poly (A) nucleotides, which is referred to as deadenylation [71], or by removing the 5’ cap by an enzyme called de-capping protein (Dcp2). The RNA degradation can either be by the exoribonuclease Xrn1 in 5'- 3' direction, or by a 3'-5' multi-protein complex called the exosome [65], [72], [73], [74], [75].

1.4.1 The eukaryotic exosome

The eukaryotic exosome is a multi-protein complex with a 3'-5' exoribonucleotic activity. It is present in the nucleus as well as in the cytoplasm. It has interactions with many other proteins. The complex was first reported in *Saccharomyces cerevisiae* [72]. The core of the exosome consists of six subunits that form a hexameric ring: Rrp41 (ribosomal RNA processing factor 41), Rrp42, Rrp43, Rrp45, Rrp46 and MTR3 (Figure 1.6). These proteins have a homology to the *E. coli* RNase PH. All subunits of the hexamer are essential, because the absence of the proteins would not lead to a functional structure [76], [77]. On the hexameric ring there is a trimetric cap which contains the proteins Rrp40, Rrp4 and Csl4 (CEP1 synthetic lethality 4). Rrp40 and Rrp4 have S1 and KH RNA binding domains and the RNA binding protein Csl4 has KH and Zn ribbon domains. This nine subunit exosome has no RNase activity. The exosome activity is due to the tenth subunit Rrp44 (DIS3), which is a hydrolytic exoribonuclease and a homology to RNase R and RNase II from *E. coli* [72], [78].

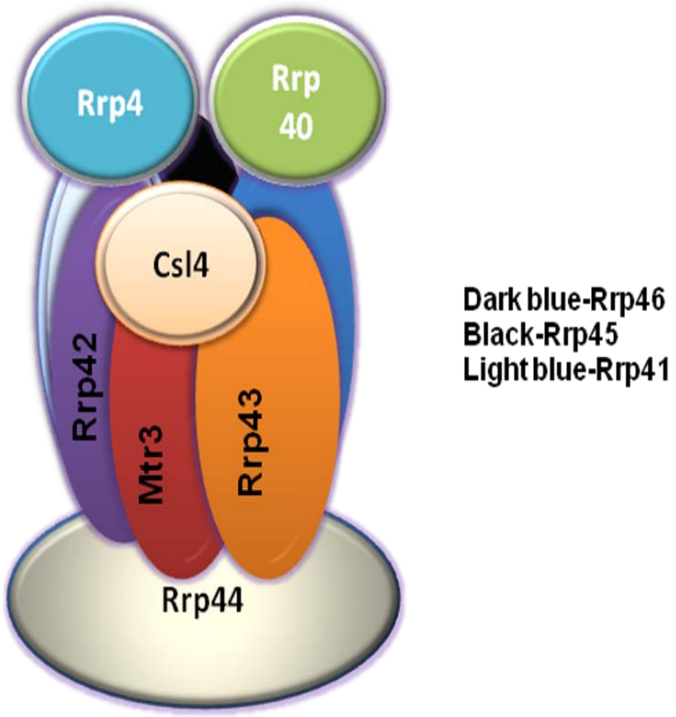

Figure 1.6 Schematic representation of the eukaryotic exosome architecture The active subunit Rrp44 is positioned below the inactive nine subunit exosome.

A characteristic of the exosome complex is that it requires additional proteins to facilitate its exonucleolytic activity in either RNA processing, turnover or RNA surveillance pathways. The cytoplasmic exosome is involved in mRNA turnover [79]. Exosome function in mRNA turnover and cytoplasmic mRNA surveillance pathways requires the associated putative GTPase (Ski7p) and the Ski complex, comprising the putative RNA helicase (Ski2p), Ski3p and Ski8p [80].

The exosome was initially identified as involved in the maturation of 5.8S rRNA [72]. In the nucleus the exosomes is involved in the early biogenesis of stable RNAs, such as ribosomal RNA, eukaryotic-specific small nuclear (snRNAs), small nucleolar RNAs (snoRNAs) and degrades unstable transcripts that originate from intergenic regions of eukaryotic genomes [81], [82].

1.5. RNA processing and degradation in Archaea

RNA processing and degradation in Bacteria and Eukarya are well researched. Nevertheless very little is known about these processes in the Archaea. Archaea show morphological similarities to Bacteria, but are phylogenetically closer to Eukarya than to Bacteria [83]. They show strong similarities to Eukarya at the molecular level, for example in the mechanisms of replication, transcription and translation. Archaeal mRNA, however, is more similar to bacterial mRNA: it is generally intron-less and lacks long stabilizing poly (A)-tail at the 3'end as well as a methylguanosine cap at the 5'end. The 5'- triphosphate stabilizes the structure [84] like in Bacteria. Interestingly the trimeric translation initiation factor (a/eIF2) binds to the 5' end of the mRNA and protects it against the degradation similarly to the 7-me-guanosine cap of the eukaryotes.

In *Sulfolobus* approximately 8% of the mRNAs have a longer half-life than 20 minutes, but 50% of the mRNAs are degraded after 4-8 minutes [85]. This is comparable to bacterial mRNAs half-lives and it also suggests the regulation of mRNA stability as a possible fast respond to changing environmental conditions.

The genome sequencing of some Archaea provided the opportunity to identify homologs to known RNases of Bacteria and Eukaryotes by comparative sequence analysis of proteins. Archaea-specific RNases, however, cannot be detected with this method. Below some archaeal homologs to bacterial and eukaryotic RNaseses with experimentally confirmed ribonucleotic activity are shortly described.

In halophilic and some methanogenic Archaea, which have no exosomes, no post-transcriptionally synthesized 3' tails were found [86]. In these exosome-less Archaea, RNA is either exoribonucleolytically degraded in 3'-5' direction by a homologue of bacterial RNase R (in halophiles) or seems to be degraded in 5'-3' direction by a homologue of the bacterial RNase J (in some methanogenic Archaea) [87]. *B. subtilis* RNase J can act as an exo and endonucleolytic enzyme at the same time. Unlike Bacteria, in Archaea, RNase J shows exo- and endonucleolytic activities separately [51], [87]. In Archaea which endure exosomes (hyperthermophiles and some methanogens), RNAs contain heteropolymeric (A)-rich tails at the 3' end, which may exert a destabilizing function [86], [88]. Furthermore this archaeal group has the bacterial RNase J homolog which has a 5'-3' exoribonucleotic activity or an

endoribonucleotic activity [87]. In RNA processing and degradation not only individual RNases, but also high molecular weight multi enzyme complexes (eg. Archaeal exosome) are also involved. Archeal exosome is highly conserved. Ribonuclease complexes which are structurally similar to archeal exosome can be found in Eukaryota (Eukaryotic exosome) and in bacteria (PNPase). The mechanisms of RNA degradation in Archaea show strong similarities to PNPase in Bacteria [89], [90]. In the following chapters the composition, structure and function of the archaeal exosome are described.

1.5.1 Composition of the archaeal exosome

The existence of an RNA-degrading multi-protein complex in Archaea, which is very similar to the eukaryotic exosome, was predicted by bioinformatic studies. For example, the prediction of the *S. solfataricus*'s exosomal subunits from orthologs of eukaryotic essential exosome subunits, Rrp41, Rrp42 and Rrp4 in a single operon and a fourth ortholog, Csl4 encoded in a different operon [91]. The first experimental evidence of the existence of an archaeal exosome was provided by co-immunoprecipitation using cell free extract of *S. solfataricus* [92]. In the following years, similar protein complexes from *Archaeoglobus fulgidus* [93] and *Pyrococcus* [94] were reconstituted and analyzed.

In addition to the predicted subunits Rrp41, Rrp42, Rrp4 and Csl4 there are other proteins which were co-precipitated with the exosome of the *S. solfataricus* such as the archaeal DnaG like protein, (a homolog of the bacterial primase), the chaperonin Cpn, the homolog of the eukaryotic protein Cdc48 (cell division cycle 48) and a 16 kDa hypothetical protein [92], [95]. The proteins Cpn and Cdc48 [96] possess chaperone properties. Cpn is also an RNA binding protein and is involved in the processing of the 16S rRNA [97]. It is unclear whether Cpn and Cdc48 were co-purified with the exosome due to a functional relationship or non-specifically. The function of the 16 kDa polypeptide is also unclear. The object of the bacterial DnaG primase is to produce an oligonucleotide RNA during DNA synthesis. The function of the archaeal DnaG in relation to RNA degradation was recently found in *in vitro* experiments. It enhances the interaction with adenine rich RNAs [98]. DnaG is not only found in *S. solfataricus* exosome but also in the exosome of other archaeal species such as, *Methanothermobacter thermoautotrophicus* and *Thermococcus kodakarensis*, which belong to different phylogenetic lines. The annotation of the archaeal DnaG protein as a bacterial type primase is based on its highly conserved central TOPRIM domain, which is

characteristic for topoisomerases and primases. Nevertheless recently it was published that DnaG of *S. solfataricus* exhibits primase activity *in vitro*. *S. solfataricus* also has a eukaryotic-type primase. This implies that this organism uses a dual system of primases [99] and that DnaG has a dual function: it is involved in the RNA metabolism and in the replication of DNA.

1.5.2. Structure and function of the archaeal exosome

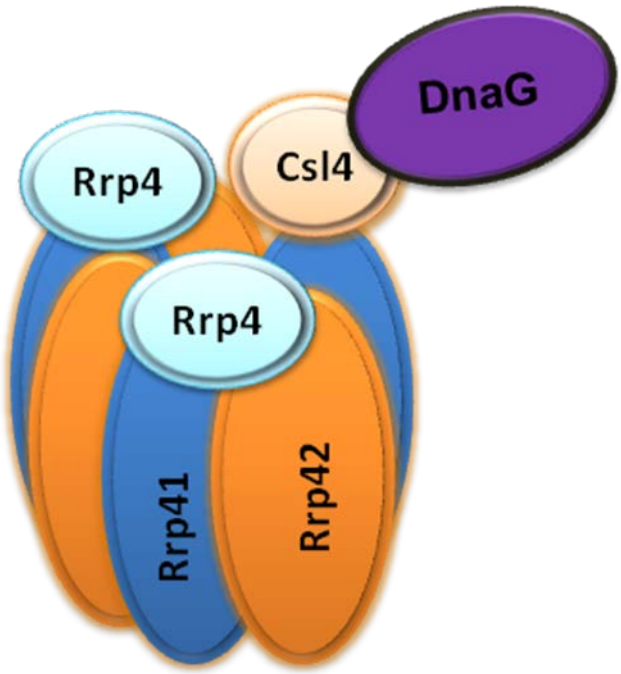

Figure 1.7 Schematic representation of the structure of the archaeal DnaG-Rrp4-Csl4-exosome. Rrp41, Rrp42, Rrp4 and Csl4 form the nine-subunit exosome, while the Archaea specific exosome protein, DnaG (tenth subunit) interacts with the Csl4 protein.

The structure and the catalytic mechanism of the reconstituted archaeal nine-subunit exosome are well understood. The Archeal exosome is a 3'-5' multi-subunit exoribonuclease complex which is involved in RNA degradation and polyadenylation [100]. It is built of a phosphorolytically active hexameric ring, containing the subunits Rrp41 and Rrp42, to which a trimeric cap of the RNA-binding proteins Rrp4 or Csl4 is bound (Figure 1.7) [93], [101], [102]. However, in addition to the two isoforms of the exosome, Rrp4 trimer bound to the

hexameric ring (Rrp4-exosome) and the Csl4 trimer bound to the hexameric ring (Csl4-exosome), exosomes with heteromeric caps can be reconstituted (Rrp4-Csl4-exosome) [93].

The archaeal exosome performs metal-dependent phosphorolysis of RNA in the presence of inorganic phosphate (Pi) and Mg^{2+}, and synthesizes RNA using NDPs without a template [86], [101], [103]. The archaeal exosome is the only enzyme which is capable of polyadenylating RNA in Archaea. It was shown by depleting the exosome from *S. solfataricus* cell-free extract which results in strong reduction of RNA polyadenylation activity [86].

The active site of the complex resides in the subunit Rrp41 while Rrp42 is inactive. The formation of the hexameric ring is essential for the phosphorolytic activity and binding of the substrate. Thus, separate Rrp41 polypeptides have no activity [101], [103].

The trimeric cap structure on the hexameric ring is formed by the RNA binding proteins Rrp4 and/or Csl4. Rrp4 has a S1 and a KH domain and Csl4 has a S1 and a Zn ribbon domain. Both proteins anchor with their N terminal domain to Rrp41. The respective S1 domains are located in the center of the proteins and form a pore (S1 pore). The S1 pore is positively charged and negatively charged RNA substrates tread through this pore to the central chamber. The positions of the KH and Zn ribbon domain differ significantly [93].

The RNA substrate enters to the central channel of the hexameric ring via the opening of the central pore. The restriction (8-10 Å) near the central channel pore only allows the entry of unstructured, single-stranded RNA [103], [104]. At the end of the duct, a chamber is formed, which represents the active site. While the surface of the hexamer is predominantly negatively charged, the central channel pore contains positive charges. The RNA must be at least ten nucleotides long for the threading into the channel [93].

The function of the RNA-binding cap was investigated *in vitro* using recombinant exosomes of Archaea belonging to the genera *Sulfolobus*, *Pyrococcus* and *Archaeoglobus*. So far homomeric caps composed of Rrp4 or Csl4 were studied in detail. Generally, the presence of Rrp4 or Csl4 increase the RNA binding and the efficiency of RNA degradation by the

archaeal exosome [93], [94], [105], [106]. It is predicted that many of the substrates of the exosome in *S. solfataricus* are adenine-rich mRNAs and adenine-rich, post-transcriptionally synthesized RNA-tails [86], [107]. Furthermore, the GC content of the *S. solfataricus* genome is 37% and short poly (A) stretches are present in its mRNAs [12], [107]. It has been shown that Rrp4 and Csl4 confer different substrate specificities to the archaeal exosome and that Rrp4 strongly prefers poly (A) [88].

1.5.3. Soluble and insoluble exosomes

Unlike in Eukarya, bacterial and archaeal cells lack organelles. In the compartmentalized eukaryotic cells, there are stress granules and processing bodies in the cytoplasm, in which RNA is translationally arrested and/or degraded. These processing bodies are involved in si- and mi-RNA mediated gene silencing and in mRNA degradation in 5'-3' direction [108] The eukaryotic exosome, which degrades RNA in 3'-5' direction, was found in the nucleus and in the cytoplasm, but not as a part of the processing bodies [109]. However, the archaeal exosomes are localized because of the need of prokaryotic cells to spatially organize RNA processing and degradation.

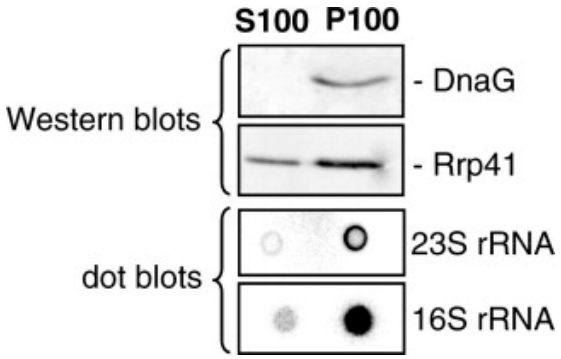

Figure 1.8 The exosomal subunits are found in the insoluble fraction. A) Western blot analysis of S100 and P100 fractions hybridized with anti-Rrp41 and anti-DnaG antibodies. B) The dot blot analysis of RNA isolated from S100 and P100 fractions with probes complementary to 16S rRNA and 23S rRNA. Taken from [110].

In a previous study most of the *S. solfataricus* exosomes were detected in the pellet fraction after 100 000 g centrifugation (P100; **insoluble exosome**) comparatively less amount of the exosomes was detected in the supernatant fraction (S100; **soluble exosome**) [110]. DnaG was exclusively detected in the P100 fraction. The dot blot analyzes showed that the 16S and 23S

rRNA were also in the P100 fraction (Figure 1.8). Detection of the 16S/23S rRNA and the exosome majorly in the P100 fraction rose the question whether RNA interfere in the exosome sedimentation pattern. The sedimentation of the RNA and the exosome was further analyzed by sucrose density gradients.

A)

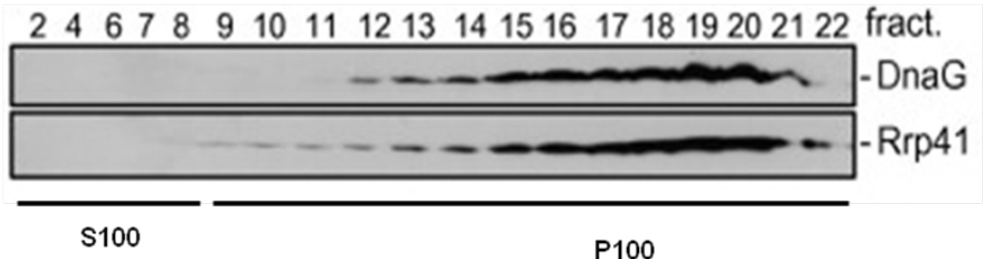

B)

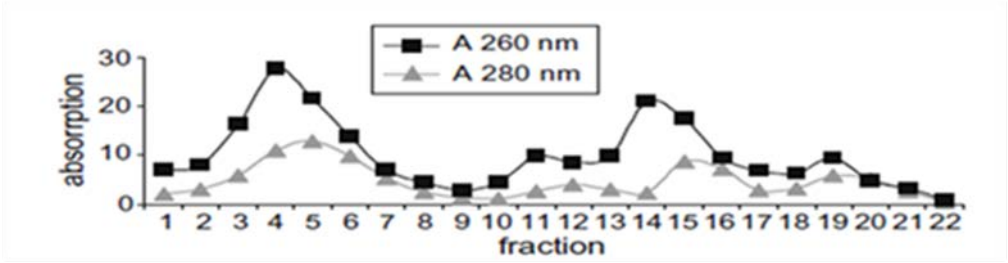

Fraction 11,12- 16S RNA, 30 S subunit
Fraction 14,15 -23S RNA, 50 S subunit

C)

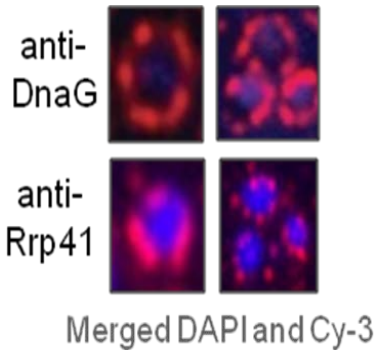

Figure 1.9 The exosome of the *S. solfataricus* is localized at the periphery of the cell and does not co-sediments with the ribosomes. A) Fractionation through a salt-containing 15–70% sucrose density gradient.

Fractionized samples were separated through SDS-PAGE, blotted and hybridized with the DnaG and Rrp41 antibodies. B) Sedimentation pattern of the ribosomal subunits in the sucrose density gradient. C) The cellular localization of *S.solfataricus* exosome by immunolabeling. The immunolabeled antibodies against DnaG and Rrp41 show that the exosomes at the periphery of the cell. Adopted from [110].

It was shown by our research group that in the 15%- 70% sucrose density gradient with salt, the yellow ring (where the membranes sediment) and the highest amount of exosomal subunits Rrp41 and DnaG were in the same fractions [110]. It was also shown that hydrophobic interactions are responsible for the co-sedimentation of the exosome with membranes, since this co-sedimentation was observed at high ionic strength only. This suggests that exosome is membrane- associated or interacts with a still unknown membrane protein via hydrophobic surfaces, but is not strongly bound to the membrane. The distribution of the exosome in the gradient was clearly different from that of the ribosomal subunits which says that there is no interference of the rRNA in the exosomal sedimentation pattern (Figure 1.9A and B). The localization of the archaeal exosome at the membrane was confirmed by immunolabelling (figure 1.9C). Rrp41 and DnaG proteins exhibited a distinct ring-shaped distribution, located almost exclusively at the membrane periphery of the cells. The mechanisms responsible for the specific subcellular localization of the archaeal exosome remain to be elucidated.

1.6. Aim of this work

The archaeal exosome is a protein complex involved in the degradation and polyadenylation of RNA. The proteins Rrp41, Rrp42, Rrp4, Csl4 and DnaG are major subunits of the exosome in *S. solfataricus. In vitro*, catalytically active hexamer can be formed with Rrp41 and Rrp42 subunits, to which an RNA binding cap of Rrp4 and/or Csl4 is attached. Rrp4 confers strong poly (A) specificity to the exosome. The contribution of the individual Rrp4 domains to its poly (A) preference was not shown so far. Therefore an important goal of the project was to analyze the domains of the Rrp4 protein in relation to poly (A) preference.

Although it was shown that *in vitro* the reconstituted exosome of *A. fulgidus* can carry a heteromeric cap containing Rrp4 and Csl4 [93] the cap composition of the archaeal exosome was not studied *in vivo* so far. Changes in the composition of the exosome may influence not only its substrate specificity, but also the interaction with other proteins and even its sub-cellular localization. To date it was not known whether Rrp4-Csl4-exosomes are present *in vivo*. Another important goal of the project was to examined where there are exosomes with heteromeric RNA binding caps *in vivo*.

The majority of the active site containing subunit Rrp41 is localized at the periphery of the *S. solfataricus* cell and is detectable in the insoluble fraction of a cell-free extract. DnaG was also detected at the cell periphery and is essentially insoluble [110]. It was not clear whether the composition of the exosome differs in the soluble and insoluble fractions. The localization of the archaeal exosome at the cell periphery and its co-sedimentation with membranes suggests that the membrane is involved in the spatial organization of RNA processing in the third domain of life. However, we do not know whether the localization of the exosome changes in different conditions, such as under different stresses. Therefore another aim of this project was to analyze whether there are differences in the composition of the soluble and the insoluble exosomes and to investigate the changes of the localization of the exosome under different stress conditions. We also wanted to know whether the localization of the exosome changes at different stages of the growth curve, in the exponential and in the stationary phase. In addition we wanted to see whether there are any potential interaction partners of the archaeal exosome under different stress conditions or at different stages of the growth curve

which can be co-purified with the exosome. The detection of the exosome will contribute to the understanding of the role and mechanisms of this protein complex in the archaeal cell.

So far there is no direct information regarding the 3-D structure of the native archaeal exosome and the exosome contain DnaG, which is essential for understanding its functional organization. Recently it was found that the DnaG interacts with the nine subunit exosome via Csl4 protein [98]. Nevertheless the archaeal DnaG protein has not been elucidated so far. Furthermore the stoichiometry between the Csl4 protein and the DnaG protein is not yet known. To address these questions, as the final part of this project we decided to analyse native and the reconstituted exosome by single particle electron microscopy (SPEM).

2. Materials

2.1. Chemicals

All chemicals which are not specifically mentioned were obtained from Applichem.

Chemical	Manufacturer
Acetic acid	Roth
Acrylamide (30% w/v)/ bisacrylamide (0.8% w/v)	Roth
Adenosindiphosphate (rADP)	Roche
Agarose (LE agarose Biozym)	Biozym
Ammonium peroxide sulphate (APS)	Aldrich
Anhydrotetracycline	IBA
Bacto agar	Difco
Bacto-peptone	Becton, Dickinson Co.
Bovine serum albumin (BSA)	Sigma
Bromophenol	Roth
Calcium chloride	Merck
Casamino acid	Difco
Coomassie Brilliant Blue G-250	Serva
Deoxyribonucleoside triphosphates (dNTPs)	Qiagen
Desthiobiotin	IBA
Dimethyl pimelimidate (DMP)	Sigma
Dithiothreitol (DTT)	Roth
Ethanol	Roth
Ethanolamine	Sigma
Ethidium bromide	Roth
Ethylene-diamine tetraacetate (EDTA)	Roth

Formaldehyde (37%)	Roth
Glucose	Merck
Glycerol	Roth
N-2-hydroxyethylpiperazine-N'-2- ethanesulfonic acid	Roth
Imidazole	Sigma
Isopropyl-β-D-thiogalactoside (IPTG)	Roth
Lumi-Light Western Blotting Substrate I and II	Roche
Phenyl-methyl-sulfonylfluoride (PMSF)	Sigma
Potassium dihytrogen phosphate	Roth
Potassium chloride	Roth
Protease inhibitor cocktail	Roche
Magnesium chloride	Roth
Magnesium sulfate	Merck
Methanol	Roth
Mineral oil	Sigma
Nickel NTA	Qiagen
Nonidet P 40 (NP 40)	Fluka
Nickel sulfate	Aldrich
Ponceau-Red	Sigma
Protein A-Separose	GE Healthcare
Ribonucleoside triphosphates (rNTPs)	Promega
Roti-Quant (Bradford-Reagent)	Roth
Sodium carbonate	Merck
Sodium dodecyl sulfate (SDS)	Roth
N, N, N ', N'-tetramethylene diamine (TEMED)	Roth
Tris-(hydroxymethyl)-aminomethane (Tris)	Roth

Triton X 100	Roth
tRNA (*Saccharomyces cerevisiae*)	Boehringer
Tween 20	Serva
Urea	Roth
Vanadyl sulfate trihydrate	Aldrich
Xylencyanol	Serva
Yeast extract	Difco
Zinc sulphate	Sigma

Table 1. Chemicals used in this thesis

2.2. Culture media and agar plates

2.2.1. LB medium

10 g	Bacto-Trypton
10 g	NaCl
5 g	yeast extract
Add 1000 ml	dH_2O

2.2.2. SOC medium

2% (w/v)	Tryptone (pancreatic digest of casein)
0.5% (w/v)	Yeast extract
8.6 mM	NaCl
2.5 mM	KCl
20 mM	$MgSO_4$
20 mM	Glucose

Glucose, which is previously sterile filtered with a 0.22 µm filter, was added only after autoclaving, just before use of the medium.

2.2.3. LB-Agar plates 1000 ml LB-medium 15g of Agar was added

2.2.3. *Sulfolobus solfataricus*

2.2.3.1. Standard medium

1.0 g	Yeast extract
1.0 g	Casamino acid
3.1 g	KH_2PO_4
2.5 g	$(NH_4)_2SO_4$
0.2 g	$MgSO_4 \cdot 7H_2O$
0.25 g	$CaCl_2 \cdot 2H_2O$
100 µl	$MnCl_2 \cdot 4H_2O$ (18 mg/ml)
100 µl	$Na_2B_4O_7 \cdot 10H_2O$ (45 mg/ml)
10 µl	$ZnSO_4 \cdot 7H_2O$ (22 mg/ml)
10 µl	$CuCl_2 \cdot 2H_2O$ (6 mg/ml)
10 µl	$Na_2MoO_4 \cdot 2H_2O$ (3 mg/ml)
10 µl	$CoSO_4$ (or $CoCl_2 \cdot 6H_2O$) (3 mg/ml)
add 1000 ml	dH_2O
10 µl/l	$VOSO_4$ (3 mg/ml) (After autoclaving the medium)

Adjust the pH value up to 4.2-4.4 by adding concentrated H_2SO_4 drop wise at room temperature. The components $MnCl_2 \cdot 4H_2O$, $Na_2B_4O_7 \cdot 10H_2O$, $ZnSO_4 \cdot 7H_2O$, $CuCl_2 \cdot 2H_2O$, $Na_2MoO_4 \cdot 2H_2O$ and $CoSO_4$ were added from previously prepared stock solutions. $VOSO_4$

solution (0.03 g/100 ml ddH_2O) which was previously sterile filtered with a 0.22 micron filter, was added only after autoclaving, just before use of the medium (10 µl/ L medium).

2.2.3.2. Brock medium

1.3g	$(NH_4)_2SO_4$
0.28g	KH_2PO_4
.25g	$MgSO_4.7H_20$
0.07g	$CaCl_2.2H_2O$
0.02g	$FeCl_3.6H_2O$
1.8mg	$MnCl_2.4H_2O$
4.5mg	$Na2B_4O_7.10H_20$
0.22mg	$ZnSO_4.7H_2O$
0.05mg	$CuCl_2.2H_20$
0.03mg	$NaMoO_4.\ 2H_20$
0.01mg	$CoSO_4$
add 1000 ml	Distilled H_20
10 µl/l	$VOSO_4$(3 mg/ml) (After autoclaving the medium)

Adjust the pH value up to 4.2-4.4 by adding concentrated H_2SO_4 drop wise at room temperature. $VOSO_4$ which was previously sterile filtered with a 0.22 micron filter, was added only after autoclaving, just before use of the medium (10 µl/L medium).

2.3. Enzymes

The enzymes were used according to the manufacturer's instructions in their respective buffers unless otherwise stated.

Enzyme	**Manufacturer**
DNase 1	NEB
RNase A	Fermentas

RNase T1	Fermentas
T4-DNA-Ligase	NEB
T4-Polynucleotid-Kinase (PNK)	NEB
T4-RNA-Ligase	NEB
Taq-DNA-Polymerase	NEB

Table 2. Enzymes used in this thesis

2.4. Markers

Product	**Manufacturer**
Prestained Protein Marker, *Broad Range*	NEB
Low Range Protein Marker	Biorad
GeneRuler 1kb DNA *Ladder* Plus	Fermentas
Low Molecular Weight Marker, 10-100 nt	Fermentas

Table 3. Markers used in this thesis

2.5 Antibiotics

Antibiotic	**Manufacturer**	**stock solution**	**End concentration for *E. coli***
Ampicillin	Roth	100mg/ml (in ddH_2O)	200 µg/ml
Kanamycin	Serva	10 mg/ml (in ddH_2O)	25 µg/ml

Table 4. Antibiotics used in this thesis

2.6. Molecular Biology KITs

KIT	**Manufacturer**

Plasmid Isolation KIT	Qiagen
P drive vector ligation KIT	Qiagen
QIAEX II Agarose Gel Extraction Kit	Qiagen

Table 5. KITs used in this thesis

2.7. Bacteria and Archaea strains

Strain	**Description**
Escherichia coli BL21-Gold(DE3)pLysS:	*E. coli* B, F^-, ompT, hsdS(r_B-rn_{B-}), dcm^+, Tet^r galλ(DE3), endA, Hte [pLysS Cam^r] (Promega)
Escherichia coli JM109	*E. coli* K, F^- , hsdR17, recA1 ,endA1, no resistance (Promega)
Sulfolobus solfataricus P2:	Wild type P2 strain
Sulfolobus solfataricus M16:	Wild type M16 strain for expression of proteins

Table 6. The strains that were used in this thesis

2.8. Plasmids

Plasmid	**Description**	**Reference**
pET-MCN	Amp^r; P_{T7}; 5,2 kb	Lorentzen *et al*, 2005
pET-MCN::*Sso*Rrp41	*rrp41* was Cloned between *Nde*I/*Xho*I restriction sites in pET-MCN; Amp^r	Lorentzen *et al*, 2005

pET-MCN::*Sso*Rrp4	*rrp4* gene was cloned between *Nde*I/*Xho*I restriction sites in pET-MCN; Amp^r	Lorentzen *et al*, 2005
pET-MCN::*Sso*Csl4	*csl4* gene was cloned between *Nde*I/*Xho*I restriction sites in pET-MCN; Amp^r	Prof. Dr. E. Conti (Max-Planck-Institute, Martinsried , Munich)
pET::*Sso*DnaG	*dnaG* gene was cloned between *Nde*I/*Xho*I restriction sites in pET30a; Amp^r	Zuo *et al*, 2010
pSP72	Amp^r; P_{T7}; SP_6; 2,46 kb	Promega
pET15b::*Sso*Rrp4NT	Gene portion corresponding to the N terminal of the Rrp4 protein was cloned between *Nde*I/*Xho*I restriction sites in pET-MCN; Amp^r	This work
pET15b::*Sso*Rrp4S1	Gene portion corresponding to the S1 domain of the Rrp4 protein was cloned between *Nde*I/*Xho*I restriction sites in pET-MCN; Amp^r	This work
pET15b::*Sso*Rrp4KH	Gene portion corresponding to the KH domain of the	This work

	Rrp4 protein was cloned between *Nde*I/*Xho*I restriction sites in pET-MCN; Amp^r	
pET15b::*Sso*Rrp4NTS1	Gene portion corresponding to the NT and S1 domain of the Rrp4 protein was cloned between *Nde*I/*Xho*I restriction sites in pET-MCN; Amp^r	This work
pET15b::*Sso*Rrp4S1KH	Gene portion corresponding to the S1 and KH domain of the Rrp4 protein was cloned between *Nde*I/*Xho*I restriction sites in pET-MCN; Amp^r	This work
pET15b::*Sso*NopF12	Gene portion corresponding to the N terminal and the middle domains of the Nop56 protein was cloned between *Nde*I/*Xho*I restriction sites in pET-MCN; Amp^r	This work

pET15b::*Sso*Nop23	Gene portion corresponding to the middle and the C terminal domains of the Nop56 protein was cloned between *Nde*I/*Xho*I restriction sites in pET-MCN; Amp^r	This work
pMS1::*Sso*Rrp4	*rrp4* gene was cloned between B*amH1/Nco1* restriction sites in pMS1; Amp^r	This work
pMS1::*Sso*Csl4	*csl4* gene was cloned between *BamH1/Nco1* restriction sites in pMS1; Amp^r	This work
pMS1::*Sso*DnaG	*dnaG* gene was cloned between *Nco1* restriction site in pMS1; Amp^r	This work
pMS1::*Sso*DnaGF12	Gene portion corresponding to the N terminal and the TOPRIM domains of the DnaG protein was cloned between *Nco1* restriction sites in pMS1; Amp^r	This work
pMS1::*Sso*DnaGF23	Gene portion corresponding to the TOPRIM and the C terminal domains of the DnaG protein was cloned	This work

	between *Nco1* restriction sites in pMS1; Amp^r	
pMJ0105:: *Sso*DnaG	*dnaG* gene was cloned between *AvrII/EagI* restriction sites in pMJ0105; Amp^r	This work

Table 7. Plasmids taken for the thesis.

2.8.1 Domains encoded by the genes used in this thesis

2.8.1.1. Domains encoded by the *rrp4* gene

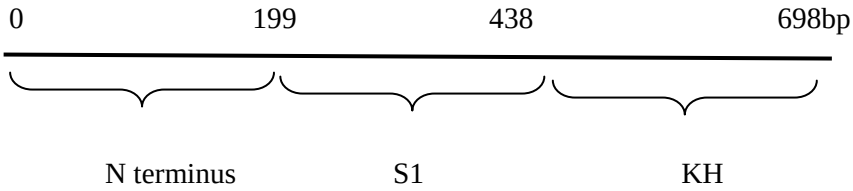

2.8.1.2. Domains encoded by the *dnaG* gene

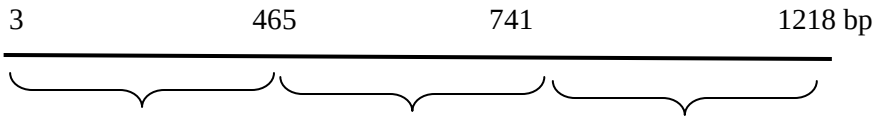

2.8.1.3. Domains encoded by the *nop5* gene

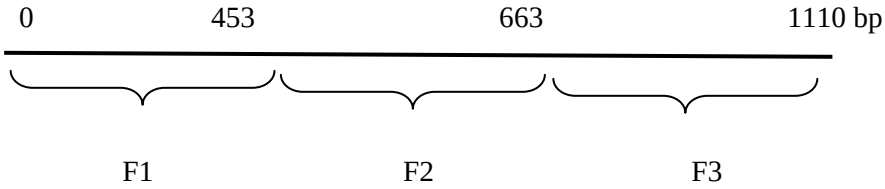

2.9. Oligonucleotides

Based on the known sequences of the genes, including their flanking regions, suitable primers were designed for the amplification. The oligonucleotides were produced by Roth, Biomers

and Eurofins companies. The concentration was adjusted to 100 pmol/µl. The stock solutions were stored at -20 ° C.

Primer name	**Sequence**	**Purpose**	**Restriction sites**
S1-Rrp4-Fwd	5’CATATGCCCTTGGAAGGCTCG3’	Cloning in pET vector	*Nde*I
S1-Rrp4-Rvs	5’CTCGAGCCCTAGATCCTTGCC3’	Cloning in pET vector	*Xho*I
KH-Rrp4-Fwd	5’CATATGGATCTAGGGCGCTGTAAG3’	Cloning in pET vector	*Nde*I
KH-Rrp4-Rvs	5’CTCGAGTGAAGCATTTCTCTCACC3’	Cloning in pET vector	*Xho*I
NT-Rrp4-Fwd	5’CGCCATATGAACATGAGTCAGTCCCAG3	Cloning in pET vector	*Nde*I
NT-Rrp4-Rvs	5’CTCGAGCGAGCCTTCCAAGGG3’	Cloning in pET vector	*Xho*I
Rrp4-Fwd	5'GGGCCATGGAACATGAGTCAGTCCCAG3'	Cloning in pMS1 vector	*Nco1*
Rrp4-Rvs	5’GGATCCTCAAGAATTAGTTTTGGTCTCTCC3’	Cloning in pMS1 vector	*Nco1*
F1-DnaG-Fwd	5’ CGCCCATGGGTGAGCTTCCAAATGAAATATG3’	Cloning in pMS1 vector	*Nco1*
F1-DnaG-Rvs	5’CAGGCGGATCCTGGTCCATATTCTGTTATTTC3’	Cloning in pMS1 vector	*Nco1*
F2-DnaG-Fwd	5’CCATGGGAAAGATTACCCGCAGG3’	Cloning in pMS1 vector	*Nco1*

F2-DnaG-Rvs	5’CCCACTCCATGGTGCCAATCGGTGCTCTTGCTAC3’	Cloning in pMS1 vector	*Nco1*
F3-DnaG-Fwd	5’GTACCATGGAGAGAGGTAGAAGAACTAACAGGG3’	Cloning in pMS1 vector	*Nco1*
F3-DnaG-Rvs	5’CAGAGGATCCAGAAGAAATAATATCGGTAAATGTC3’	Cloning in pMS1 vector	*Nco1*
F1-Nop-Fwd	5’CCATGGATGAAAATATACCTAATTGAGCATGTTATTGG3’	Cloning in pMS1 vector	*Nco1*
F2-Nop-Fwd	5’GGGCCATGGAAGAGAGACCTTTTAGCTATTCAAGC3’	Cloning in pMS1 vector	*Nco1*
F2-Nop-Rvs	5’GCGCCATGGCATTTTAGCTAATTCATCTAAACTCC3’	Cloning in pMS1 vector	*Nco1*
F3-Nop-Rvs	5’CAATGGTCACTTTCTTTTACCTCTTCTCTTTC	Cloning in pMS1 vector	*Nco1*

Table 8. Primers used for subcloning exosome genes of *S. solfataricus*. Fwd, forward primer; Rvs, reverse primer.

2.10. Radioactive nucleotides

Product	**Manufacturer**
[α-^{32}P]-ATP, 3000 Ci/mmol	Hartmann Analytic
[γ-^{32}P]-ATP, 3000 Ci/mmol	Hartmann Analytic

Table 9. The radioactivity used in this thesis.

2.11. Antibodies

Antibody	Manufacturer	Reference
Anti-*Sso*Rrp41 (Rabbit, Antiserum)	Davids Biotechnology GmbH	Evguenieva-Hackenberg, *et al*., 2003
Anti-*Sso*DnaG (Rabbit, Antiserum)	Biogenes	Walter , P., *et al*., 2006
Anti-SsoRrp4 (Rabbit, Antiserum)	Davids Biotechnology GmbH	Witharana, C., *et al*., 2012
Anti-*Sso*Csl4 (Rabbit, Antiserum)	Davids Biotechnology GmbH	Witharana, C., *et al*., 2012
Anti-*Rabbit* IgG, Peroxidase Conjugates	Pierce	

Table 10. The antibodies used in this thesis.

2.12. Buffers and solutions

De ionized water was used for the preparation of buffers.

2.12.1. Buffers for gel electroporesis

1 x TBS :	200 mM	NaCl
	50 mM	Tris-HCl
		pH 7,4
1 x TBE	89 mM	Tris-HCl
	89 mM	Sodium borate
	2,5 mM	EDTA
		pH 8.3
4 x Separation buffer	1,5 M	Tris-HCl
	0,4% (w/v)	SDS
		pH 8.8

4 x Stacking buffer	0,5 M	Tris-HCl
	0,4% (w/v)	SDS
		pH 6.8
1 x Laemmli-buffer	25 mM	Tris-HCl
	192 mM	Glycin
	0,1 % (w/v)	SDS
		pH 8.2

2.12.2. Buffers for Western blotting

Transfer buffer	25 mM	Tris-HCl
	192 mM	glycine
	20%	Methanol
10x TBS	0.5 M	Tris-HCl
	2 M	NaCl
		pH 7.4
Blocking solution	5% (w/v)	Milk powder
Stripping buffer I	500 mM	NaCl
	200 mM	glycine
		pH 2.8
Stripping buffer II	500 mM	NaCl
	200 mM	glycine
		pH 2.2

Stripping buffer III	200 mM	Tris
		pH 7.2

2.12.3. Other buffers

1 x PBS	137 mM	NaCl
	2,7 mM	KCl
	10 mM	Na_2HPO_4
	2 mM	KH_2PO_4
		pH 7,4
1 x TE-Puffer	10 mM	Tris-HCl
	1 mM	EDTA
		pH 7,5
MES-Low salt buffer	20 mM	MES
	2 mM	DTT
	1 mM	PMSF
	0,5 mM	EDTA
		pH 6,5
MES- High salt buffer	20 mM	MES
	2 mM	DTT
	1 mM	PMSF
	0,5 mM	EDTA
	500 mM	NH_4Cl
	10 mM	Mg-Acetate
		pH 6,5

10x TMN	100 mM	Tris-HCl (pH 7.5)
	1.5 M	NaCl
	50 mM	$MgCl_2$
	1 %	$NaPO_4$
Po buffer	10 mM	Tris-HCl (pH 7.0)
	5 mM	$MgCl_2$
	0.5 mM	EDTA
	200 mM	NaCl
	0.05 %	Tween 20
	0.2 %	DTT
	5 %	99.5 % glycerol
Lysis buffer (Ni-NTA purification)	50 mM	Tris-HCl (pH 8.0)
	400 mM	NaCl
	10 mM	Imidazole
Elution buffer (Ni-NTA purification)	200 mM-400 mM	Imidazole
5 x RNase Buffer	100 mM	HEPES pH 7
(Degradtion assay)	40 mM	$MgCl_2$
	300 mM	KCl
	0,5 mM	EDTA
	10 mM	DTT
	100 mM	HEPES pH 7,9
5 x RNase Buffer	20 mM	$MgCl_2$

(Polyadenylation assay)	300 mM	KCl
	0,5 mM	EDTA
	10 mM	DTT

2.13. Equipments

Equipment	**Manufacturer**
Centricon 10 membrane	Millipore
Cooling centrifuge, Sorvall RC-5C+	Kendro
Cooling centrifuge, Sorvall -5B	Kendro
Cooling centrifuge Z 323K	Hermle
Dialyse tubes (Type 20/32)	Roth
Electroporator (Micro Pulser)	Biorad
FPLC system (Akta)	GE Amersham
Filter paper, Whatman	Hartenstein
Fusion SL4 –Chemiluminasence detector	Biorad
Glass wool	Serva
Incubator Shaker (Model G 25)	New Brunswick Scientific
Microcon (MWCO 3000)	Millipore
Nitrocellulose membrane (BA Protran)	Schleicher & Schuell
NanoDrop spectrophotometer	Biorad
Optima TLX Ultra centrifuge	Beckman Coulter
Phosphoimager (*Molecular Imager* FX)	Biorad
Phosphoimager Screens	Biorad/Fuji
Screen Eraser K	Biorad
Semi dry blot- Apparatus(Novablot)	Pharmacia
Sterile filter 0,22 µm	Nalagene

Superdex^{TM}75,*HiLoad*^{TM}16/60 (Gel filtration)	Pharmacia
Scintillation counter (LS 6500)	Beckman Coulter
Tabletop centrifuge Biofuge 13 and fresco	Kendro
Ultrasound machine Sonoplus GM70 (Sonifier)	Bandelin
Ultra centrifuge Discovery 90	Kendro
UV-*Stratalinker*^{TM} 1800	Stratagene

Table 11. Equipments used in this thesis

3. Methods

3.1. General microbiology techniques

3.1.1. Preparation of cultures

3.1.1.1. Cultivation of *E. coli*

The liquid cultures of *E. coli* were grown aerobically at 37 °C on a shaker, shaking at 180 rpm. The culture was filled up to 25% of the total volume of the Erlenmeyer flasks. If necessary, an appropriate amount of antibiotic was added in to the culture to prevent cells lose the plasmid with resistance after a few cell divisions.

The grown culture was plated on the LB agar plates (with appropriate antibiotics) with an inoculating loop. The agar plates were incubated at 37 °C over night.

3.1.1.2. Cultivation of *S. solfataricus*

3.1.1.2.1. Standard conditions

In Duran bottles*: S. solfataricus* P2 was grown in liquid culture at 75 °C. The Duran bottles were filled up to 30% of the total volume with the medium and inoculated with 10% *S. solfataricus* pre-grown culture. Approximately in every 7 days a new culture was inoculated.

In fermenter: Five Duran bottles containing 200 ml of *S. solfataricus* medium was grown as pre cultures on the shaker at 75 °C. Then 10 l of autoclaved media was inoculated with the pre cultures and was grown in the fermenter [92] at 75 °C aerobically.

Growth was monitored by optical density measurements at 600 nm every 12 hours.

3.1.1.2.2. Growth of *S. solfataricus* in stress experiments

The *S. solfataricus* was grown in the fermenter for the stress experiments. Five litres out of the 10 l of exponentially growing cultures (OD_{600} ~ 0.3) were harvested as the control experiments while stresses were applied to the rest of the cultures (heat stress 88 °C, cold stress 65 °C, pH low stress pH 2, pH high stress pH 6.5 deviating from the normal growth temperature 75 °C and pH 4) for 30 min. For the stationary phase experiment, the cultures were grown till they reached a constant OD (OD_{600} ~ 0.7) for 48 hours prior to harvesting.

3.1.2. Preparation of competent cells

The production of heat-competent cells and electro-competent cells were based on the document "Preparation of competent *E. coli*" by Qiagen (Qiagen 2003). The competent *E. coli* cells were stored in aliquots at -80 °C.

For the preparation of the Sbl4 cells, first a LB agar plate was streaked out with the original stock and following day, 4 ml of self mixed LB medium was inoculated with 1 colony and incubated over night at 32 °C. Next day, 60 ml of self mixed LB medium was inoculated by 1% of the overnight grown culture and incubated at 32 °C until the OD_{600} reached 0.4-0.5. There after all the steps were performed on ice. The cells were harvested at 4 °C for 10 min at 4000 g and supernatant was discarded. The cells were resuspended in 10 ml ice cold Glycerin-MOP-buffer (15% (w/v) glycerin and 1 mM MOPS), centrifuged and the last step was repeated. The cell pellet was resuspended in 1 ml ice cold Glycerin-MOP-buffer and it was transferred into Eppendorf tubes. Again the cells were centrifuged for 10 min at 4 °C at 4000 g, the supernatant was removed and the pellet was resuspended in 200 µl Glycerin-MOP-buffer. The cells were aliquoted (each 50 µl) in Eppendorf tubes, frozen it in liquid nitrogen and stored it in -80 °C.

3.1.3. Transformation of *E. coli* cells

3.1.3.1. Transformation by heat shock

For each transformation, competent *E. coli* cells (50 µl) from -80 °C were thawed on ice. Plasmid DNA (approximately 50 ng) was added to the cells, mixed gently, and incubated on ice for 30 min. To facilitate the uptake of DNA, cells were heat-shocked by incubating the cells at 42 °C for 30 s, and cells were then placed back on ice for a further 2 min and 1 ml of LB medium without any antibiotics was added. The cells were allowed to recover at 37 °C for 1 h with shaking (180 rpm) before plating onto LB agar plates with antibiotics. Plates were then incubated overnight at 37 °C to allow for colony growth.

3.1.3.2. Transformation by electroporation

The electro competent cells (JM 109 and DH5α), which were stored at -80 °C, were thawed on ice. Plasmid DNA (approximately 50 ng) was added to the cells and mixed gently. The mixture was added in to a pre-cooledd cuvette and the cuvette was placed in the electroporator. The electro pulse (EC2- 2.5 kv) was applied to the cells and immediately 1 ml

of LB medium without any antibiotics was added. Cells were allowed to recover at 37 °C for 1 hour with shaking (180 rpm) and then the procedure same as the heat shock trasfomation was followed.

The procedure for the Stl4 electro competent cells was slightly different. Approximately 200-250 ng of plasmid DNA was added to the cells and an electro pulse of 2.5 kv was applied. Immediately 1 ml of SOC medium was added without any antibiotics. Cells were allowed to recover at 32 °C for 1.5 hours.

3.1.4. Preparation of electrocompetent *Sulfolobus solfataricus* M16 cells

Two cultures of *Sulfolobus solfataricus* M16 (ΔpyrEF/lacS double mutant) were started to ensure that the negative control without uracil did not grow over an OD_{600} of 0.3. The culture with uracil was grown for 2 days. After 2 days growth, 500ml culture was inoculated and allowed to grow overnight to an OD_{600} of between 0.2-0.3. The overnight culture was cooled on ice, and centrifuged at 4000 g at 4 °C for 20 min. The cell pellet was resuspended in 1 ml cold sucrose water (6.9 ml 20% sucrose in 200 ml water) and then diluted into a total of 50 ml sucrose water and centrifuged again. This was repeated with the pellet resuspended in a total of 10 ml sucrose water and centrifuged again. The cell number was adjusted to 10^{10} cells/ml (e.g. if the OD_{600} of a 50 ml culture was 0.1 the cells would be resuspended in 200 µl sucrose or if original OD_{600} was 0.15 then 300µl of sucrose water should be added). Cells were incubated on ice before electroporation.

3.1.4.1. Electroporation of *Sulfolobus solfataricus* M16 cells

Twenty nanogram of the plasmid DNA was mixed with 50 µl of cells, and transferred to a chilled cuvette. Cells were electroporated at 1.5kV, 25µF and 400Ω, with a time constant of approximately 10 ms. After electroporation 1ml of Brock medium + uracil (2%w/v) were added and the cells were transferred to a 1.5 ml Eppendorf tube. Cells were regenerated at 75°C for 1h and aerated every 20 min by opening the tube. 50ml pre-warmed medium plus uracil was inoculated with the transformed cells and grown for 2-3 days until the cells reached an OD_{600} of 0.5. After this time, cells were transferred to selective medium without uracil and with 0.1 % N-Z Amine and grown for 2 days. When the cells were grown to an OD of 0.3 or higher glycerol stocks were prepared (3.1.5.2.). The induction was done with 0.2% D-arabinose and when the culture reached OD 0.7 cells were harvested.

3.1.5. Preparation of the glycerol stocks

3.1.5.1. Preparation of glycerol stocks of *E. coli*

To create glycerol stocks of *E. coli*, 3 ml of a liquid culture was grown overnight and cells were pelleted at 4000 g for 10 min. The cells were washed with 1 ml of medium without added antibiotics. The cell pellet was resuspended in 1 ml of medium without antibiotics, glycerol was added to a final concentration of 20% and mixed gently. They were stored in special cryogenic tubes that were initially frozen in liquid nitrogen and then stored at -80 °C.

3.1.5.2. Preparation of glycerol stocks of *S. solfataricus*

To create glycerol stocks of *S. solfataricus,* 5 ml of a culture in the exponential growth phase was taken. The cultures were centrifuged for 10 minutes at 4000 g at 4 °C. The cells were resuspended in 1 ml of medium and glycerol was added to a final concentration of 20%. Mixed gently. They were stored in special cryogenic tubes at -80 °C.

3.2. Molecular biology methods

3.2.1. Nucleic acid techniques

3.2.1.1. Polymerase chain reaction (PCR)

The PCR is a method in which nucleic acid segments can be amplified exponentially. The primers used are listed in 2.9.

Reaction mixture used for the PCR

Fwd primer	1 µl (100 pmol/µL)
Rvs primer	1 µl (100 pmol/µL)
Taq Polymerase buffer (x10)	5 µl
template DNA	1 µl (5 ng of plasmid DNA)
dNTPs	0.4 µl (100 mM)
Taq Polymerase enzyme	1 µl (5 Units/µl)
Water	40.6 µl
Total volume	50 µl

Annealing temperature was generally between 45 and 60 ° C and the extension time of the primer (about 1 min/kb template) were individually optimized for each PCR. The PCR product was purified (if necessary) using an agarose gel (see 3.2.10.1.).

3.2.1.2. Preparation of plasmid DNA from *E. coli*

To prepare small amounts of plasmid DNA in microgram quantities (termed 'miniprep'), *E. coli* cells were transformed with plasmid DNA, and a single colony was inoculated in LB medium with appropriate antibiotics (5 ml) to stationary phase by incubation at 37 °C overnight in a shaking incubator. After centrifugation at 6000 g for 10 min at 4 °C, plasmid DNA was extracted from the cell pellet by sequential lysis, precipitation and extraction of DNA. After the cell lysis under alkaline conditions (NaOH 500 mM, SDS 1% v/w) acetate containing neutralizing buffer was added for the precipitation of proteins and large chromosomal fragments. The sample was centrifuged for 20 min at 13 000 g and supernatant was taken in to another Eppendorf tube. The DNA was precipitated with 70% (v/w) isoproponal. The pellet was then re-suspended in RNase free water and typically yielded 100-300 μg/ml plasmid DNA.

To prepare larger quantities of plasmid DNA, 'maxi-preps', were performed using the Qiagen DNA Maxi Kit. A single bacterial colony, transformed with the relevant construct was used to inoculate LB (5 ml) containing the appropriate antibiotic and then a larger volume (250 ml). After an overnight incubation at 37 °C, the cells were pelleted by centrifugation at 6,000 rpm for 10 min at 4 °C. Plasmid DNA was purified according to the manufacturer's instructions. Overnight cultures of 250 ml typically yielded 0.5-1 mg plasmid DNA.

3.2.1.3. Enzymatic dephosphorylation

The linearized plasmids were subjected for dephosphorylation to avoid self ligation. For the dephosphorylation of the 5' terminus of DNA molecules, Antarctic Phosphatase (NEB) was used as specified by the manufacturer in the provided buffer.

3.2.1.4. DNA cloning

3.2.1.4.1. Use of cloning vectors

To simplify the cloning in *E coli*, PCR fragments which were amplified by *Taq* polymerase were ligated in to the P Drive vector (Fermentas) as specified by the manufacturer in the

provided buffer for 2 hours at room temperature or at 16 °C over night. This is an open vector with (U) overhangs. PCR fragments can be directly ligated in to the P Drive vector because *Taq* polymerase synthesized (A) overhangs in the PCR products.

3.2.1.4.2. Ligation

Ligations were performed with T4 DNA ligase (Fermentas) in 1x ligase buffer. All ligations (except the P Drive vector ligation) were incubated at 16 °C overnight. The ligations are due to the covalent linkage between vector DNA and the DNA fragment (insert).

3.2.1.4.3. Cloning in the shuttle vector for the expression in *S. solfataricus* M16

Homologous expression of the exosomal proteins was attempted using the method in [111]. The *S. solfataricus* uracil auxotroph strain (ΔpyrEF/lacS double mutant) was kindly provided by Dr. Sonja-Verena Albers (Max Planck Institute for Terrestrial Microbiology, Germany). The genes *dnaG*, *csl4*, *rrp4* and gene fragments corresponding to the N terminus and C terminus of the DnaG protein, were PCR amplified using the primers shown in 2.9 and cloned into the vector pMZ1 using the restriction sites *Nco*1 and *Bam*H1 (Csl4 and Rrp4) or single restriction site *Nco*1 (DnaG and its fragments).

This vector contains an upstream D-arabinose inducible promoter and downstream His and Strep-tags at either side of the gene insertion site. The promoter, gene and tags were then restricted from the vector as a single piece of DNA using the restriction sites *Avr*II and *Eag*1, and ligated into the modified viral vector pMJ0503. This vector contains a pUC18 region to allow propagation in *E. coli* before transformation into *Sulfolobus*, and a selectable pyrEF gene which complements the *Sulfolobus* uracil auxotroph mutant, allowing transformants to be grown under selective conditions. After ligation, the pMJ0503 vector containing the insert was transformed into the Stbl4 strain of *E. coli* engineered for the propagation of large vectors. The cells were grown on LB agar plates, with 50 µg/ml ampicillin and 0.5% glucose at 32 °C for 1.5 days. The successfully transformed cells (colonies) were picked and grown in LB supplemented with 0.5% glucose at 30 °C over night. Plasmids were extracted by Minipreps (3.2.1.2.) and transformed into *S. solfataricus M16* (3.1.4.1.) and cells were grown on Brock medium at 75 °C for 5-7 days to allow successful transformants to grow.

3.2.1.5. Detection of DNA by ethidium bromide

Ethidium bromide (EtBr) intercalates into the DNA helix. When exposed to UV light EtBr florescence with orange colour. The agarose gels was dipped in EtBr solution (5 g/ ml) for 10 min and non-intercalated EtBr was removed by brief washing with double-distilled water and then exposed to UV light for the visualization.

3.2.1.6. Isolation of DNA fragments from agarose gels

For the isolation and purification of DNA fragments from agorose gels, the peqGOLD Gel Extraction Kit (peqlab, Erlangen, Germany) was used as instructed by the manufacturer.

3.2.1.7. DNA sequencing

Sequencing of either plasmid DNA or PCR product DNA was performed by the sequencing Service, Life sciences, University of Giessen.

3.2.1.8. RNA Isolation

To isolate RNA from cell free extract, the TRIzol method (according to peqGOLD TriFast^{TM} Manual) was used. Here, the 200 µl of cell free extract was added to 1 ml of TRIzol solution and mixed well and kept for 2-3 min at room temperature. Then, 200 µl of chloroform was added and mixed with the TRIzol solution by short, vigorous shaking. After centrifugation of the samples (11000 x g, 20 min, room temperature) three phases were formed. An upper aqueous phase with RNA, an interphase and a lower phenol-chloroform phase containing the DNA and the proteins respectively. The upper phase was carefully removed and then used to precipitate the RNA. For this purpose, 500 ml of ice-cold 96% ethanol was added and samples were left at least 30 min at -20 °C. After centrifugation (11000 x g, 20 min, 4 °C), the RNA was extracted as a visible pellet and washed once with 70% ethanol and centrifuged again briefly (4500 x g, 5 min, 4 °C). The pellet was then air dried and re-suspended in 30 µl sterile RNase free water.

In order to avoid the amplification of possibly existing genomic DNA in this RNA solution, a DNA digestion by DNase was performed. This was done as stated by the manufacturer in the provided buffer. After the DNA digestion, samples were filled up with 150 µl of RNase free water and 200 µl of phenol / chloroform mixture (1:1), mixed well and centrifuged (11000 g, 10 min, 4 °C). The upper phase was removed and mixed again with 200 µl phenol:isoamyl alcohol(25:24:1) and chloroform. Samples were vortexed for 1 min and centrifuged at 13000

g for 5 min at room temperature for the phase separation. The upper aqueous layer containing the RNA was precipitated with ice cold 96% ethanol. The RNA pellet was then resuspended in about 15-30 µl RNase free water and RNA concentration was determined photometrically by the NanoDrop spectrophotometer at a wavelength of 260 nm.

3.2.1.9. Estimation of purity and quantification of nucleic acids

Quantification of RNA was performed on NanoDrop spectrophotometer using the solution which the RNA/DNA was in, as the reference. Both RNA and DNA absorb light at 260 nm wavelength. However, proteins have an absorption at 280 nm. Therefore, the ratio A260/280 gives an estimation of the degree of contamination of RNA samples with protein. For pure RNA, the ratio A260/280 is between 1.9 and 2.1 (1 unit of absorption= 40 ng/ml of RNA). A ratio lesser than this range means that the prepared RNA is contaminated with proteins and aromatic substances (phenol).

The quantification of DNA in aqueous solutions was measured as mentioned above. The ratio (260/280) 1.8 was considered as pure DNA (1 unit of absorption= 50 ng/ml of DNA). The integrity of plasmid DNA was assessed by agarose gel electrophoresis.

3.2.2. Overexpression of proteins

3.2.2.1. Overexpression of recombinant proteins in *E. coli*

For expression of the recombinant proteins Rrp41, Rrp42 Rrp4, DnaG with an N-terminal hexa histidine tag (genes ligated in pET vector) and Csl4 with an N-terminal Strep-tag (gene ligated in pASK-IBA 3 vector) the *E. coli* strain BL21 Gold (DE3) pLysS was used.

For the overexpression, 1 liter of LB medium was inoculated with the 1 ml of overnight culture with the appropriate antibiotic. Then the culture was incubated at 37 °C with shaking (180 rpm). When the OD_{600} was approximately 0.3-0.4, the culture with the cells which contain pET vectors were induced with 1 mM IPTG (final concentration) and incubated further for another 3 hours. Cells were harvested at 6000 g for 20 minutes. The proteins were either immediately isolated using Ni NTA affinity chromatography or stored at -80 °C.

It was not possible to overexpress DnaG in *E. coli* strain BL21 Gold (DE3) pLysS. Therefore *E.coli* Archtic express cells were used for overexpression. As mentioned before the culture was grown until OD_{600} 0.3-0.4 at 37 °C shaking at 180 rpm. Then the temperature was

lowered to 22 °C. After 2 hours, the culture was induced with 0.5 mM IPTG (final concentration) and left over night shaking at 22 °C. The next morning the cells were harvested at 6000 g for 20 minutes at 4 °C.

Csl4 protein was overexpressed same as DnaG protein. The induction was performed with (0.02 mg/ml, final concentration) anhydrotetracycline. After harvesting the cells the proteins were either immediately isolated using Strep-tag isolation or Ni-NTA chromatography or stored at -80 °C.

3.2.2.2. Overexpression of recombinant proteins in *S. solfataricus* M16

The fermentation was carried out at 75 °C in Duran bottles on the shaking incubator (220 rpm). Growth was monitored by optical density measurements at 600 nm every 12 hours. At an OD_{600} ~0.3-0.4 protein expression was induced by 0.2 % D-arabinose. After 36 hours the cells were harvested (6000 g for 10 min at 4° C) and stored at -80 °C.

3.2.3. Isolation and purification of proteins from *E. coli*

3.2.3.1. Ni-NTA chromatography

For the purification of His-tagged proteins metal chelate chromatogrpahy was used as described in [112]. Ni^{2+} ions are coupled via nitrilotriacetic acid (NTA) on an agarose matrix. The cell free extract of *E. c*oli or *S. solfataricus* was prepared by using 2 g or 1.5 g of wet pallet (respectively) mixing with 15 ml of lysis buffer and subjecting to sonification as mentioned in 3.2.7. Cell free extract of *E. coli* or *S. solfataricus* was added to the Ni-NTA beads (400 µl of slurry) and tumbled for 2 hours at 4 °C. The beads were washed with the 20 ml of lysis buffer. Imidazole (400 mM) was used for the elution of the proteins. Six times of elutions were done with 100 µl of elution buffer each time. The elution of bound proteins was carried out by the addition of imidazole, which occupies its binding to the matrix due to the structural similarity to histidine.

For the DnaG purification the lysis buffer was adopted as follows:

50 mM	Tris-HCl (pH 8.0)
150 mM	NaCl
10 mM	Imidazole

3.2.3.1.1. Co-purification of RNA bound to the native exosome

The experiments were carried out at 4° C. Following the Ni- NTA purification of the native exosome by the His-tagged DnaG directly from *S. solfataricus*, I tried to isolate RNA from the elution fractions by the Trizol (Invitrogen) RNA purification method (as described in 3.2.1.8.) Control experiment was carried out with the wild type *S. solfataricus*. Portions of the purified RNA were treated with RNAse T1, RNase A or with DNase 1. To confirm that the purified, DNase treated sample was DNA free, we carried out a PCR reaction.

3.2.3.2. Strep-tag purification

Cell free extract of *E. coli* was added to pre- activated *Strep*-tactin beads and tumbled for 2 hours at 4 °C. The beads were then washed with 20 ml of washing buffer and eluted the proteins with the provided elution buffer.

Strep-tag washing buffer

100 mM	Tris-HCL
400 mM	NaCl
1 mM	EDTA
0.1% (w/v)	Triton X-100

3.2.3.3. Size exclusion chromatography

The size exclusion chromatogrpahy was used for further purification of the native exosome complex.

In this work the gel filtration column Superdex ™ 200, HiLoadTM 16/60 (Pharmacia) was used. The column was installed according to the manufacturer's specifications. First the column was washed and filled with ddH_2O (filtered, 0.45 micron and degassed) and subsequently with the gel filtration buffer (filtered, 0.45 micron and degassed). The gel filtration took place with a flow rate of 1.0 ml/min. After 30 ml of flow 1.5 ml fractions were collected, immediately placed on ice and then analyzed by SDS-PAGE for their protein content. The UV absorption of proteins at 280 nm, which was measured as soon as the proteins leave the column, was used for the graphical representation of the elution profile.

Based on the known molecular weights of marker proteins, a standard curve was created which was used to verify the molecular sizes of the protein complexes [95].

Gel filtration buffer:	10 mM	Tris pH 7.6
	150 mM	NaCl

3.2.4. Dialysis of proteins

The proteins (minimum of 1 ml and maximum of 3 ml volume) were dialyzed in 1 l of P_0 buffer for 2 hours.

3.2.5. Concentration measurements of protein samples

Protein concentrations were measured by the Bradford method [113]. A standard curve was prepared according to the manufacturer's protocol, by adding increasing amounts of BSA to a final volume of 0.1 ml with water, and then mixing with 0.9 ml Bradford reagent. The mixture was allowed to stand at room temperature for 5 min. The optical density of the standards was measured at 595 nm (OD_{595}) in 1.5 ml plastic cuvettes against a reference cuvette containing water (0.1 ml) and Bradford reagent (0.9 ml). This was used to construct a standard curve that was employed to determine protein concentrations of cell lysates. On average the linear range of protein Bradford measurements lies between OD_{595} 0.1 and OD_{595} 0.7. Cell lysates were diluted so that the OD_{595} lay in this range. Bradford measurements were performed in triplicates.

3.2.6. *In vitro* reconstitution of complexes using native recombinant exosome protein subunits

3.2.6.1. Reconstitution of the Rrp4-exosome the Csl4- exosome and the Rrp4-Csl4-exosome

All the dialysis steps were done at room temperature.

Freshly isolated Rrp41 and Rrp42 were mixed briefly in an Eppendorf tube (0.5 mg each) in a final volume of 1.5 ml. The mixture was then transferred in to a dialysis tube which incubated for 2 h at room temperature in the P_0 buffer for the formation of the hexameric ring. Thereafter excess amount of Rrp4 or Csl4 was added (0.7 mg each) to reconstitute Rrp4-

exosome and Csl4-exosme, respectively. For the preparation of Rrp4-Csl4-exosome, excess amount Rrp4 and Csl4 proteins were added (0.7 mg each). The incubation took place at room temperature for 2 hours dialyzing in P_0 buffer. After the heat treatment at 75 °C for 10 min and centrifugation for 20 min at 13,000 g, the supernatant was used directly for the activity assays or stored at -80 °C in portions of 10 µl. The frozen portions were always thawed on ice and second thawing was avoided.

3.2.6.2. Reconstitution of the DnaG-Csl4-exosome

Csl4-exosome was reconstituted as described in (3.2.6.1.). Subsequently excess amount of DnaG protein (0.7 mg) was added in to the dialysis tube and incubated for 2 hours at room temperature. Rrp41, Rrp4 and DnaG were His-tagged proteins while Csl4 was the only Strep-tagged protein in this complex. Afterwards, Strep-tag purification was done to avoid of all the monomers of His-tagged proteins and the complexes without Csl4. Subsequently the elution fractions of the Strep-tag purification were subjected to a Ni-NTA chromatography to evade all the monomers of the Strep-tagged Csl4 protein. The elution fractions were separated in the SDS-PAGE gels and visualized by silver staining.

3.2.6.3. Reconstitution of the ΔKH-Rrp4-exosome (for RNA assays)

The hexameric ring was reconstituted as mentioned above (3.2.6.1.). Then the full length or the truncated Rrp4 subunits (0.7 mg) were mixed together and dialyzed at room temperature in a modified P_0 buffer with 500 mM NaCl instead of 150 mM NaCl.

3.2.7. Cell free extract of *S. solfataricus*

The cells (1.5 g) were thawed resuspended in 3 ml MES buffer with 30 µl protease inhibitor cocktail, 2 mM DTT and 1 mM PMSF. The suspension was subjected to ultrasound sonification for 3 times, 20 seconds with 50% power (pulsed). Subsequently, the sample was centrifuged for 20 min at 4 °C and 5,000 g to get rid of the cell debris. The supernatant, (cell free extract) was taken for the further experiments.

3.2.8. Fractionation experiments

The cell free extract was subjected to ultra centrifuged at 100 000 g and 4 °C for 1 hour to obtain S100 (soluble fraction) and the P100 (insoluble fraction).

3.2.8.1. Analysis of the change in the protein content in the soluble and non soluble fractions in the individual exosomal subunit after stress

The cell free extract was fractionized as described in 3.2.8. 10 µl of S100 and P100 fractions were loaded in to a SDS-PAGE gel as described in 3.2.10.3. Thereafter a Western blot analysis was conducted and the band intensities were measured using the Fusion SL4 software.

3.2.8.2. Sedimentation of the exosome under different relative centrifugal forces

To analyse the sedimentation properties after applying different relative centrifugal forces (RCF) the cell lysate, which was prepared as mentioned in 3.2.7., was subjected to the 2500 g and 14 000 g RCFs for 10 min.

3.2.8.3. Sucrose density gradients

In this work the sucrose density gradient centrifugation is used to separate the membranes of *S. solfataricus* and to demonstrate the interaction between the membrane fractions and the exosomal proteins.

The gradients were prepared under high salt conditions. The gradient was prepared by increasing the concentration of sucrose starting with the highest concentration at the bottom of the ultra centrifuge tubes. Thereafter the next highest concentrated segment was pipetted very carefully on top of the bottom layer without mixing. Likewise the sucrose density gradient was prepared from 70% -15% w/v concentrations. Eight hundred micro liters of the cell free extract was pipetted on to the sucrose density gradient.

The centrifugation was carried out in an ultracentrifuge for 24 hours at 25000 g at 4 °C. After centrifugation, the tubes were carefully removed from the rotor and immediately separated into 22 fractions of 0.5 ml. These fractions were further analyzed by Western blot, Co-IP and absorption measurements.

Sucrose density buffer

20 mM	MES
2 mM	DTT
0.5 mM	EDTA
500 mM	NH_4Cl

10 mM Mg-Acetate

15-70% Sucrose (15, 30, 40, 55 and 70%)

3.2.9. Co-immunoprecipitation experiments

Co-immunoprecipitation experiments with polyclonal antibodies covalently coupled to protein A-Sepharose were performed as previously described [95]. We used 800 μl of cell-free extract and 0.04 g of beads with coupled antibodies in PBS buffer. The antibody-bead conjugate was incubated with cell free extract for 2 h at 4 °C on a tumbler and then centrifuged for 3 min at 4000 g at 4 °C. The supernatant was carefully discarded and the beads were washed seven times with 1 ml of lysis buffer. Then the proteins were eluted with the low pH-elution buffer.

3.2.10. Gel electrophorosis

The electrophoresis can be used for separating proteins and nucleic acids according to their molecular weight. The migration velocity of the molecules depends primarily on the net charge, shape and size. Large molecules move slower through the matrix than smaller ones.

3.2.10.1. Separation of DNA by agarose gel elecrophoresis

The separation of the DNA was done with the use of agorose gels. The samples were mixed with (4X) loading buffer (25% of the total volume) before loading to the gel. The electrophoresis was carried in TBA buffer (1X) at 70 mA. The visualization of the DNA was done as mentioned in 3.2.1.5.

3.2.10.2. Separation of RNA by urea polyacrylamide gel electrophoresis (PAGE)

For the separating of short RNA fragments that occur in RNA activity assays, 18% polyacrylamide gels containing 8 M urea was used. The 20 x 20 cm glass plates, spacers and comb were cleaned first with pure H_2O and then with 70% ethanol. The "ears plate" was silanized with "Acrylease" in order to easily get the gel off the glass plates after electrophoresis.

It is important that the urea is completely dissolved before the addition of APS and TEMED to the gel solution. The RNA samples were mixed with formamide-urea buffer (50% of its volume) before loading onto the gel and denatured for 10 min at 65 °C. The electrophoresis

was carried out for about 1 to 2 hours at 400 V in 1 x TBE buffer. The gels were transferred onto Whatman paper and dried on a vacuum drier for about 45- 60 min at 80 °C. The RNA bands were visualized by phosphoimaging.

10-18% Urea PAGE	5-9 ml	40% (w/v) Polyacrylamid
	2 ml	10 x TBE-buffer
	9.6 g	Urea
	add 20 ml	ddH_2O
	70 µl	6% APS (w/v)
	7 µl	TEMED

3.2.10.3. Separation of proteins by sodium dodecyl sulphate (SDS)-polyacrylamide gel electrophoresis (PAGE)

The 20 x 20 cm glass plates, spacers and comb were cleaned first with pure H_2O and then with 70% ethanol. The gel was sealed with melted agorose. First the separation gel was poured between the glasses. Subsequently 96% ethanol was layered carefully over the acrylamide solution and polymerisation was allowed to continue for at least 30 min- 1 hour. The ethanol was removed, washed with pure water and rest of the water was removed with filter paper. Thereafter stacking gel was poured onto the separating gel and a 22-well comb was added prior to polymerisation and left to set for at least 1 hour. Gel electrophoresis was carried out at 180 to 240 V in 1 × Laemmli buffer. Before loading, the protein samples were mixed with one-third its volume of 4 × SDS-PAGE loading buffer and denatured for 5 minutes at 90 °C. The separated proteins were then visualized by silver staining or Coomassie stain of the gel or subjected for a Western blot analysis.

3% Stacking gel:	1.2 ml	40 % (w/v) Acrylamide:Bisacrilamide solution
	2 ml	4 x SDS-Stacking gel buffer
	120 µl	6 % APS (w/v)
	12 µl	TEMED
	add 16 ml	ddH_2O

12% Separation gel:	7.5 ml	40 % (w/v) Acrylamide:Bisacrilamide solution
	6.25 ml	4x SDS-Separation buffer
	200 µl	6% APS (w/v)
	20 µl	TEMED
	add 25 ml	ddH_2O

3.2.11. Protein detection on SDS-PAGE

3.2.11.1. Detection of proteins in SDS-PAGE gels by silver stain

This is a very sensitive staining method which enables the detection of even small amounts of protein (below 20 ng) on a SDS-PAGE gel. After the electrophoresis, the gel was fixed in the fixing solution for 1 hour to over night to prevent the diffusion of separated proteins from the gel. The gel was washed with 50% ethanol, three times for 20 minutes. Then it was sunk in solution 1 for one minute and again rinsed three times, each for about 20 seconds, with deionized (DI) water. The incubation was carried out in solution 2 for 20 minutes at room temperature. After the washing with DI water for three times for 20 sec, solution 3 was added for the development of bands. The development of the bands was reached the desired intensity; the reaction was stopped by adding of acetic acid. The gel was rinsed with water and scanned for documentation.

Fixing solution:	50%	Methanol
	12%	Acetic acid
	500 µl/l	37% Formaldehyde (prior to use)
Solution 1:	0.1 g	$Na_2S_2O_3$ x 5 H_2O
	add 500 ml	ddH_2O
Solution 2:	0.4 g	$AgNO_3$

	add 250 ml	ddH_2O
	187.5 µl	37% Formaldehyde (prior to use)
Solution 3:	15 g	Na_2CO_3
	5 ml	Solution 1
	add 250 ml	ddH_2O
	125 µl	37% Formaldehyde (prior to use)

.

3.2.11.2. Detection of proteins in SDS-PAGE gels by Coomassie stain

To visualize proteins after SDS-PAGE, gels were stained in Coomassie stain. The gel was dipped in the staining solution for 30 min at room temperature on a shaker (80 rpm). Gels were destained with destaining solution and then with water, using several changes of solution until the background staining was greatly reduced. The gels were scanned for documentation.

Coomassie blue stain	50% (w/v)	Water
	40% (w/v)	Methanol
	10% (w/v)	Acetic acid
	0.2% (w/v)	Coomassie Brilliant Blue (G-250)
Coomassie destain solution	20%	Methanol
	10%	Acetic acid
	70%	Water

3.2.12. Mass spectrometry for protein identification

Identification of proteins in silver stained SDS-PAGE gels were performed by mass spectrometry analysis in the lab of Prof. Dr. Günter Lochnit, Biochemistry institute, University of Giessen.

3.2.13. Western blot analysis

For this purpose, at first a SDS-PAGE was performed as described under 3.2.10.3. Protein gels were assembled into a gel-membrane sandwich. Nitrocellulose membrane (or PVDF membrane) was placed on the gel, and this assembly was placed between three pieces of filter paper (3 mm), and all were piled up over one another. All components were pre-soaked in transfer buffer (PVDF membrane was activated by soaking it in 96% ethanol for 1 min and then washing with water and then with the transfer buffer). This assembly was loaded into a blotter, and proteins were transferred at 1-2 mA/cm^2 for at least 1 hour and 20 min.

Nonspecific bindings on the membranes were saturated by incubation with a blocking solution (5% fat-free milk powder in TBS) for 1 h at room temperature. Thereafter the membrane was washed with TBS buffer for 10 min. Primary antibodies were diluted (DnaG antibody, 1:500, Rrp41 antibody 1:1000, Rrp4 antibody, 1: 2000, Csl4 antibody, 1: 1000) in TBS buffer and incubated for 3 hours at room temperature. Membranes were washed with TBS buffer for 3 times at room temperature for 10 min and incubated with secondary antibodies conjugated to alkaline phosphatase for one hour on the tumbler at room temperature (secondary antibody was diluted at 1:10000 dilutions in TBS buffer).

After washing for 3 times with TBS buffer for 10 min, membranes were developed with enhanced chemiluminescence reagent (ECL). To detect secondary antibodies bound to primary antibody, ECL reagents 1 and 2 were mixed in equal volumes and 1 ml of this mix was added to each blot for 1 min. The membrane was then placed in a clean piece of polythene roll. The membrane was then exposed to Medical X-Ray film and developed or the membrane was exposed to Fusion SL4 chemiluminescence detection machine to detect the chemiluminescence. The produced luminescence can be then recorded using a corresponding detection system (Fusion SL4 software).

3.2.14. RNA assys

3.2.14.1. *In vitro* RNA degradation assay and polyadenylation assay

Degradation and polyadenylation assays using the reconstituted exosomal complexes were carried out with a 5’ end-labeled 30-meric poly (A) substrate in the presence of inorganic phosphate and ATP, respectively, and incubated at 60 °C. As a control instead of the protein complex double distilled water or the reaction buffer was used under the same reaction

conditions. The assays with proteins bound to the protein A-Sepharose beads were done as described in [95]. The salt concentration in the reaction mixtures was adjusted to 150 mM NaCl. Yeast tRNA or a 30-meric MCS-RNA was used as competitors. To stop the reactions, (1:1) formamide: urea buffer (1:1) was added immediately. The mixture was heated for 10 min at 65 °C and then it was loaded on an 18% denaturing urea-polyacrylamide gel for the separation. 1,000 cpm RNA substrate was used per reaction.

Degradation assay reaction:

1 µl	RNA-Substrate (6-90 fmol, 1.000 cpm/µl)
2 µl	5 x degradation-buffer
1 µl	10 mM K_2HPO_4
60 ng/each polypeptide	Exosome-complex
add 10 µl	ddH_2O

Polyadenylation assay reaction:

1 µl	RNA-Substrate (6-90 fmol, 1.000 cpm/µl)
2 µl	5 x Polyadenylation buffer
1 µl	10 mM ADP
60 ng/each polypeptide	Exosome-complex
add 10 µl	ddH_2O

3.2.14.2. Phospho imaging

The Phospho imaging method is used for the detection of radioactively labeled samples by exposure of gels to phosphoimager screens. In these specific screens BaFBr:Eu crystals are embedded, which are excited by radioactive radiation. By irradiation with a He/Ne laser (Imager FX from BioRad) at 600 nm wavelength, the latent image was developed, which was stored by the excited BaFBr:Eu crystals in the optical disk. The result is a photo stimulated luminescence, which can be registered by a photomultiplier. With the appropriate software (Bio-Rad Quantity One) the visualized bands were evaluated quantitatively.

3.3. Single particle electron microscopy

3.3.1. Negative-stain EM sample preparation and data collection

The protein complexes were applied to glow-discharged holey carbon grids with a thin layer of carbon over the holes. After 1 min, grids were stained consecutively in 3 droplets of 2% (w/v) uranyl formate solution and excess stain removed by blotting with filter paper. Negative staining and sophisticated computer programs such as spider and Imagic software were used to sort images into classes and average them. Prof Tomas Walz (Harvard University, Boston, USA) and Dr. Janet Vonck (Max Planck Institute for Biophysics, Germany) kindly helped us in single particle EM to determine the structure of the complex from images of individual particles or single particle projections.

4. Results

4.1. Heterogeneous complexes of the RNA exosome in *Sulfolobus solfataricus*

The structure and the function of the nine subunit exosome of Archaea are well understood. Nevertheless little is known about the regulation of the functions of the exosome *in vivo*. It was found that the exosomes are localized in the periphery of the *S. solfataricus* cells [110]. Thus, the archaeal exosome may be localized due to the need of prokaryotic cells to spatially organize RNA processing and degradation. Furthermore it was also found that there is a minor amount of exosomes in the soluble fraction, in which DnaG protein was not detected [110]. It is very important to know whether the compositions of the soluble and insoluble exosomes differ because the composition may directly influence its substrate specificity, the interaction with other proteins and even its sub-cellular localization.

An aim of this work was to analyze the composition of the soluble and the insoluble exosomes.

4.1.1. Differences in the composition of the soluble and the insoluble exosomes

In the sucrose density gradients DnaG subunit was only found in the high density fractions while Rrp41, partly in the low density fractions and majority in the high density fractions. Furthermore the active subunit Rrp41 was mainly in the P100 fraction while DnaG was exclusively detected in the P100 fraction [110]. These findings raised the question whether there are different compositions of the exosome in the soluble (S100) and insoluble (P100) fractions.

To answer this, first of all, polyclonal antibodies were raised against recombinant His-tagged, Rrp4 and Csl4 proteins of *S. solfataricus.* The antibodies against DnaG and Rrp41 were available in the lab. Then DnaG, Rrp41, Rrp4 and Csl4 were detected in quantitative Western blot analyses of the S100 and P100 fractions. In three independent experiments, 21±3% of Rrp4 and 23 ±3% of Rrp41 were detected in the S100 fraction. In contrast, Csl4 and DnaG were detected in the P100 fraction only (Figure 4.1.1A). However, the sensitivity of the anti-Csl4 and anti-DnaG antibodies were lesser than the sensitivity of the antibodies directed against Rrp41 and Rrp4. This result does not necessarily imply the different subunit contents

of the soluble and the insoluble exosomes, but confirms that the majority of the exosome is insoluble.

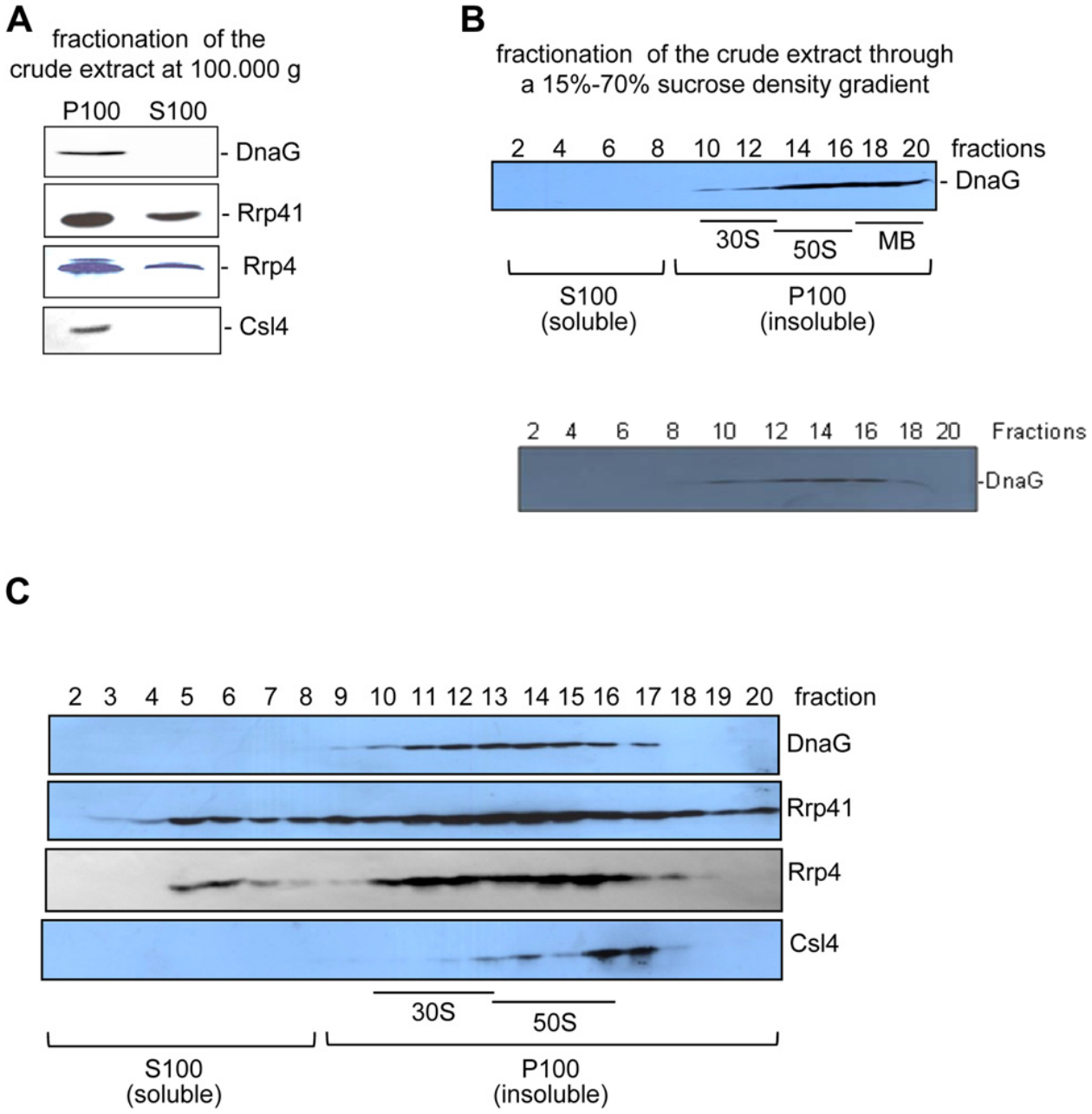

Figure 4.1.1 Detection of DnaG, Rrp41, Rrp4 and Csl4 in fractions of the *S. solfataricus* cell-free extract by Western blot analysis. A) Western blot analysis of S100 and P100 fractions. Equal volume amounts of the S100 and the P100 fractions were separated in 12% SDS-PAGE, blotted and hybridized with sera directed against the exosomal subunits indicated on the right side of the panels. B) Top panel- Schematical representation of the sedimentation of the small (30S) and large (50S) ribosomal subunits, and of membranes (MB) with surface layer proteins in fractions of a sucrose density gradient with 500 mM salt. Shown is also the relationship

between sucrose density gradient fractions and S100 and P100 fractions. The sedimentation of the exosome is shown on the example of DnaG detected by Western blotting of selected fractions. The sedimentation of the exosome is in the 18th fraction as in the published result by [110]. Fractionated was the crude extract. Bottom panel- The sedimentation of the exosome is in the 12-16 fractions. This was the most recurrent result in my work. C) The cell-free extract was subjected to low speed centrifugation to remove the membranes with the surface layer proteins and the associated exosome. The supernatant was fractionated through the sucrose density gradient and the fractions were analyzed for the presence of DnaG, Rrp41, Rrp4 and Csl4 by Western blot hybridization. The analyzed fractions are given above the panels, the detected proteins are marked on the right side. The relationship between density gradient fractions, S100 and P100, and the sedimentation of the ribosomal subunits is given below the panels.

To see the composition of the soluble and insoluble fractions of the exosome, Co-IP was attempted. Co-IPs were performed with the S100 and the P100 fractions with beads coupled to anti-Rrp41 antibody. However, it was not possible to immunoprecipitate the exosome from the P100 fraction due to less solubility (it formed clumps which were difficult to dissolve). In order to compare the exosomal complexes corresponding to the S100 and P100 fractions, fractionation of the cell free extract was done in 15-70% sucrose density gradients (4.1.1B and C). The fractions were analysed by SDS-PAGE and Western blot hybridization with anti-DnaG, anti-Rrp41, anti-Rrp4 and anti-Csl4 antibodies. It was expected that the exosome should co-sediment with the membrane fractions (18th and 19th fractions) in the sucrose density gradients [110]. I could not observe the highest amount of sedimentation of the exosome with the membrane fractions constantly. Only one of the ten attempts was successful to reproduce the published results (Figure 4.1.1B-Top panel). Recurrent result was the exosome sedimentation at the 11-16 fractions (4.1.1B – Bottom panel). Consistent with previous results [110], DnaG was not detected in the low density fractions. Surprisingly Csl4 also was not detected in the low density fractions. The sedimentation of Rrp41 and Rrp4 were considerably similar: The majority was in the high density fractions and a minor part was in the low density fractions.

In the sucrose density gradient, 1-8 fractions correspond to the S100, while 9-22 fractions correspond to the P100 fraction (Figure 4.1.1C). The Co-IP was done with fraction 6 (soluble), 12 (insoluble, not with the membrane) and 19 (insoluble, with the membrane). However, the Co-IP with the 19th fraction failed. Therefore we compared the results from the

Co-IP from fraction 6 and 12 (Figure 4.1.2). This Co-IP was done by Verena Roppelt. Interestingly there was a protein which was co-immunoprecipitated with the soluble exosome which was identified by mass spectrometry as EF1α. Furthermore the proportion of DnaG was lesser in comparison to the hexameric ring in the soluble exosome and the proportion was higher in comparison to the hexameric ring in the insoluble exosome (compare Figure 4.1.2A and B). The identity of DnaG was also confirmed by mass spectrometry.

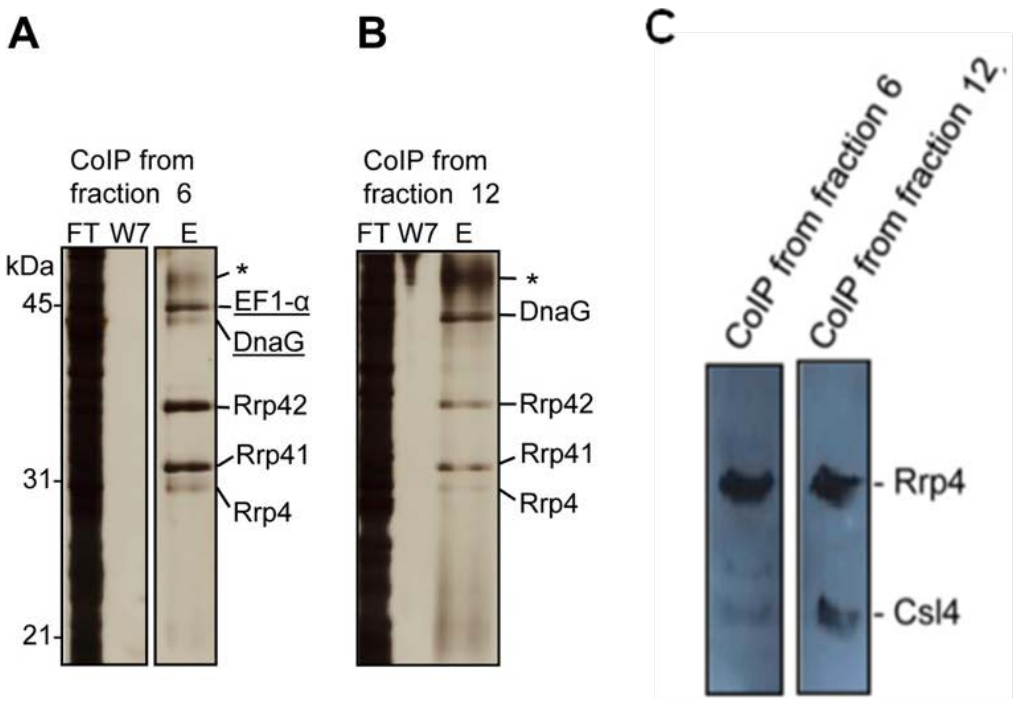

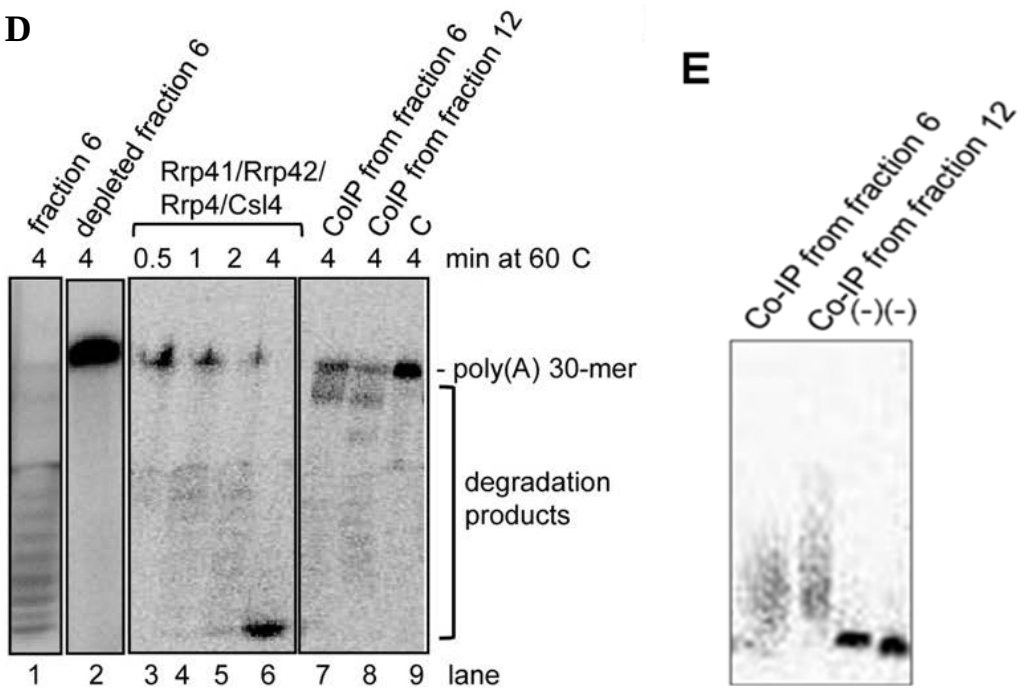

Figure 4.1.2 Exosomal complexes with different sedimentation behaviours are active and differ in their composition. A) and B) Silver stained SDS-gels showing proteins purified by Co-IP with Rrp41-specific antibodies from different sucrose density gradient fractions. The Co-IP was done by Verena Roppelt. A) The soluble exosome was purified from fraction 6. B) The insoluble exosome was purified from fraction 12. FT, flow-through; W7, last, seventh washing fraction; E, elution fraction. The migration of marker proteins is marked (in kDa). Underlined proteins were identified by mass spectrometry, bands with known migration behaviour are marked with the names of the respective proteins. The band corresponding to antibodies is marked with an asterisk. C) Western blot analysis of the elution fractions shown in A) and B). To estimate the relative amounts of Csl4 and Rrp4, the membranes were hybridized simultaneously with Csl4- and Rrp4-directed antibodies. The detected proteins are marked on the right side. D) Phosphorimages of degradation assays with fraction 6 (lane 1), depleted fraction 6 (the flow-through after three rounds of immunoprecipitation of the exosome with Rrp41-specific antibodies lane 2 [95]), exosomes reconstituted by mixing of equimolar amounts of Rrp41, Rrp42 and the RNA-binding proteins Rrp4 and Csl4 (lanes 3-6), the co-immunoprecipitated exosome from fraction 6 (lane 7), the co-immunoprecipitated exosome from fraction 12 (lane 8), and water (negative control C, lane 9), as indicated above the panels. The incubation time in minutes (min) is also indicated. The 5'-labelled 30-meric poly (A) RNA and the degradation products are marked on the right side. E) Phosphoimages of the polyadenylation assay with the co-immunoprecipitated exosome from fraction 6 and the co-immunoprecipitated exosome from fraction 12 and water, negative control (-) as indicated above the panel.

Though Csl4 was not detectable in silver stain gels it was possible to detect it in Western blot hybridization. The relative amounts of the cap proteins, Rrp4 and Csl4 were also different in

the soluble and insoluble exosomes (Figure 4.1.2C). In relation to Rrp4, the insoluble exosome contains higher amounts of Csl4 than the soluble exosome. These results strongly suggest that the composition of the soluble and the insoluble exosomes is different.

Then I wanted to investigate the functional relevance of the soluble and insoluble exosomes. For that, I performed an activity assays with the co-immunoprecipitated complexes which were bound to the protein A-Sepharose beads (Figure 4.1.2D). Lane 7 and 8 show that the soluble exosome (fraction 6) and insoluble exosome (fraction12) are active. The amount of remaining substrates (poly (A) 30-mer) was lesser in lane 8 than in lane 7. We also performed polyadenylation assays with the complexes which were bound to the protein A-Sepharose beads (Figure 4.1.2E). That further proved that the soluble and the insoluble exosome complexes were active.

We confirm that the major RNA degrading nuclease in fraction 6 of the gradient is the exosome. The exosome was depleted from a portion of this fraction with three rounds of Co-IP using anti-Rrp41 antibodies. The assays were performed, using the flow though after the depletion. In lane 2 (Figure 4.1.2D), we saw that the RNA was not degraded at all. It clearly says that in that fraction the main RNA degrading nuclease is the exosome.

It is important to note that DnaG and Csl4 were not detected by Western blot analysis in the S100 fraction (Figure 4.1.1A) and in fractions of low sucrose density like fraction 6 (Figure 4.1.1C), but co-immunoprecipitated along the exosome from those fractions (Figure 4.1.2A). This means that the protein complexes with Csl4 and DnaG were under the limit of detection in the low density fractions and were enriched by the Co-IP.

4.1.2. The sedimentation properties of the exosome are independent of the ribosomal subunits

To rule out the hypothesis that DNA or RNA has an influence on the exosome sedimentation in the sucrose density gradient we treated the cell free extract with DNase I (40 units) or RNase A (40 units) and RNase T1 (40 units). The treated cell free extract was loaded onto the sucrose density gradient and centrifuged as mentioned in 3.2.8.3. Every second fraction was analysed by Western blot by hybridizing with anti-Rrp41 and with anti-DnaG antibodies. It

was not possible to see any major difference in Western blots between the standard and the treated cell free extracts (Figure 4.1.3). Following the anti-Rrp41 antibody hybridization, a signal was observed in the fractions 2-4 under the standard conditions which was not observed in the treated cell extracts. The signal at the low density fractions were not observed 50 % times out of the ten repetitions (under the limit of detection). There was no major difference between the RNA sedimentation patterns in the standard condition, DNase treated cell free extract. Nevertheless, in the sucrose density gradient with the RNase treated cell free extract, RNA sedimentation was different from the standard. Here, 30S and 50S (ribosomal subunits) peaks were not seen.

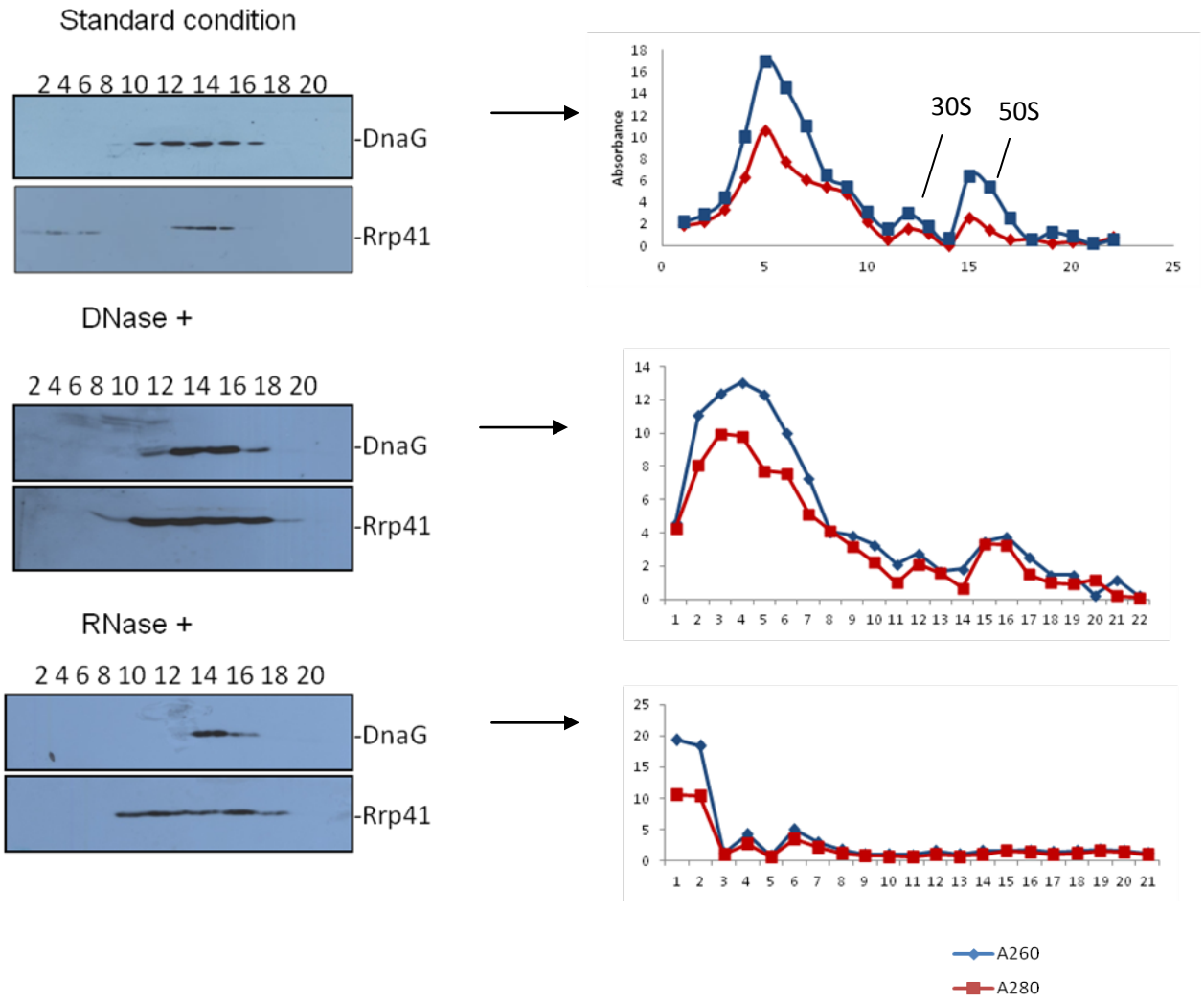

Figure 4.1.3 The effect of RNA and DNA on the sedimentation pattern of the exosome. To verify that there is no influence of RNA and DNA for the sedimentation patterns of the exosome in the sucrose density gradient, the cell free extract was treated with of DNase and RNase before loading. The sucrose density gradient was fractionized and fractions were analysed by Western blotting with anti-Rrp41 and anti-DnaG antibodies. The sedimentation pattern of RNA in the sucrose density gradient is on the right side of the Western blots.

4.1.3. The amount of soluble exosomes under different RCF (relative centrifugal forces)

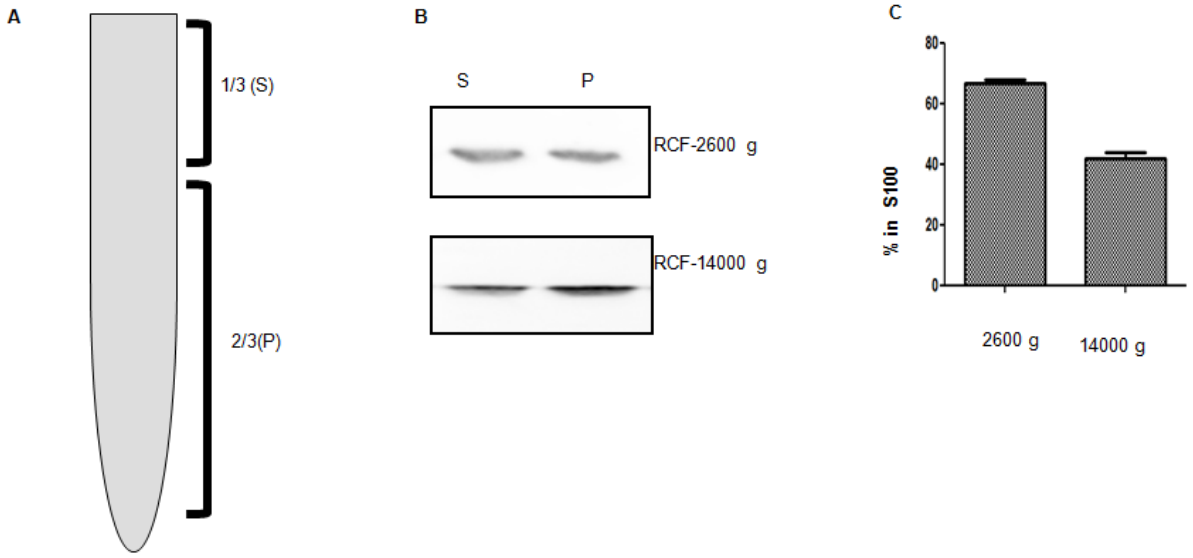

Figure 4.1.4 Western blot analysis to detect differences in solubility (S and P) of Rrp41, the catalytic subunit of the exosome, under different RCF (relative centrifugal forces). A) Cell free extract of *S. solfataricus* (OD600 ~0.4) was centrifuged in an eppendorf tube at 2600 g and 14000 g RCFs for 20 min. After centrifugation the 1/3 on the top of the eppendorf tube was separated and analysed as the supernatant fraction (S) and the rest 2/3 was analysed as the pellet fraction (P). B) Equal volume of S and P fractions were loaded on a SDS-PAGE gel for separation of the proteins and blotted and hybridized with sera directed against Rrp41. The applied RCFs are indicated on the right side of the panel. C) Graphical representations of the results from two independent experiments and two technical replicates in which the percentage of the S100 fraction is indicated in relation to the total amount of proteins (S100+P100) after centrifugation at 2600 g and 14000 g.

To elucidate whether we lose exosomes by centrifuging the cell free extract before adding to the sucrose density gradient we conducted another experiment. The cell free extract was subjected to different RCFs in eppendorf tubes and checked the whether the exosome is in the supernatant or the pellet fraction (Figure 4.1.4A) by Western blot analysis (4.1.4B). After applying different RCFs (2600 g and 14000 g) to the *S. solfataricus* cell free extract we found that increasing the RCF pulls the exosome towards the pellet fraction (Figure 4.1.4B and C).

The percentage of the exosomal subunit Rrp41 in the S100 fraction relative to the total amount of proteins (S100+P100) was 67% after centrifugation at 2600 g and 42 % at 14000 g RCFs. Thereafter we decided to add the crude extract on to the sucrose density gradient (15%-70%) without any prior centrifugation step to avoid the loss of the exosomes. Following the fractionation of the crude extract, the yellow ring where the membrane fractions sediment, was more intense. However, even after fractionation of the crude extract, the exosome sedimentation pattern in the sucrose density gradient was not as previously published [108], but it was in the fractions 12-16 fractions (Figure 4.1.1.B- bottom panel).

4.1.3. DnaG is an integral part of the soluble exosome

To verify the interaction of EF1α with the exosome, another experiment was conducted. The exosome was co-immunoprecipitated from the S100 fraction using anti-DnaG antibodies. The fished exosome contained the expected exosomal subunits, Rrp41, Rrp42, Rrp4, Csl4 and additionally, EF1α. The identity of DnaG and EF1α was confirmed by mass spectrometry (Figure 4.1.5A) (Appendix 1).

To find out whether only a part of the soluble exosomes contains DnaG, depletion assays were conducted. If the hypothesis was correct, it should be possible to deplete the DnaG containing exosome from the soluble exosome pool. Three rounds of Co-IPs were carried out with beads coupled to anti-DnaG antibodies to deplete DnaG containing exosomes (4.1.5A) and the remaining exosome was fished with Co-IP using beads coupled to anti-Rrp41 antibodies (4.1.5B). We were able to see the decrease of the signal of the Rrp41 in the flow through in sequential rounds of Co-IP by Western blot analysis (Figure 4.1.5C). However, in the remaining exosome, the presence of Csl4 and DnaG was detectable by SDS-PAGE and silver staining and was confirmed by mass spectrometry. This strongly suggests that DnaG and Csl4 are integral parts of the soluble exosome. Surprisingly, EF1α was co-immunoprecipitated with the rest of the exosomal subunits from the S100 fraction using anti-DnaG antibodies. The identity of EF1α and DnaG were confirmed by mass spectrometry (Appendix1). EF1α was not present in the remaining exosome after depletion; instead there was TIP49 protein (same migration pattern as EF1α). This indicates that EF1α was already removed with the exosome during the depletion with the anti-DnaG antibodies. EF1α and TIP49 were not found in the control experiments with the pre-immune serum (4.1.5D).

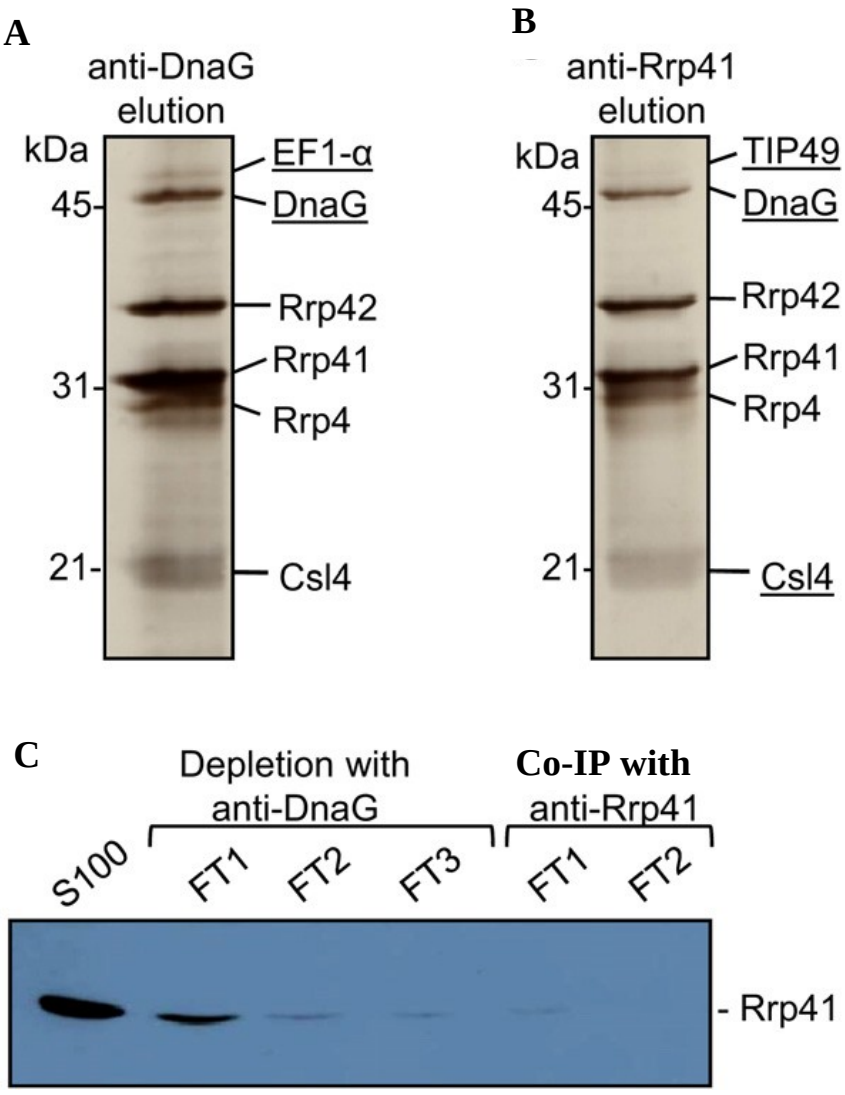
A
anti-DnaG
elution
kDa
45
31
21
EF1-α
DnaG
Rrp42
Rrp41
Rrp4
Csl4
B
anti-Rrp41
elution
kDa
45
31
21
TIP49
DnaG
Rrp42
Rrp41
Rrp4
Csl4
C
Depletion with
anti-DnaG
Co-IP with
anti-Rrp41
S100
FT1
FT2
FT3
FT1
FT2
- Rrp41

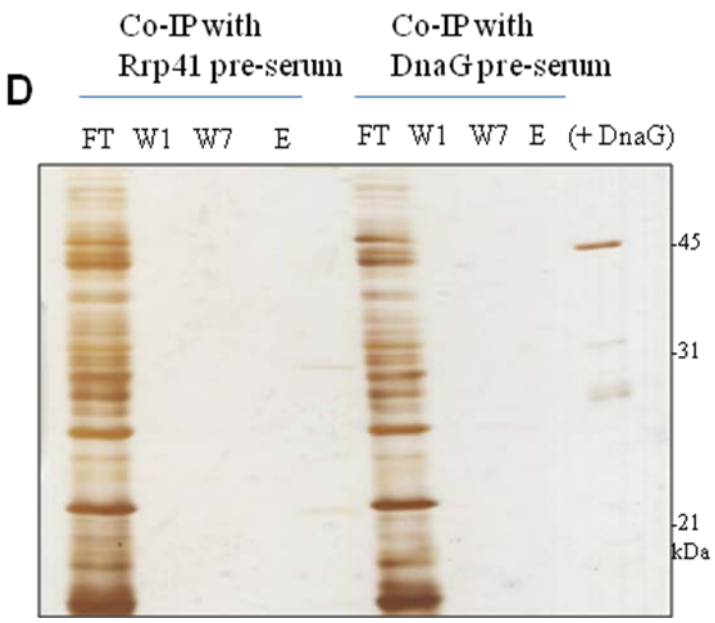

Figure 4.1.5. **Co-immunoprecipitation (Co-IP) of EF1α with the soluble exosome using DnaG-specific antibodies**. The S100 fraction was subjected to three rounds of Co-IP with anti-DnaG antibodies. Subsequently, two rounds of CoIP with anti-Rrp41 antibodies were performed. A) Silver stained SDS-gels showing the proteins, which were co-precipitated during the first Co-IP round with anti-DnaG antibodies B) Silver stained SDS-gels showing the proteins, which were co-precipitated during the first Co-IP round with anti-Rrp41antibodies. C) Western blot analysis of the flow-through fractions (FT) after each Co-IP round. The antibodies used for Co-IP are marked above the panels. The FT fractions (depleted S100) were separated on a 12% SDS-PAGE and hybridized with anti-Rrp41antibodies. The detected Rrp41 is marked on the right side of the panel. D) Co-IPs with Rrp41 and DnaG pre-immune serum using S100 fraction was performed as a control experiment. (+DnaG), DnaG purified protein was added in order to locate the position of the DnaG, and EF1α.

4.2. The RNA binding cap of archaeal exosome

The RNA binding cap of the exosome plays a major role, in regard to the function of the exosome. The function of the cap proteins in the recombinant exosome have been investigated in *Sulfolobus, Pyrococcus* and *Archaeoglobus.* In general, in the presence of the RNA binding cap proteins, the efficiency of the RNA degradation and polyadenylation is higher. Recently it was shown that Rrp4 and Csl4 confer different substrate specificities and that Rrp4 strongly prefers poly (A) [88]. In addition, it is known that the KH domain has less RNA affinity compared to the S1 domain in *E. coli*- PNPase which has structural and functional similarities to the archaeal exosome. Furthermore S1 domain of the PNPase in chloroplast is responsible for the poly (A) specificity [39], [114], [115]. Nonetheless we do not know which domain of the Rrp4 protein in the archaeal exosome is responsible for this RNA specificity.

Even though it was shown that *in vitro* the reconstituted exosome of *Archaeoglobus fulgidus* can carry a heteromeric cap containing Rrp4 and Csl4 [93], the cap composition of the archaeal exosome was not studied *in vivo* so far.

An important goal of this work was to investigate whether heteromeric caps exist *in vivo*. Additionally an aim of this study was to investigate the contribution of the individual Rrp4 domains to its poly (A) preference.

4.2.1. The KH domain of Rrp4 is not responsible for poly (A) preference but is necessary for efficient RNA degradation

4.2.1.1. Reconstitution of the exosome with truncated Rrp4

The exosomal RNA binding protein Rrp4 confers a strong poly (A) affinity to the *S. solfataricus* exosome [88]. Nevertheless the mechanism of this poly (A) preference and the contribution of the individual domains of Rrp4 for poly (A) preference were not known. Rrp4 protein has three domains, an N terminal domain, a S1 domain and a KH domain which is at the C terminus (2.8.1.1.). The individual domains (Nl, S1 and KH) or truncated versions lacking either N terminal or the C terminal domains (ΔNT or ΔKH respectively) were cloned in *E. coli* with a His-tag, overexpressed and purified under native conditions by Ni-NTA chromatography (3.2.3.1.) Exosomes were reconstituted with Rrp41, Rrp42 and with either of

the truncated Rrp4 polypeptides (3.2.6.). First it was necessary to test whether the truncated proteins interact with the hexameric ring. The hexameric ring was reconstituted as mentioned in 3.2.6.1. and then the truncated protein was added in excess amounts (3.2.6.). Co-IP was performed with anti-Rrp41 antibodies. The complexes were eluted with 40 µl of elution buffer and the whole elution fraction was loaded on to a SDS-PAGE gel and analyzed by silver stain. Unfortunately, under standard conditions (150 mM NaCl) none of the truncated proteins except the ΔKH variant interacted with the hexameric ring (4.2.1A). However, the interaction between the hexamer and the ΔKH variant was very weak in comparison to the control experiment done with the full length Rrp4 protein (compare 4.2.1A and B). Usually the Rrp41:Rrp42:Rrp4 stoichiometry is 1:1:1. In a previous work it was shown that under high ionic strength (1 M $MgCl_2$ and up to 2 M NaCl) it was not possible to separate the reconstituted exosome in to individual subunits [116]. Therefore the NaCl concentration was increased up to 500 mM. The cap proteins interact with the ring via hydrophobic interaction [93]. Under higher ionic strength, hydrophobic interactions are forced and we expected that the truncated proteins will interact with the hexameric ring. Out of all the variants only the ΔKH truncated protein was able to interact with the hexameric ring successfully to form the ΔKH-Rrp4-exosome at high salt (4.2.1C). However, in the standard buffers for degradation and polyadenylation assays, the concentration of the salt is 60 mM and the reconstituted exosome is active at salt concentrations up to 300 mM [105]. Therefore it was necessary to test whether the ΔKH-Rrp4-exosome is still stable under salt concentration suitable for activity assays. After the reconstitution of the exosome under high salt (500 mM NaCl) Co-IP was performed with anti-Rrp41 antibodies. Prior to elution, the beads were washed with 150 mM NaCl containing washing buffer. The elution buffer also contained 150 mM NaCl. The elution fractions were separated in a SDS-PAGE gel and analyzed by silver staining. Figure 4.2.1D shows that, when the ΔKH-Rrp4-exosome was reconstituted at 500 mM NaCl, the protein complex was stable even though the complexes were washed with low salt (150 mM NaCl) buffer (4.2.1D).

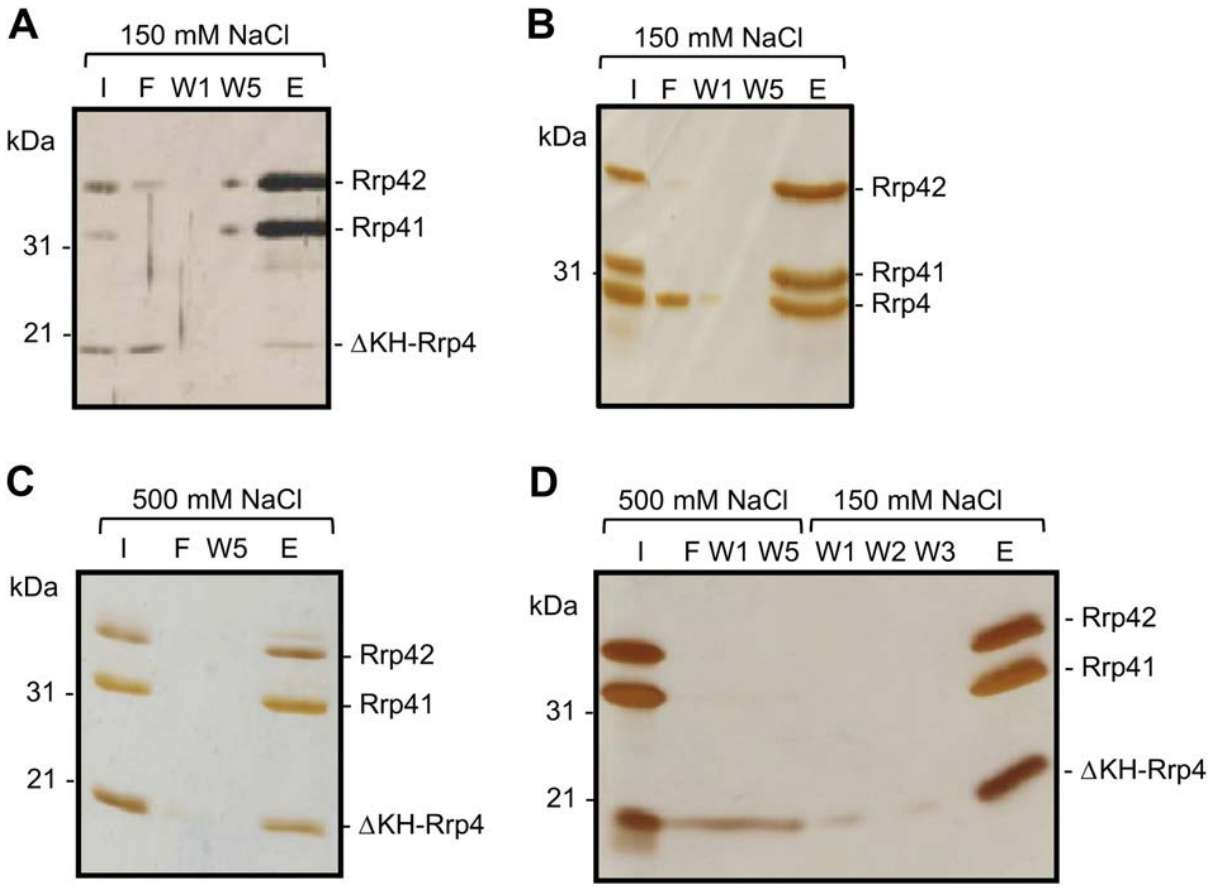

Figure 4.2.1. Reconstitution of the ΔKH-Rrp4-exosome. Silver stained SDS-PAGE gels showing detection of protein-protein interactions by co-immunoprecipitation with Rrp41-specific antibodies. I, input; F, flow through, W1, W5, washing fractions 1 and 5; E, elution fraction. The NaCl content of the buffers is shown above the panels. The detected proteins are marked on the right side of the panels, the migration of protein markers (in kDa) in the gel is indicated on the left side. A) An attempt to reconstitute the ΔKH-Rrp4-exosome at 150 mM NaCl. B) Control reconstitution of the Rrp4-exosome at 150 mM NaCl. C) Successful reconstitution of the ΔKH-Rrp4-exosome at 500 mM NaCl. D) The reconstituted ΔKHRrp4- exosome is stable at 150 mM NaCl.

4.2.1.2. Activity assays

The comparison of the degradation and the polyadenylation assays with the reconstituted Rrp4-exososme and the ΔKH-Rrp4-exosome were done in the presence of 150 mM NaCl with the radioactively labeled poly (A) 30-mer. In line with the previously published results, the nine-subunit Rrp4-exosome was very efficient in degradation, leading to the fast disappearance of the substrate band and the accumulation of the final degradation product, while the hexamer performed this step less efficiently: The substrate disappeared but we did

not observe the accumulation of the final products [105] (Figure 4.2.2A, compare lanes FL and H). The ΔKH-Rrp4-exosome suppressed the degradation. The substrates were was not fully degraded after 4 min of incubation time. The degradation activity of the ΔKH-Rrp4-exosome was lower than the degradation activity of the Rrp41-Rrp42 hexamer and the Rrp4-exosome (compare the lane ΔKH to the lanes FL and H in Figure 4.2.2A).

Furthermore the polyadenylation efficiency of ΔKH-Rrp4-exosome was similar to that of the hexameric ring. Rrp4-exosome had higher polyadenylation efficiency than the ΔKH-Rrp4-exosome and the hexameric ring (Figure 4.2.2B). The ΔKH polypeptide does not appear to enhance the RNA degradation or the polyadenylation activity of the hexamer like the full length Rrp4 protein.

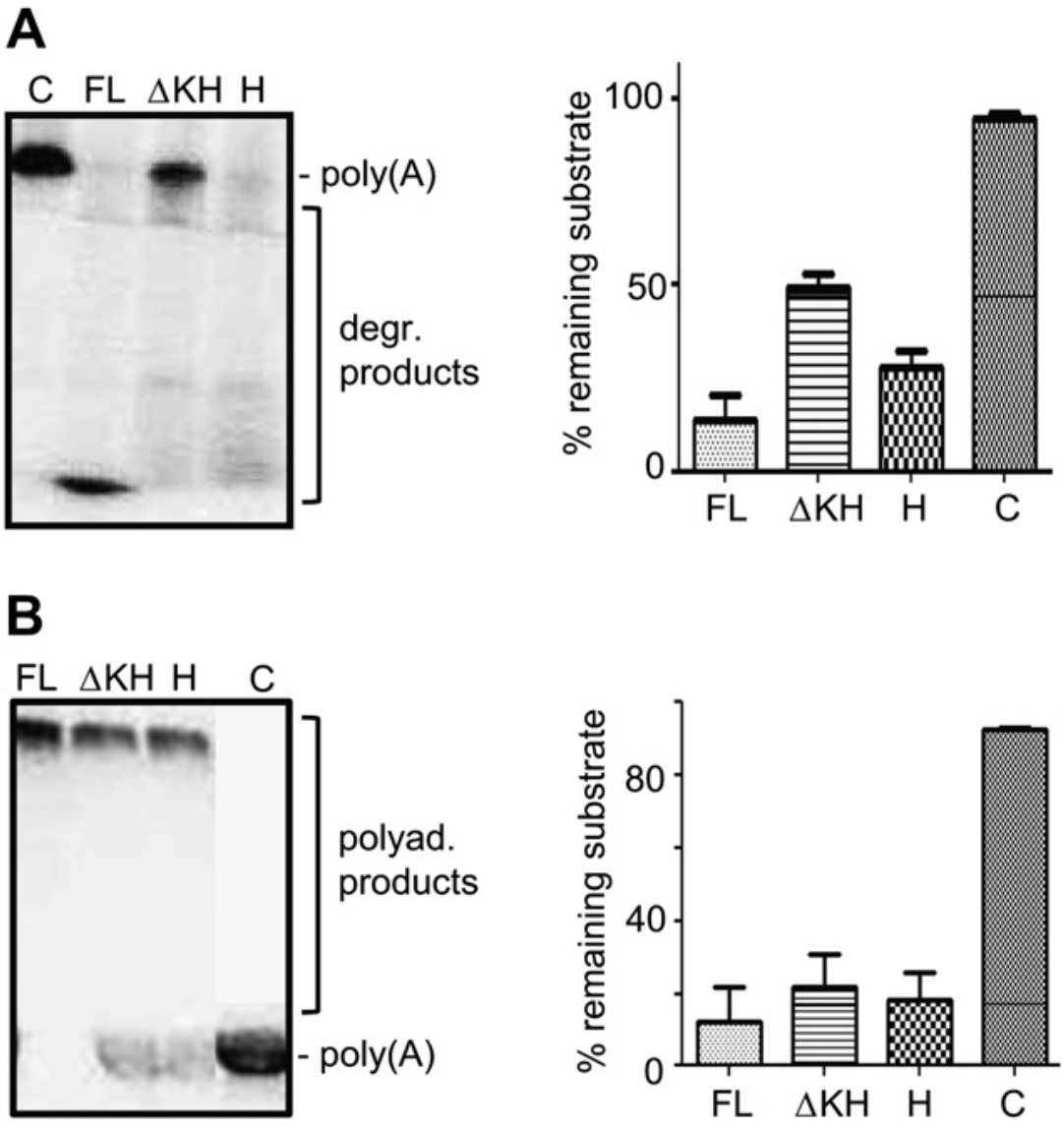

Figure 4.2.2. Comparison of the degradation and the polyadenylation activities of the ΔKH-Rrp4-exosome, the Rrp4-exosome and the hexameric ring. A) Degradation assays. B) Polyadenylation assays. Shown are representative phosphorimages of denaturing polyacrylamide gels with resolved radioactively labelled substrate (30-meric poly(A) and degradation (degr.) or polyadenylation (polyad.) products, and graphical representations of the results from three experiments, in which independently purified ΔKH-Rrp4 proteins were tested. The used protein complexes are indicated: exosome with full-length Rrp4 (FL), exosome with ΔKH-Rrp4 (ΔKH) and hexameric ring (H). C, control reaction without protein. In each reaction 8 fmol substrate was incubated with 0.6 pmol of the respective protein complex for 4 min (degradation assays) or for 2 min (polyadenylation assays) at 60 °C.

To analyze whether the KH domain is important for the poly (A) preference, competition assays were conducted with radioactively labeled poly (A) and over excess amounts of non labeled tRNA. In the degradation assays the ΔKH-Rrp4-exosome clearly conferred a poly (A) preference in comparison to the hexamer (4.2.3A). Furthermore, the poly (A) preference was slightly lesser than the Rrp4-exosome. The results were confirmed by the polyadenylation competition assays. Irrespective to the over excess amounts of tRNA, the ΔKH-Rrp4-exosome preferably polyadenylated the lesser amount of the poly (A) RNA (4.2.3B). The efficiency of the polyadenylation of the labeled poly (A) RNA in competition with the enormous amount of tRNA was lesser with the ΔKH-Rrp4-exosome compared with the Rrp4-exosome. The hexameric ring did not show any poly (A) preference in the degradation and the polyadenylation assays. In comparison to the poly (A) 30-mer, tRNA is a longer and highly structured molecule. Therefore the competition assay was performed with a short heteropolymeric RNA, 30-meric MCS-RNA [88]. The Rrp4-exosome and the ΔKH-Rrp4-exosome preferably polyadenylated the RNA, which confirms the poly (A) specificity of the ΔKH-Rrp4 variant (4.2.3C). However, the efficiency of the ΔKH-Rrp4-exosome was lesser than the Rrp4-exosome. These results show that the KH domain of Rrp4 is not necessary for the poly (A) preference.

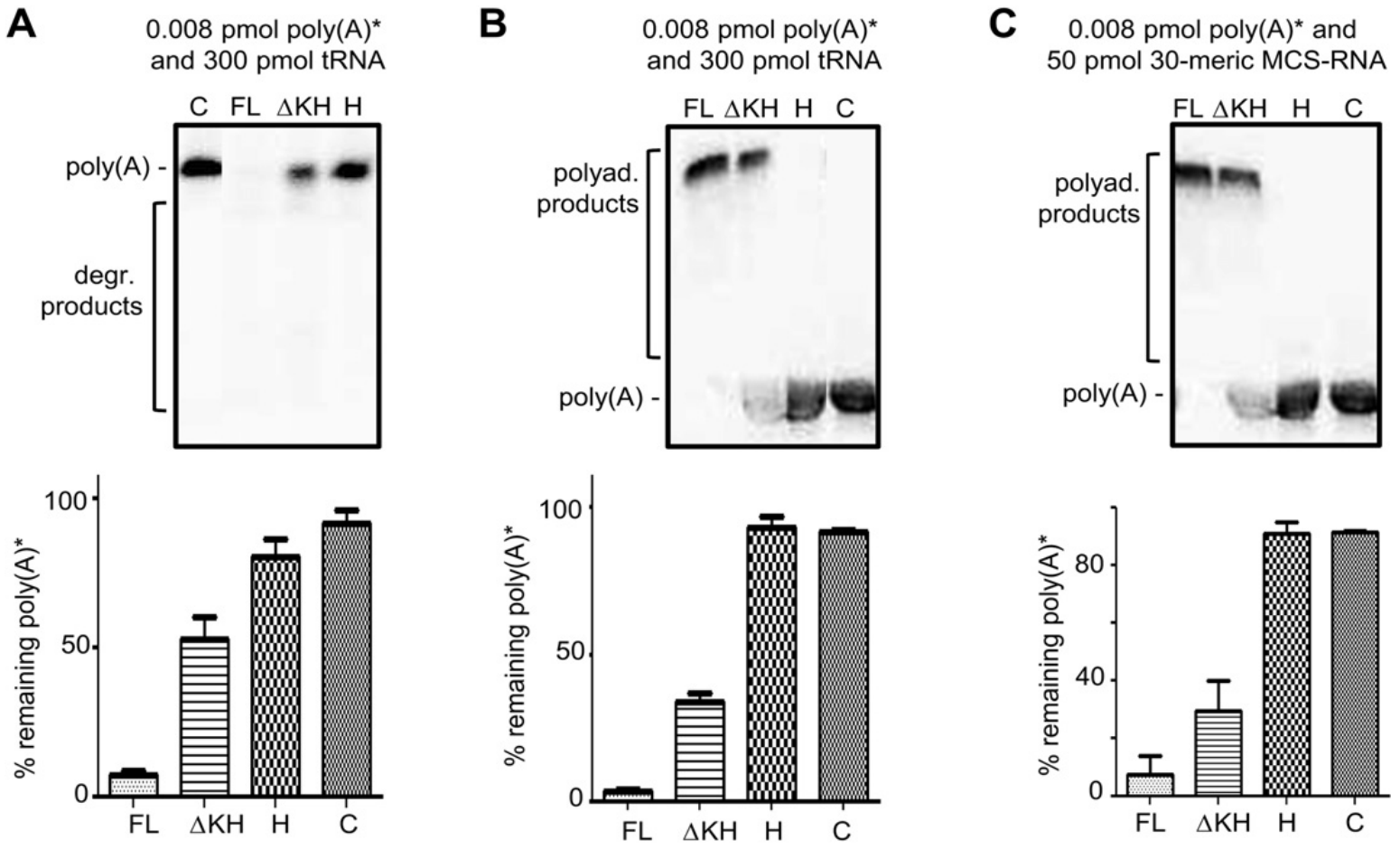
A
0.008 pmol poly(A)*
and 300 pmol tRNA
C FL ΔKH H
poly(A) -
degr.
products
% remaining poly(A)*
100
50
0
FL ΔKH H C
B
0.008 pmol poly(A)*
and 300 pmol tRNA
FL ΔKH H C
polyad.
products
poly(A) -
% remaining poly(A)*
100
50
0
FL ΔKH H C
C
0.008 pmol poly(A)* and
50 pmol 30-meric MCS-RNA
FL ΔKH H C
polyad.
products
poly(A) -
% remaining poly(A)*
80
40
0
FL ΔKH H C

Figure 4.2.3. Competition assays for comparison of the poly(A) specificities of the ΔKH-Rrp4-exosome, the Rrp4-exosome and the hexameric ring. In each competition assay, 0.6 pmol protein complex, 0.008 pmol labelled poly(A) RNA and an excess of non-labelled competitor RNA were incubated for 4 min (degradation assays) or for 2 min (polyadenylation assays) at 60 °C. A) Degradation assays in presence of 300 pmol non-labelled tRNA. B) Polyadenylation assays in presence of 300 pmol non-labelled tRNA. C) Polyadenylation assays in presence of 50 pmol 30-meric MCS-RNA. Shown are representative phosporimages and graphical representations of the results from three independent experiments.

4.2.2. Rrp4 and Csl4 form heteromeric RNA-binding caps *in vivo*

It was shown that exosomes of *A. fulgidus* can be reconstituted with heteromeric caps (Rrp4-Csl4-exosome) *in vitro* [93]. Nevertheless it was not investigated whether these heteromeric caps containing Rrp4 and Csl4 exist in Archaea, *in vivo*. Co-IPs were performed with anti-Rrp4 antibodies and anti-Csl4 antibodies with the cell free extract of *S. solfataricus* and the S100 fractions. Figure 4.2.4A and B show the elution fractions of the Co-IPs performed with anti-Rrp4 and anti-Csl4 antibodies with the cell free extract and the S100 fraction respectively. The presence of Rrp4 and Csl4 proteins in the co-purified exosome with anti-Rrp4 and anti-Csl4 antibodies were identified by mass spectrometry and Western blot analysis (Appendix 1, and Figure 4.2.4C). Figure 4.2.4 shows that when Co-IP was done with anti-Csl4 antibodies, Rrp4 was fished out with the rest of the exosomal subunits and vice verse. It is important to note that the proportion of Csl4 was higher in the Co-IP performed with anti-Csl4 antibodies than in the Co-IP performed with anti-Rrp4 antibodies. Rrp4 and Csl4 were not found in the control experiments with the pre-immune serum (4.2.4D). Figure 4.2.4 further shows that different relative amounts of Rrp4 and Csl4 are immunoprecipitated from the S100 fraction when the two different antibodies were used suggesting cap composition differs in the soluble exosome.

To exclude the possibility of the existence of free monomers of Rrp4 or Csl4, we analyzed the pooled fractions 1 and 2 of the sucrose density gradient Co-IP. It was not possible to precipitate Rrp4 or Csl4 monomers using the anti-Rrp4 or anti-Csl4 antibodies. This clearly shows that Rrp4 and Csl4 do not exist as monomers in the cell. Thus the Csl4 and Rrp4 which were co-immunoprecipitated in Figure 4.2.4A and B are parts of the exosome. Therefore we conclude that exosomes with heterogeneous RNA-binding caps are present in the soluble fraction of *S. solfataricus*.

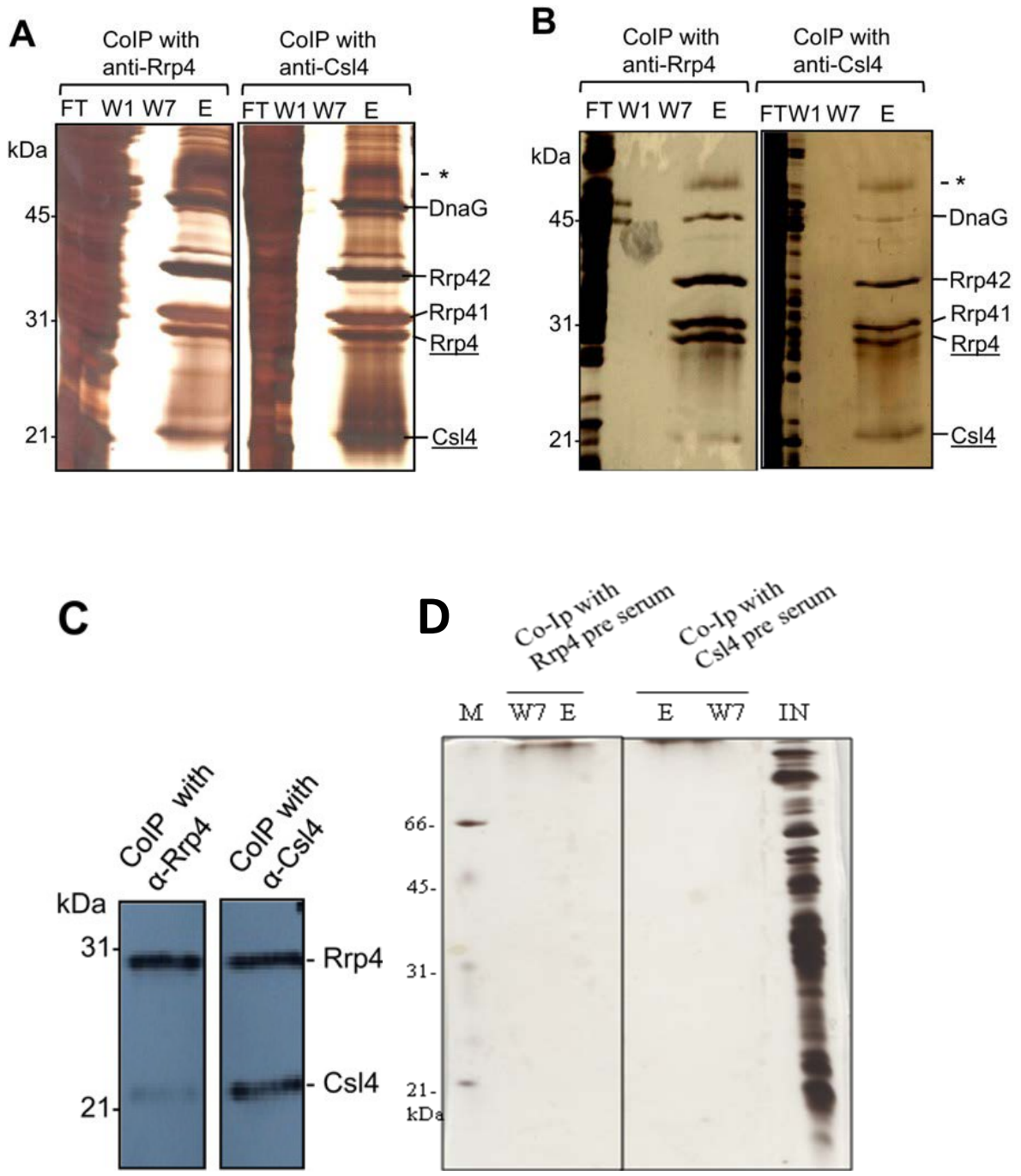

Figure 4.2.4 *In vivo* analysis of the RNA-binding cap of the *S. solfataricus* exosome. A), B) and D) show silver stained SDS-PAGE gels, C shows Western blot analysis. A) Co-immunoprecipitation (Co-IP) experiments with anti-Rrp4 and anti-Csl4 antibodies from a clarified cell-free extract. B) Co-IP with anti-Rrp4 and anti-Csl4 antibodies from S100 fractions. FT, flow through, W1, first washing fraction, W7, last washing fraction, E, elution fraction. C) Western blot analysis of exosomes immunoprecipitated from S100 fractions with anti-Rrp4 and anti-Csl4 antibodies (marked above the panels). To estimate the relative amounts of Csl4 and Rrp4 in the immunoprecipitated complexes, the membranes were hybridized simultaneously with Csl4- and Rrp4-directed

antibodies. The detected proteins are marked on the right side. D) Co-IPs with Rrp4 and Csl4 pre-immune serum using S100 fraction was performed as a control experiment.

4.3. The *Sulfolobus solfataricus* RNA-exosome under stress conditions

Environment influences physiology of an organism and changes occur at cellular and molecular level. In the majority of studies on the Achaea, the third domain of life, response to environmental changes have been limited to just one level of information processing, transcription. Nevertheless information on quality control pathways, RNA processing and degradation under stress conditions are lacking.

The bacterial RNases, polynucleotide phosphorylase (PNPase) and RNase R are the only exoribonucleases so far shown to be inducible under at least one stress condition, cold stress [117-119]. PNPase is essential for adaptive growth resumption of cold stress treated cells at the end of the acclimation phase [120]. Under cold stress, bacterial degradosome changes the protein composition, leading to the replacement of RNA helicase, RhlB, with another helicase, CsdA [121].

We previously found that the composition of the soluble and the insoluble exosomes differ (4.1.). Furthermore we found that DnaG is an integral part of the exosome. Nevertheless it is not known whether the exosome composition differs in different stress conditions to sustain the viability of the cell in problematical circumstances. Moreover it is important to elucidate how the archeal exosome performs under different stress conditions. In this study we examine changes in the exosome of the archaeon *S. solfataricus* to provide an insight on stress adjustments by describing whether there is any response to five different perturbations (cold, heat, pH high, pH low, and stationary phase).

4.3.1 Changes of the exosome amount under stress conditions

To study whether the total amount of the exosomal proteins change after 30 min of stress, I compared the total amount of exosomal proteins in the cell free extract before and after stress by Western blot analysis. Figure 4.3.1A shows representative growth curves of two independent experiments before applying the stress conditions of two independent experiments. The growth curves are comparable to each other. The stress was applied after 48 hours of growth for 30 min and the OD was measured. In all four cases the ODs do not decline after the stress (Figure 4.3.1B). Western blot analysis revealed that the *S. solfataricus* exosome is induced upon cold stress conditions (Figure 4.3.1C). For this analysis, signal

intensities of two fold dilutions were measured to ensure that two fold dilutions give two fold less signal intensities (Figure 4.3.1D). The amount of the exosomal proteins increased by an average of 1.5 fold after a down shift of the temperature from 75 °C to 65 °C. No marked change in the exosomal protein level was observed before and after the heat, pH high and pH low stress (Figure 4.3.1E, Appendix 2).

A

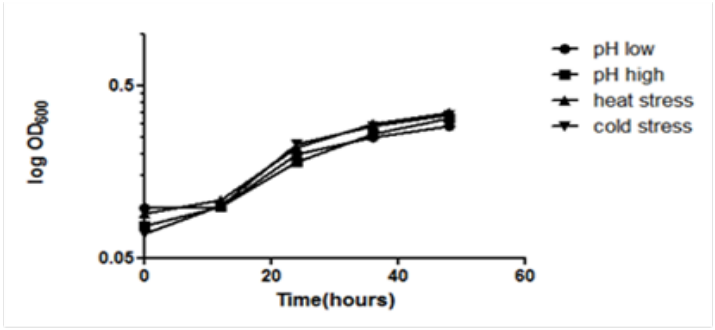

B

Stress condition	OD600 before stress	OD600 after stress
pH low	0.290	0.290
pH high	0.324	0.325
Heat stress	0.350	0.35
Cold stress	0.337	0.337

C

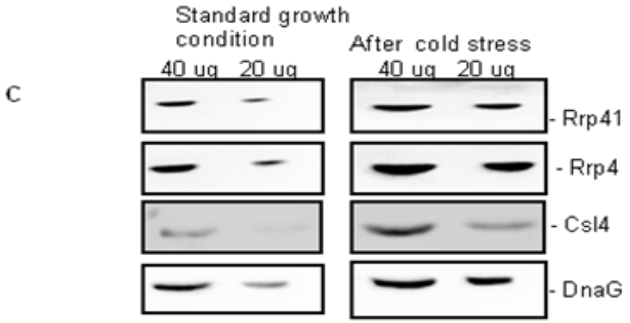

D

	Standard growth condition		After cold shock	
	40 ug	20 ug	40 ug	20 ug
Rrp41	69	29	111	51
Rrp4	105	46	182	99
Csl4	64	32	90	59
DnaG	108	45	170	88

E

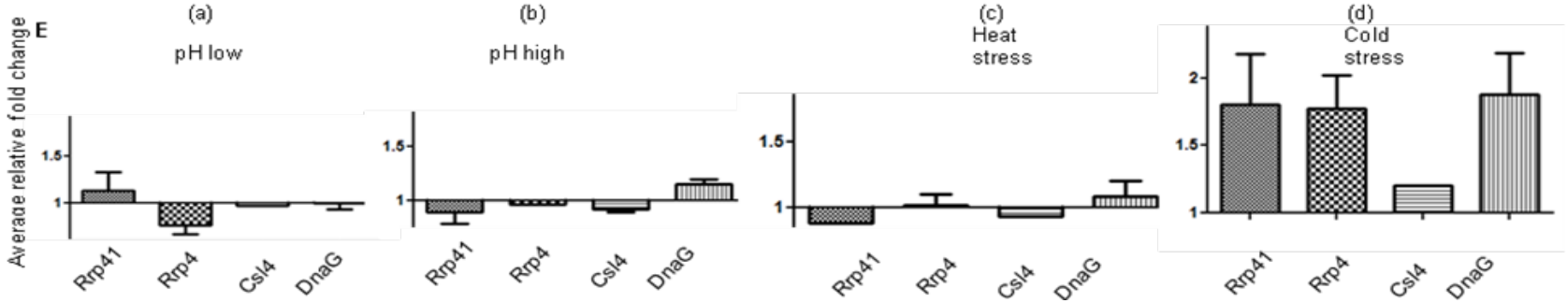

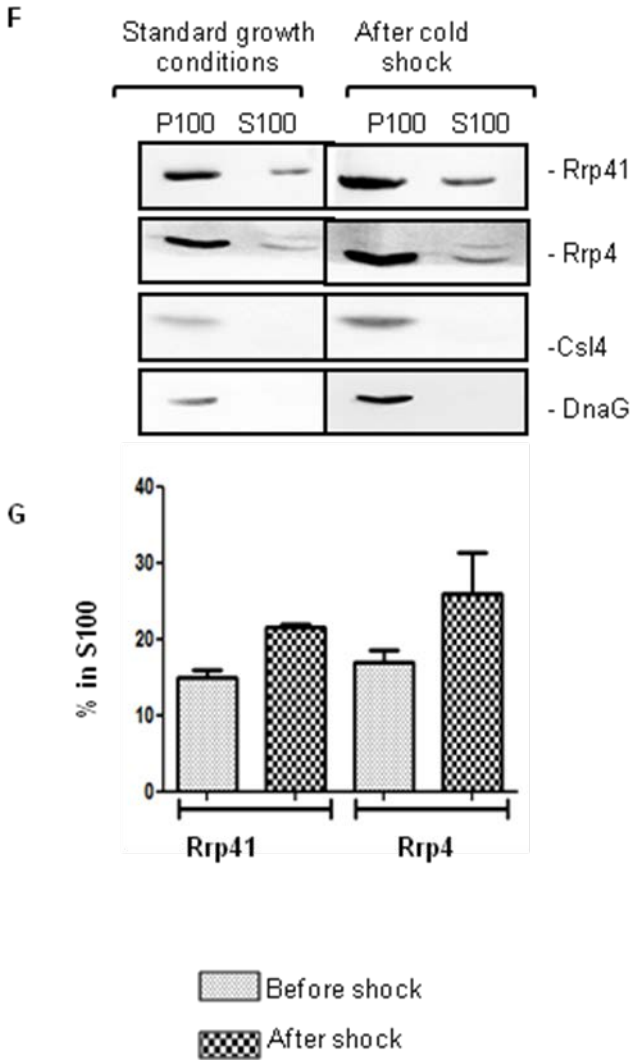

Figure 4.3.1 Detection of exosomal subunits Rrp41, Rrp4 Csl4 and DnaG of *S. solfataricus* before and after stress by Western blot analysis.

A) Comparison of the growth curves. The figure indicates the growth curves of *Sulfolobus solfataricus* before applying the stress. *S. solfotaricus* growth was determined using optical density data (OD) recorded for duplicates at 600 nm for 48 hours under normal growth conditions and then pH low, pH high, heat stress or cold stress were applied for 30 min. B) The optical density data (at 600 nm) before applying the stress and after 30 min of stress. The ODs do not change before and after the stress. C) Detection of exosomal subunits in *S. solfataricus* cell-free extract before and after stress by Western blot analysis. Example for the comparison of the Western blot analysis of changes in the amount of the total protein of the exosomal subunits. Equal weight (µg) amounts of protein were separated in 12% SDS-PAGE, blotted and hybridized with sera directed against the exosomal subunits indicated on the right side of the panels. D) Quantification of the of signals. The chemiluminescent signals in the Western blot was detected by a digital imaging system in fusion X4 machine and signal intensities were quantified by the fusion X4 software. The intensities are divided by 1000 and rounded to the nearest decimal point. E) Graphical representation of the quantification of the total amount of proteins of the exosomal subunits under different stress conditions (a-pH low, b-pH high, c- heat stress, d-cold stress), relative to the control standard growth conditions. Shown are graphical representations of the results from two independent experiments and two technical replicates. Graphs for Csl4 protein under ph low, heat and cold stress were drawn by one measurement from one experiment due to the less sensitivity of the Cls4 antibody. F) Western blot analysis to detect differences in solubility of the exosomal subunits in different stresses. Equal volume of S100 and P100 fractions were loaded on a SDS PAGE gel for separation of the proteins and blotted and hybridized with sera directed against the exosomal subunits indicated on the right side of the panels. The figure indicates an example (cold stress) for the Western blot analysis carried out for S100 and P100 fractions of standard conditions and after the stress. G) Graphical representation of the results from two independent experiments in which the percentage of the S100 fraction is indicated in relative to the total amount of proteins (S100+P100). DnaG and Csl4 were exclusively in the P100 fraction.

Further we analysed the changes in solubility of the exosome after the stresses in comparison to the standard conditions. We observed that the solubility does not change after the above mentioned stress conditions other than the cold stress (Figure 4.3.1F and G). Following the cold stress, the proportion of the exosomal proteins, Rrp41 and Rrp4 in the (S100) soluble fraction were increased by 7% and 10% respectively. DnaG and Csl4 were detected exclusively in the pellet fractions.

To indentify the possible interaction partners of the exosome under stress, Co-IP experiments were done with anti Rrp41 antibody coupled beads and *S. solfataricus* cell free extracts from cells harvested under standard conditions and after applying different stress conditions. There are no interaction partners fished with the exosome in any of the stress conditions (Figure 4.3.2). The additional bands which obtained were either in the elution fractions of the Co-IP in the control experiment or the bands were not reproducible.

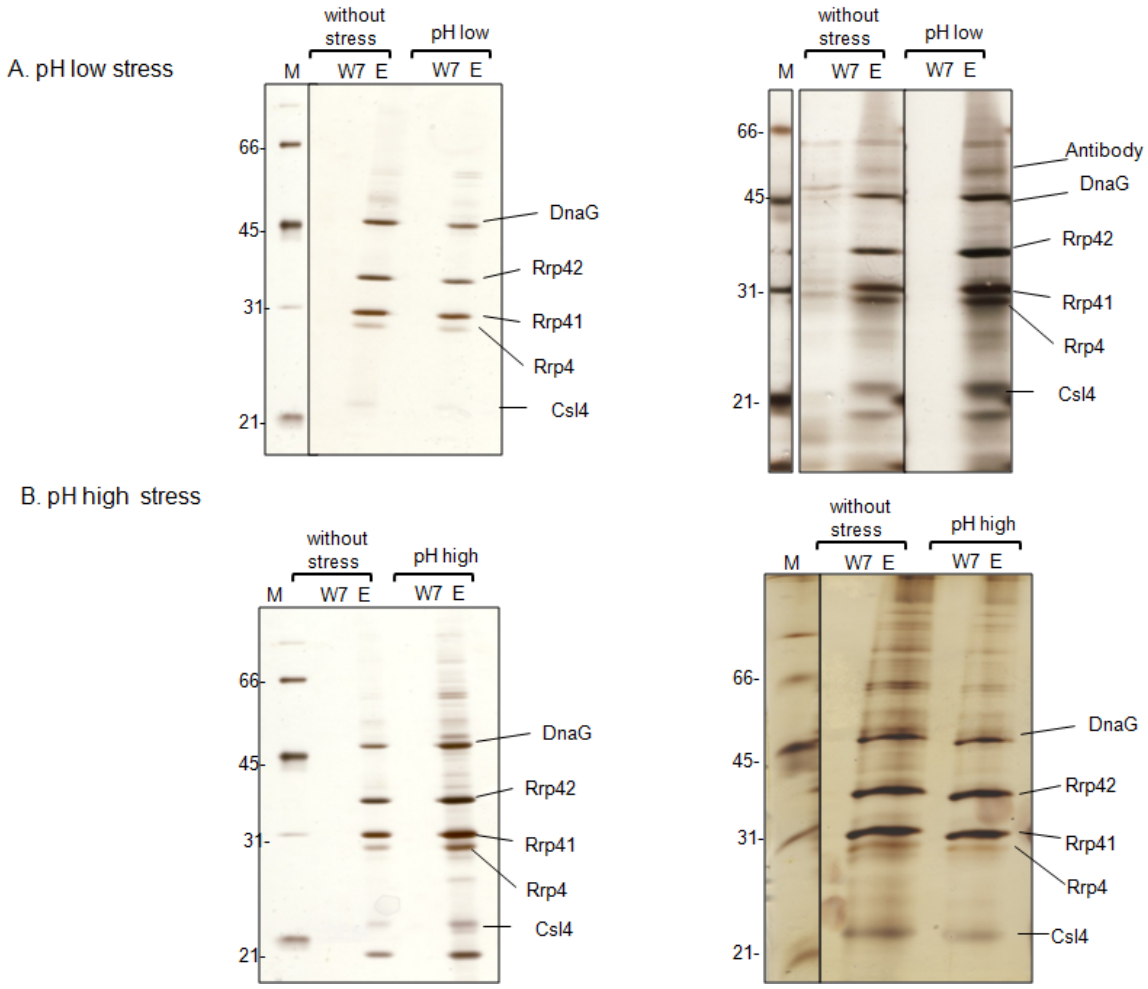

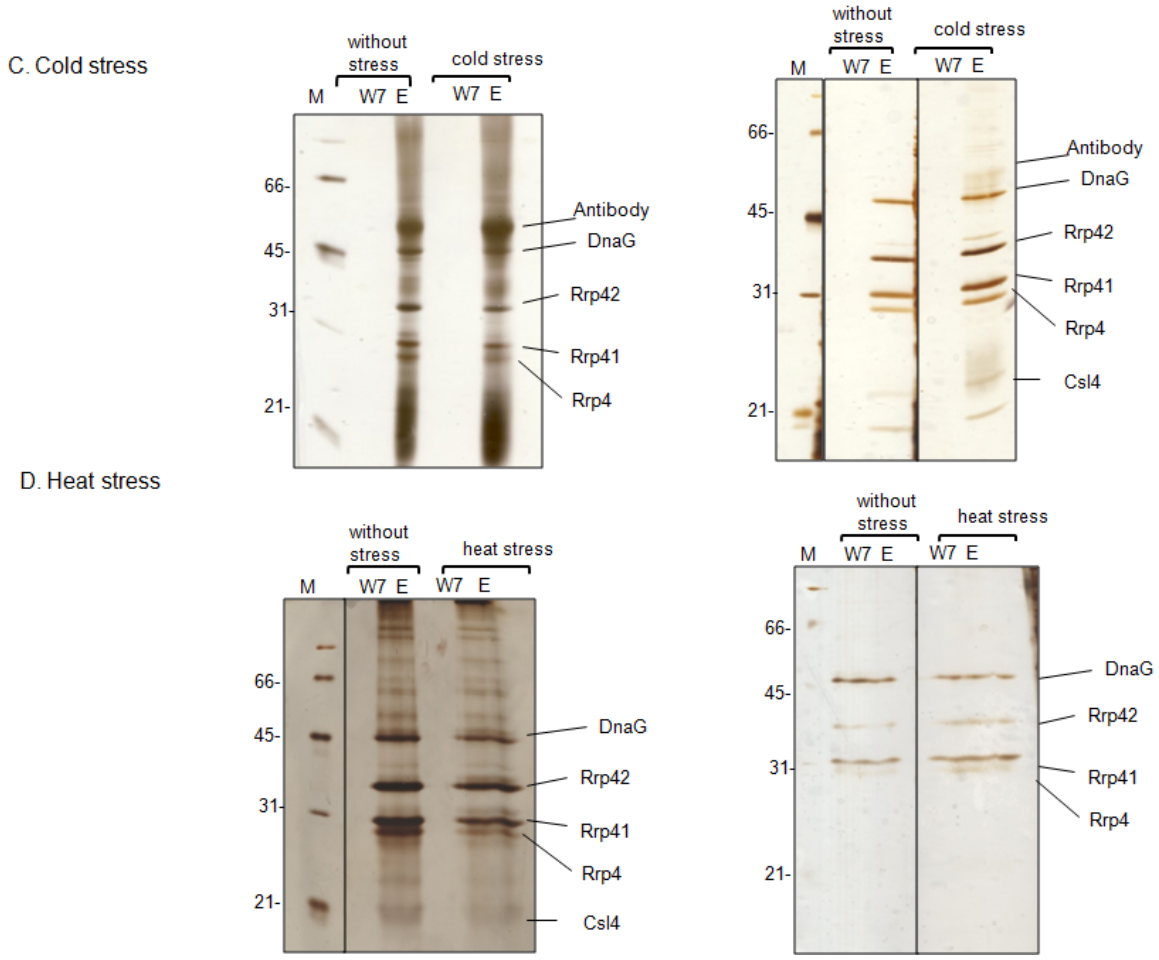

Figure 4.3.2 Silver stained SDS-gels showing proteins purified by co-immunoprecipitation (Co-IP) for two independent experiments with Rrp41-specific antibodies from *S. solfataricus* cell free extract under standard condition and under different stress conditions (A, pH low B, pH high C, heat and D, cold stress). W7, last, seventh washing fraction; E, elution fraction. The migration of marker proteins is marked (in kDa).

4.3.2. Changes of the archaeal exosome in the stationary phase

The experiments were done to study changes in the exosome in different stages of the growth curve. The figure 4.3.3A shows a typical growth curve (exponential and stationary stages) for *S. solfataricus* under standard growth conditions. The viability of the cells was approximately 90% during the growth [122]. The total amount of exosomal proteins do not change except Csl4 protein when exponential and stationary phases were compared [123]. Nevertheless I was able to observe that there is 1.3 fold increase in the amount of the Csl4 protein and 1.1 fold increases in the amount of the Rrp4 protein in the stationary phase relative to the exponential phase (Figure 4.3.3B and C).

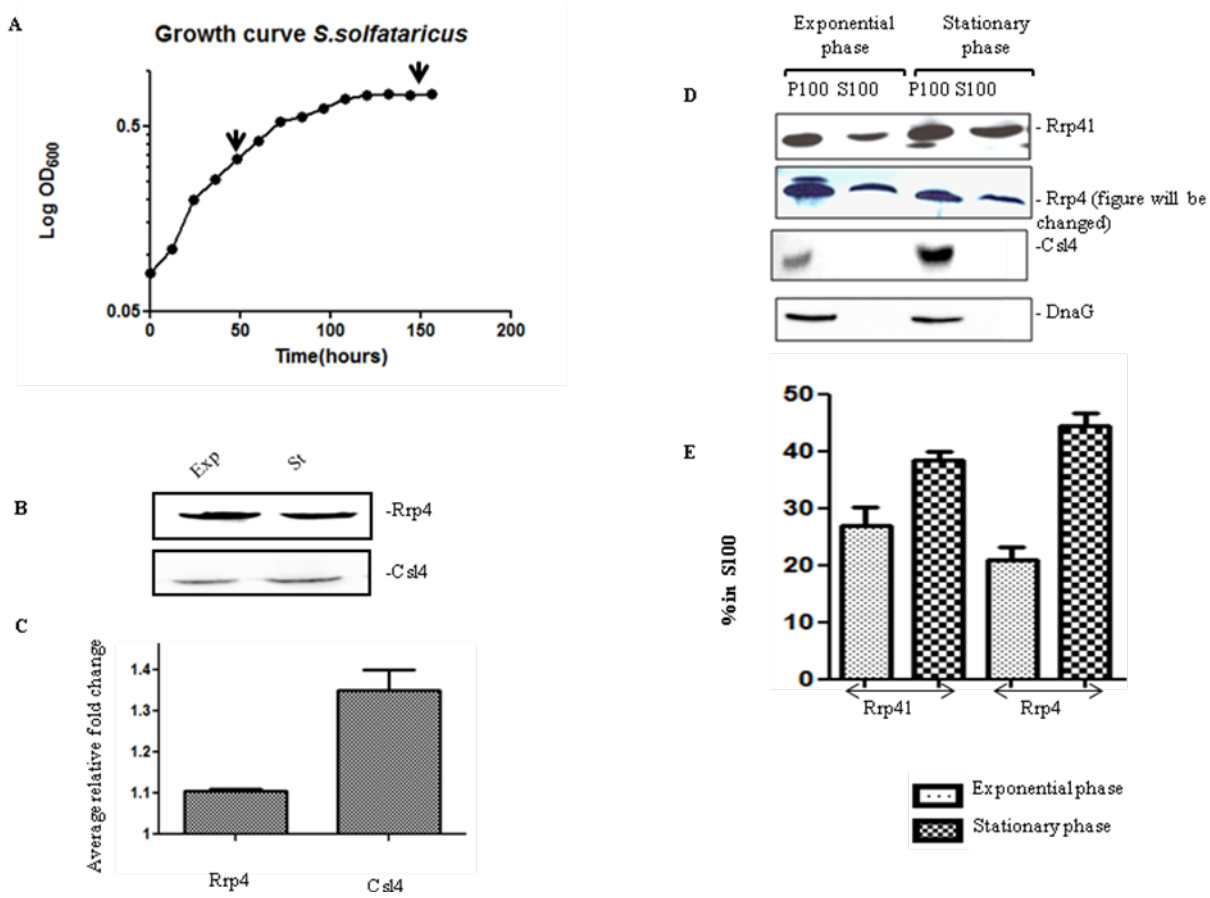

Figure 4.3.3 Detection of exosomal subunits Rrp41, Rrp4 Csl4 and DnaG of *S. solfataricus* in exponential and stationary phase by Western blot analysis.

A) A typical growth curve of *S. solfotaricus* was determined using optical density data (OD) recorded for duplicates at 600 nm for 144 hours. Arrows indicate the exponential (OD600 ~ 0.3) and stationary phase (OD600 ~ 0.7). B) Total amount of cap protein, Cls4 increases in the stationary phases. The cap proteins Rrp4 and Csl4 in *S. solfataricus* cell-free extract in the exponential phase (OD600 ~ 0.3, arrow in A) and in the stationary phase (OD600 ~ 0.7, arrow in A) were detected by Western blot analysis. Equal weight (µg) amounts of protein were separated in 12% SDS-PAGE, blotted and hybridized with sera directed against the cap proteins indicated on the right side of the panels. C) Graphical representation of the results from two independent experiments and two technical replicates. It shows the quantification of the increase of the proteins, Csl4 and Rrp4 in the stationary phase in relative to the exponential phase. D) Western blot analysis carried out for S100 and P100 fractions of cells from the exponential and stationary phase. Equal volume of S100 and P100 fractions were loaded on a SDS-PAGE gel for separation of the proteins and blotted and hybridized with sera directed against the exosomal subunits indicated on the right side of the panels. E) Graphical representations of the results from two independent experiments and two technical replicates in which the percentage of the S100 fraction is indicated in relative to the total amount of proteins (S100+P100). DnaG and Csl4 were exclusively in the P100 fraction.

Based on our previous study we know that there are different compositions of the soluble and the insoluble exosomes (4.1). DnaG and Csl4 are not detected in the S100 fractions whereas Rrp41 and Rrp4 are found in soluble fractions in the exponential and stationary phase. Interestingly the solubility of the exosomal Rrp41 and Rrp4 subunits increased in the stationary phase regardless the fact that the total Rrp41 content was not changed among phases in the growth cycle (Figure 4.3.3D and E).

In 2010 Roppelt *et al* found that both ribosomal subunits, (30S and 50S) were in the P100 fraction, in agreement with the previously described co-sedimentation of Rrp41 with ribosomal subunits in glycerol density gradients ([92] and chapter 4.1). It was also found that the archaeal exosome localizes at the cell periphery and co-sediments with membranes [110]. To clarify whether the sedimentation behaviour of the exosome changes during the growth circle, sucrose density gradients were applied (Figure 4.3.3A).

In agreement with the results shown in Figure 4.3.3D and E, we have been able to show the increment of the soluble exosome in the stationary phase by sucrose density gradients (Figure 4.3.4A and B). In addition we found that DnaG is not present in the low density fractions (S100) in the exponential and the stationary phases whereas the protein content of Rrp41 and Rrp4 increased the low density soluble fractions in the stationary phases. Nevertheless we did not observe the highest exosome proportion to co sediment with the membrane fractions.

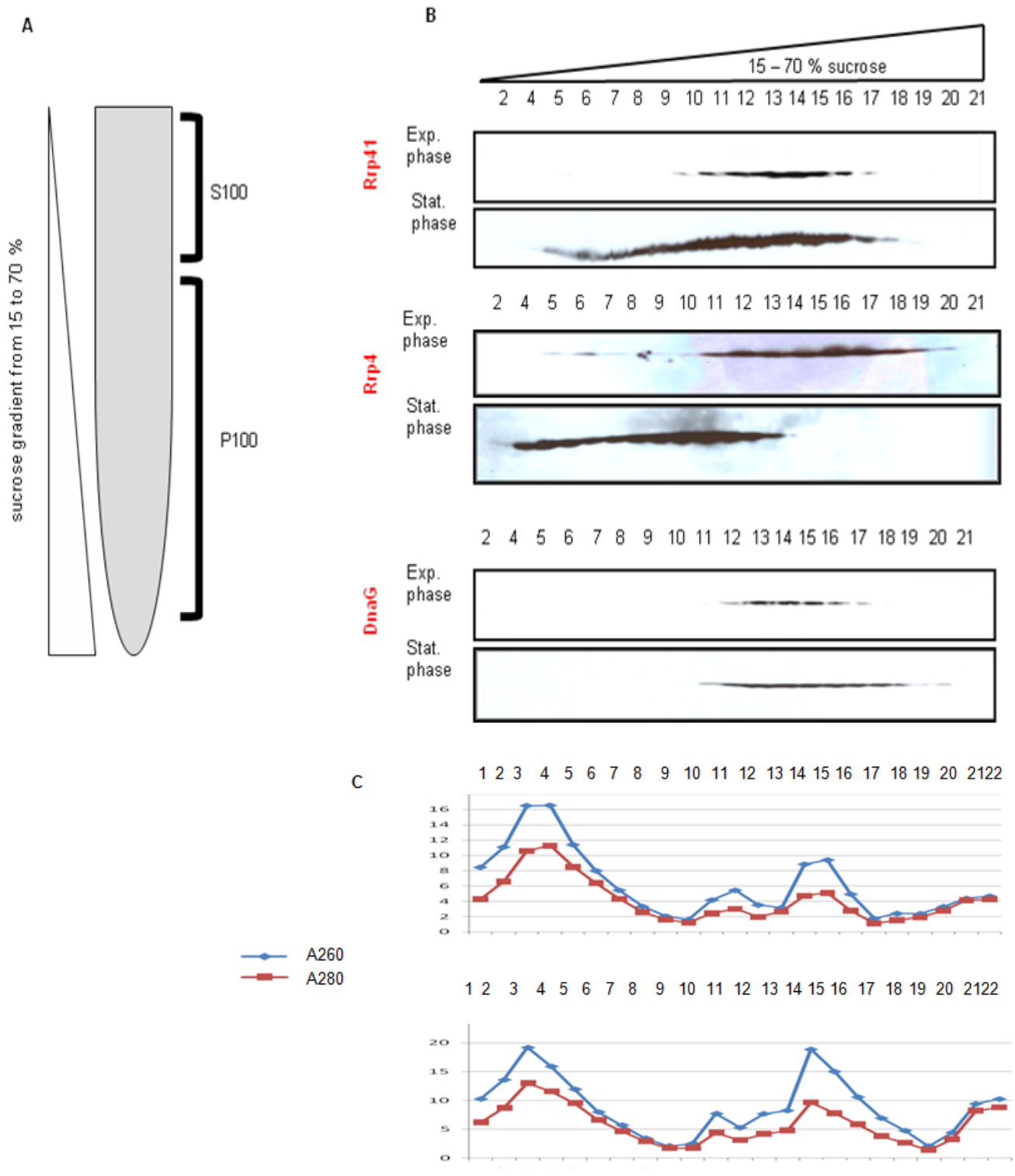

Figure 4.3.4. Fractionation through a 15–70% sucrose density gradient with salt.

A) Cell free extract of the *S.solfataricus* was added on to the 15-70% sucrose density gradient. B) The cell-free extracts of *S. solfataricus* in exponential and stationary phase were fractionated through the sucrose density gradient and the fractions were analyzed for the presence of Rrp41, Rrp4 Csl4 and DnaG by Western blot

hybridization. The analyzed fractions are given above the panels, the detected proteins are marked on the left side. C) Absorption of the gradient fractions of exponential (top) and stationary (bottom) at 280 or 260 nm.

RNA and protein content of each fraction was monitored at 280 and 260 nm absorption, of the cell free extract of the *S. solfataricus* in the exponential phase and the stationary phase (Figure 4.3.4C). Peaks were detected in fraction 4 (contains tRNAs (not shown))and in the fractions 10-14 (contain 30S and 50S ribosomal subunits) [110] in both cell free extracts.

4.4. Exosome under the single particle electron microscope

It was found in *in vitro* experiments that DnaG interacts with the reconstituted 9 subunit exosome via the Csl4 protein [98]. Although crystal structure of the Csl4-exosome from *A. fulgidus* [93] and of DnaG from *E. coli* [124] are known there is no direct information about the three-dimensional (3D) structure of the archaeal exosome with DnaG, which is essential for understanding its functional organization. Despite the recent study about the shape of *E. Coli* DnaG protein as crescent shaped protein with a groove in the middle, [124] the archeal DnaG has not yet been elucidated. To address these questions we decided to analyse native and the reconstituted exosome by single particle electron microscopy (SPEM).

4.4.1. Reconstituted exosome under SPEM

As the first step of reconstitution of the exosome, the proteins were overexpressed and purified from *E. coli* BL21 (DE3) at 37° C. The recombinant exosomal proteins Rrp41, Rrp42, Rrp4 and Csl4 were purified to near homogeneity (Figure 4.4.1A, B, C, and D). However, it was not able to achieve any expression of DnaG protein in BL21 (DE3) cells. The construct was then transformed into the *E. coli* strain Arctic Express for the overexpression (Figure 4.4.1E) [98].

The concentrations of DnaG and Csl4 were less in comparison to other recombinant exosomal proteins. The typical concentration of DnaG and Csl4 were about 0.2-0.3 mg/ml and the typical concentration of Rrp41, Rrp42 and Rrp4 were about 0.7-1 mg/ml. All the recombinant exosomal proteins (Rrp41, Rrp42 and DnaG) contain a His- tag except the Csl4 protein which contains a Strep- tag at the C terminus. Reconstitution of the Csl4-exosome and the DnaG-Csl4-exosome was done as described in 3.2.6.2. In order to avoid monomers with the His- tag and complexes without Csl4 protein, we first purified the complexes by a *Strep*-tactin column. The elution fraction, which contains the Strep-tag Csl4 monomers and the complexes with Csl4 protein, was then subjected to a Ni-NTA column to avoid the monomers of Strep- tagged protein, Csl4. By this method I was able to achieve concentrated (total protein content-0.5 mg/ml) complexes without monomers. Prior to visualizing the samples under SPEM, samples were analyzed by silver staining, in a 12% SDS-PAGE denaturing gel (Figure 4.4.2A). Csl4 protein band was not visible in the silver stained gel. Nevertheless, as the first purification was done with *Strep*-tactin column, the protein

complexes should contain Strep-tagged Csl4. Previously it was shown that His-tagged proteins and samples do not stick to *Strep*-tactin beads [98].

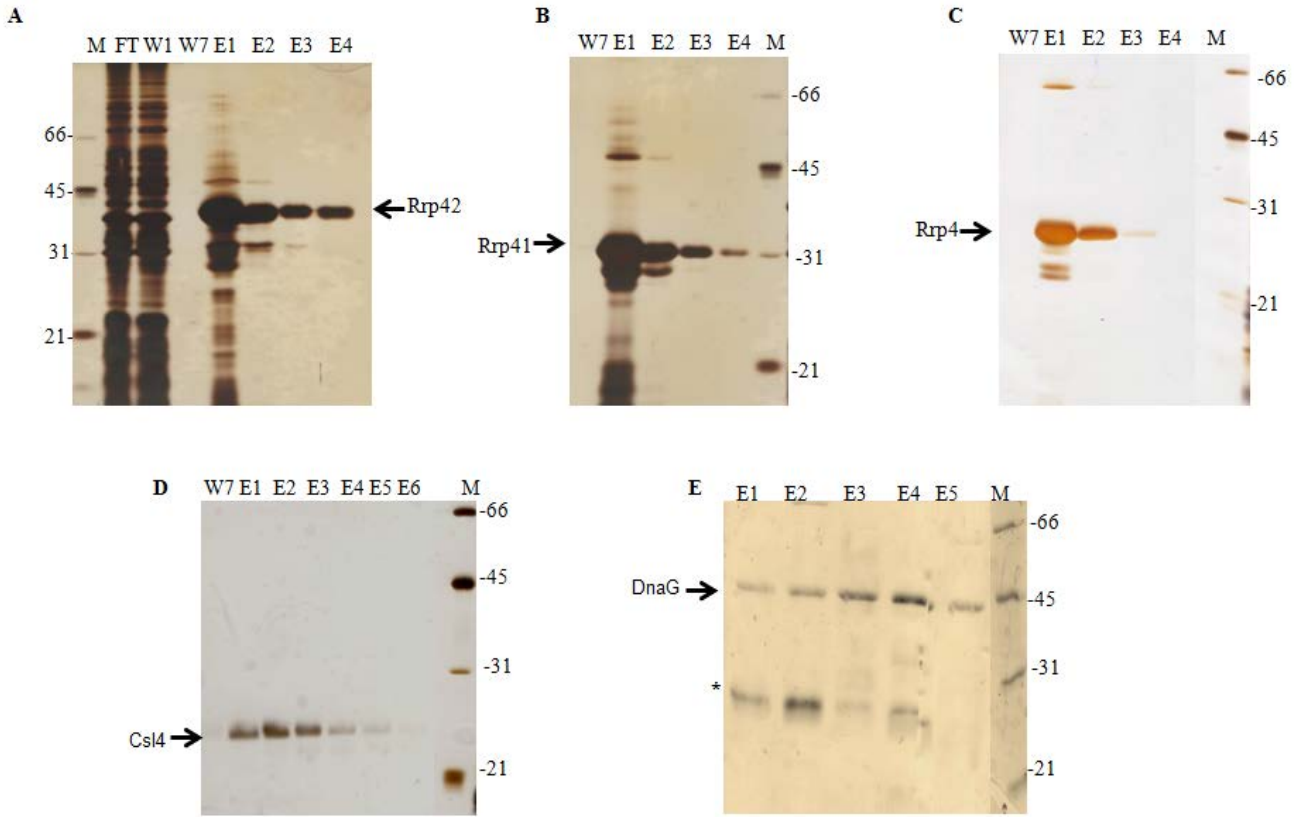

Figure 4.4.1 Overexpressed recombinant exosomal proteins were separated in a 12 % SDS-PAGE gel and visualised with silver staining. FT, flow-through; W1, W7, the first and the last washing fractions; E, the elution fraction. The bands of the expected size for the recombinant A) Rrp42 (35 kD) , B)Rrp41 (30 kD), C) Rrp4 (28k D) and DnaG (45 kD) with His-tags and Csl4 (20 kD) with Strep-tag can be seen in the elution fractions (E1- E6, marked with an arrow). An *E. coli* protein binding to Ni-NTA, which was routinely present in the DnaG-fractions used for the reconstitution experiment, is marked with an asterisk (D). In the last washing fraction (W7) no proteins were detected. The sizes of the Low-Range markers (Biorad) are shown in the lane marked as M in kDa.

The Csl4 exosomes and the DnaG-Csl4-exosomes were directly applied to a grid and negatively stained. In the SPEM we could not observe any images of monomers or any impurities. Approximately 15000 particles were picked (pointed by the arrow heads in Figure 4.4.2B) from each complex, with different projections before the translational and rotational alignment. Figure 4.4.2C shows the 25 classes resulting from classification. Though the crystal structure of the Csl4-exosome of *A. fulgidus* was known [93], the structure of the exosome of *S. solfataricus* was never revealed. We were able determine the structure of the *S.*

solfataricus Csl4-exosome by SPEM (Figure 4.4.2C). The bottom view of Csl4-exosome of *S.solfataricus* and *A. fulgidus* is similar (Figure 4.4.2D). The Csl4-exosome of *S.solfataricus* contains a ring shape structure with trimetric symmetry and appeared rather homogeneous when visualized by negative stain EM. We were not able to see any difference between the Csl4-exosome and the DnaG-Csl4-exosome.

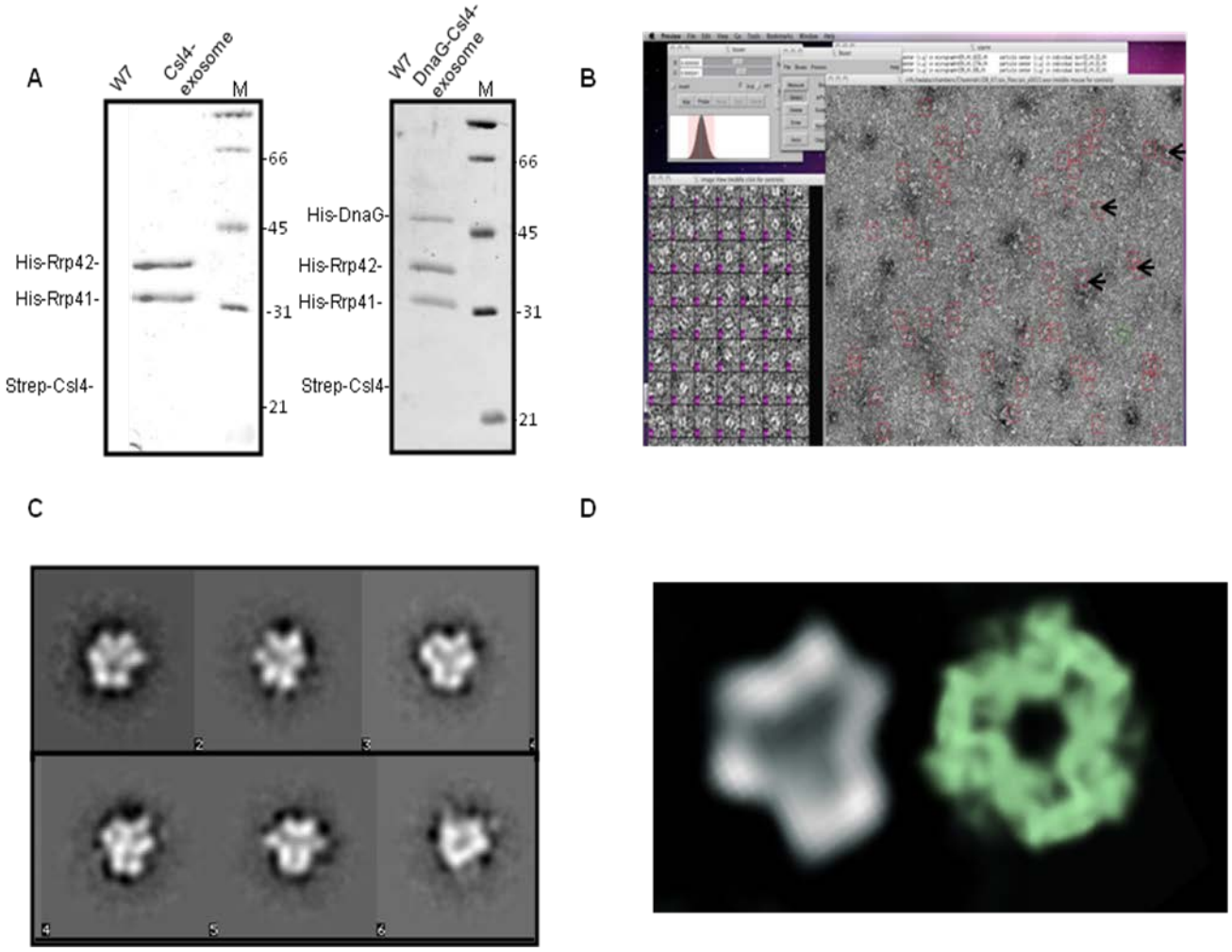

Figure 4.4.2 The analysis of the reconstituted Reconstitution of the Csl4-exosome and the DnaG-Csl4-exosome. A) The exosomes were reconstituted by mixing Strep-tagged Csl4 and His-tagged Rrp4, Rrp41, Rrp42 and DnaG proteins. Subsequent to the sequential purification by the *Strep*-Tactic followed by Ni- NTA chromatography, in the elution fraction, the Csl4-exosome and the DnaG-Csl4-exosome were detected by silver staining. Nonetheless Csl4 protein was not visible in both cases. M, protein marker, the migration behavior of the proteins is given in kDa on the left side. B) The particles were picked (pointed by the arrow heads), with different projections before the translational and rotational alignment. Approximately 15 000 particles were picked from each sample. C) Different views of the Csl4 exosome. Analysis of single particles projections gives the structure of Csl4 exosome from images of individual particles. Resolution 47 000x D) Alignment of the bottom view of the SPEM analysed Csl4 exosome (left) and bottom view of the crystal structure of the Csl4 exosome (right) using the Chimera software.

4.4.2. Native exosome under SPEM

Homologous cloning system was used to express exosomal proteins in *S. solfataricus* (Figure 4.4.3A). It was possible to clone the genes *rrp4, csl4* and *dnaG,* as well as the *dnaG* parts encoding the N terminal and the C terminal portions of the protein, in to the pMJ0503 vector. However it was possible to transform and express only the full length DnaG-His_6 in *S. solfataricus* M16. The comparison of the growth curves between the wild type and the strain containing the DnaG-His_6 construct (without and with induction) is shown in Figure 4.4.3B. *S. solfataricus* cultures which contained other constructs failed to grow over OD_{600} 0.1, which says that the expression of those construct were deleterious for the cells. The DnaG construct containing *S. solfataricus* M16 culture did not grow more than an OD_{600} of 0.3-0.4 (Figure 4.4.3B). Induction for the overexpression was done in the stationary phase (OD_{600} 0.3-0.4, indicated by the arrow head). The induction in the exponential phase (OD_{600}, 0.15) resulted a higher amount of His-tagged DnaG protein in relative to the native DnaG protein (Figure 4.4.3C and D). However, the induction in the stationary phase resulted a His-tagged DnaG and the native DnaG in similar stoichiometry.

A

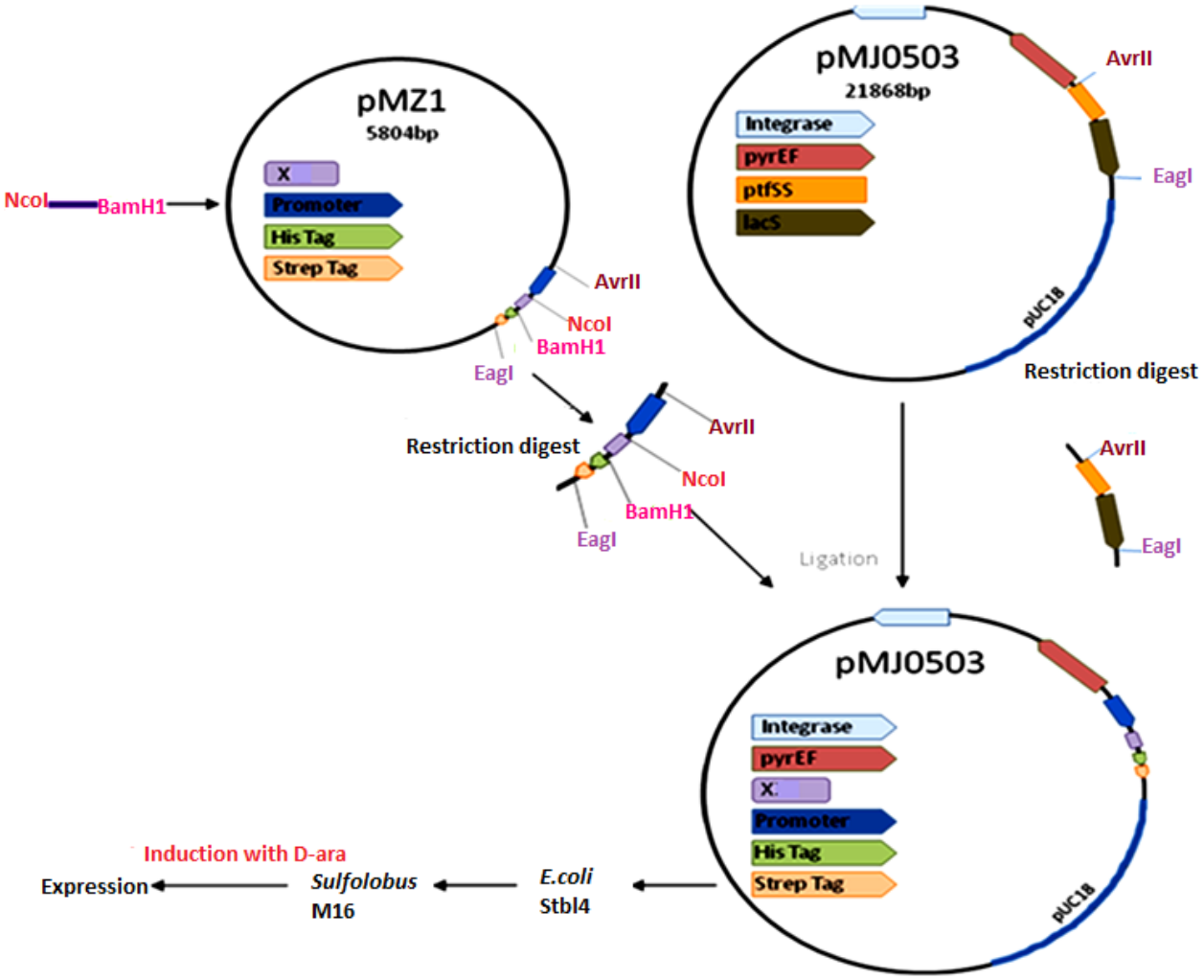

B

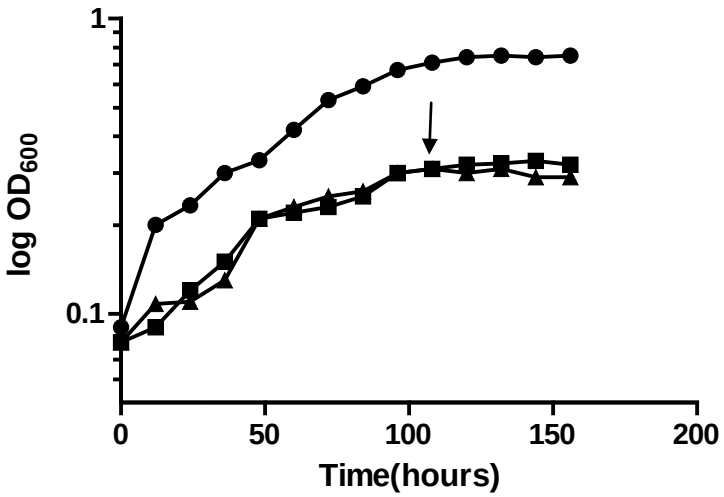

Wt -*S. solfataricus* M16

S. solfataricus M16 DnaG-His_6 (Without induction)

S. solfataricus M16 DnaG-His_6 (with induction)

C

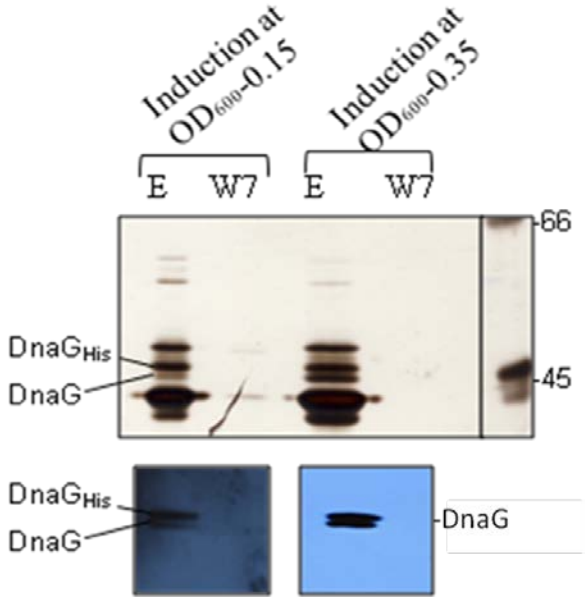

D

Induction at → / Intensity (mean) ↓	OD_{600} 0.15	OD_{600} 0.35
DnaG-His_6	322	467
Native DnaG	145	436

Figure 4.4.3 Induction of DnaG-His_6 construct in *S. solfataricus* M16. A) Overview *of S. solfataricus* homologous expression system. X resembles the gene of interest, eg., *rrp4*, *csl4* or *dnaG*. Adopted from [125]. B) The figure indicates the typical growth curve of *Sulfolobus solfataricus M16* (wild type) and *S. solfataricus* with the $DnaG_{His\text{-}6}$ construct (without induction and with induction). *S. solfotaricus* growth was determined using optical density data (OD) recorded for duplicates at 600 nm for 144 hours under normal growth conditions. The arrow indicates the point of induction. C) Comparison of the purified exosomes which was induced at different time points in the growth circle. The cultures were induced for the expression of proteins at the exponential and stationary phase. The exosomes were purified by Ni-NTA chromatography. The elution fractions were separated in a 12% SDS-PAGE gel and analysed by silver stain and Western blot. W7, last washing fraction, E, Elution fraction. D) Quantification of the signals. The chemiluminescent signals in the Western blot was detected by a digital imaging system in fusion X4 machine and signal intensities were quantified by the fusion X4 software. The intensities are divided by 1000 and rounded to the nearest decimal point.

4.4.2.1. Characterization of the DnaG-His_6 protein

4.4.2.1.1. Solubility and sedimentation pattern in sucrose density gradient

We wanted to see whether DnaG-His_6 in *S.solfataricus* M16 strain performs same as the native DnaG in *S. solfataricus* P2 strain. Thus, we checked the solubility of DnaG-His_6 after ultracentrifugation of the cell-free extract at 100,000 g and the sedimentation pattern of DnaG in sucrose density gradient. Consistent with the previous results (chapter 4.1), only a minor part of Rrp41 was detected in the soluble, supernatant fraction (S100) and DnaG was detected only in the insoluble, pellet fraction (P100) (Figure 4.4.4A). Furthermore we observed 2 bands (45 kDa and 48 kDa) after hybridizing with anti DnaG antibody and one band (48kDa) after hybridizing with anti His antibody. DnaG was also not observed in the low density fractions in the sucrose density gradient of 15 % to 70% (Fractions 2 to 10, Figure 4.4.4B) and the sedimentation patterns of DnaG and Rrp41 were similar to the previous results which were obtain by the cell free extract of the *S. solfataricus* P2 strain (chapter 4.1).

Finally we concluded that DnaG-His_6 performs similarly as the native DnaG in *S. solfataricus*. Thereafter we wanted to fish the complete exosome by Ni-NTA chromatography.

4.4.2.1.2. Interaction partners of the soluble and non- soluble exosomes

Prior to the examination of the native exosome under the SPEM, we wanted to know whether there are any additional proteins which co-purify with the exosome or novel interaction partners of the complex. Hence, cell free extract from the D-arabinose induced sample was subjected to Ni-NTA chromatography (Figure 4.4.4C). A negative control was performed in which the cell free extract of *S. solfataricus* (wild type) was subjected to the same purification steps. Some of the protein bands which were seen in the elution fractions were disappeared after the treatment with RNases. The bands in the second elution fraction after the RNase treatment (corresponds to lane 6 in Figure 4.4.4C) were given for the mass spectrometry analysis and further identified by Western blotting (Figure 4.4.4F and G). The underlined proteins were identified by mass spectrometry (Appendix 1). There were 2 bands of DnaG protein in the SDS-PAGE. The content of the DnaG protein was visibly more than the other exosomal proteins in the silver stained SDS-PAGE gel. Bands which are marked with asterisks were found in the control elution fractions (Figure 4.4.4H and I). I did not find

any interaction partners. However, RNA chaperone Hfq [bacillus coagulan 2-6] protein, which was identified by mass spectrometry, was co purified together with the exosome. This was not reproducible. This experiment was repeated three times. Silver stained gel with the last washing fraction and the elution fractions is in Appendix 3.

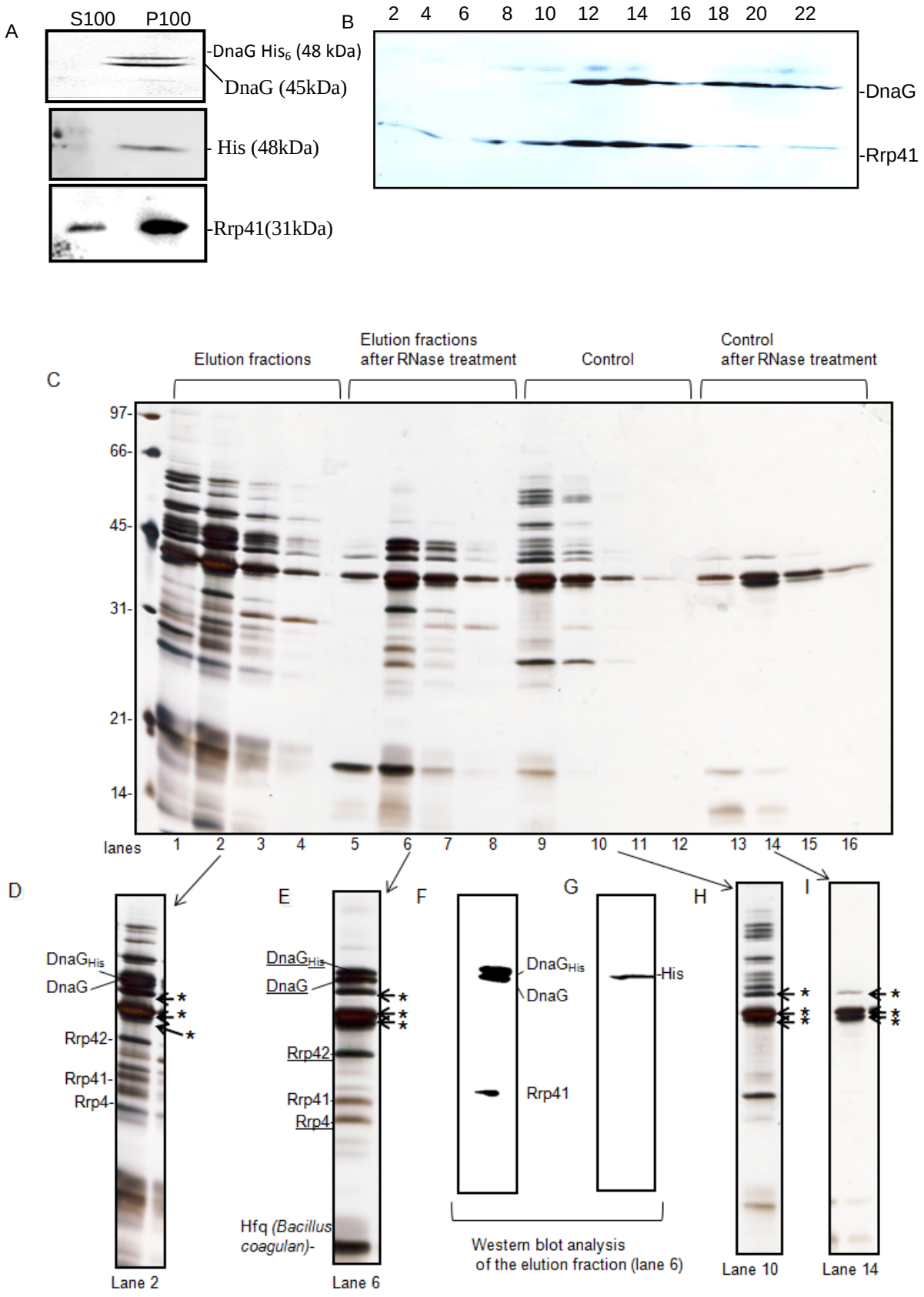

Figure 4.4.4 Characterization of DnaG His6 in *S. solfataricus* M16 and purification of the exosome by Ni – NTA chromatography.

A) Western blot analysis of S100 and P100 fractions of the overexpressing strain. Equal volume amounts of the S100 and the P100 fractions were separated in 12% SDS-PAGE, blotted and hybridized with sera directed against the exosomal subunits indicated on the right side of the panels. Anti- His antibody gives one signal at 48 kDa while anti-DnaG antibody gives 2 signals at 48 kDa and 45 kDa which correspond to the tagged DnaG and the native DnaG. Only a minor amount of Rrp41 protein was detected in S100 fraction which is consistent with the results in chapter 4.1. B) The cell free extract of the overexpressing strain was fractionated through a 15–70% sucrose density gradient with salt. Western blot analysis of the gradient fractions is shown with the use of specific antibodies in the right side of the panel. The number of the individual fractions is given above the panel. C) Elution fractions of the Ni-NTA chromatography from RNase treated, and non-treated and control samples. D) Elution fraction of the DnaG protein with the exosome protein complex. E) Before the elution, the beads were treated with RNases for 15 min at 37 °C to avoid the interactions of the exosome with other proteins due to RNA. The beads were washed with 6-column bed volumes and eluted. F) and G) DnaG, Rrp41 and His-DnaG were detected in elution fractions of Ni-NTA chromatography purification by Western blot analysis. Anti DnaG antibody gives 2 signals while anti His antibody gives one signal at the 45 kDa. The used antibodies are marked on the right side of the panel. H) Control experiment was carried out with the cell free extract of S *solfataricus* P2 without expression of DnaG. I) The RNase treatment was done in the control experiments same as mentioned in D. The last washing fraction did not contain any protein bands in any of the pull down assays (not shown). Protein bands of lane 6 were given for mass- spectrometry identification. The proteins which are underlined were detected by mass spectrometry, and the bands which are marked with an asterisk were present in the control experiments (Lane 10 and 14).

4.4.2.2. RNA and the native exosome

The aim of the experiment was to determine the specific RNAs which the exosome prefers and binds. To purify the RNAs which were bound to the native exosome isolated by the Ni-NTA chromatography from *S. solfataricus*, I treated the elution fraction of the Ni-NTA chromatography with TRIzol. The nucleic acid content was measured in the sample by NanoDrop spectrophotometer. The concentration of nucleic acids which were eluted with the exosome was 283.1 ng/µL and the in the sample of the control experiment the concentration was 38.8 ng/µL. After a portion of the Ni-NTA purified sample was treated with DNase, the concentration was 236,2 ng/µL and after an RNase treatment the concentration was dramatically decreased to 45.7 ng/µL. Therefore I concluded that the nucleic acids which were co-purified using Ni-NTA and further purified by TRIzol were mainly RNA molecules.

The RNA sample which was treated with DNase was then subjected to PCR experiment to see whether there is any DNA undigested. The control experiment was done with chromosomal DNA of *S. solfataricus* with the same primers. The PCR gave an intense signal

similar to the signal of control which means that there was DNA which was failed to be digested by DNases. We could not get rid of the undigested DNA.

4.4.2.3. Shape of the archaeal DnaG protein

The RNases treated elution fraction from Ni-NTA chromatography, was subjected to gel filtration before the examination under SPEM. There were two peaks which correspond to 290 kDa (size of the exosome) and 90 kDa (data not shown). Both fractions were analysed with the SPEM. In the 290 kDa peak, concentration of the protein was too less. Thus, we failed to see the exosome protein complex under the microscope. However, we were able to visualize the protein in relatively high concentration, which gave a peak around 90 kD in the gel filtration. It was a symmetric, dimeric protein with a central pore. Each monomer contained two lobes (figure 4.4.5). The monomer of the protein is 45 kDa, which is the size of the DnaG protein.

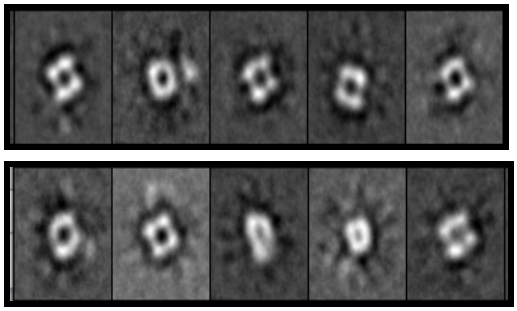

Figure 4.4.5 The native DnaG protein under SPEM. The DnaG protein was analysed and identified as a doubled lobed protein with a central pore from the technai T12 SPEM under 67000x resolution

4.5. Could Nop5 be a novel interaction partner of the soluble exosome of *Sulfolobus solfataricus?*

DnaG was co-immunoprecipitated with the *S. solfataricus* exosome and it was identified as an integral part of the exosome [92, 95](chapter 4.1). However DnaG is present in the soluble exosome in lower amounts compared to the insoluble exosome. The amount of the soluble exosome is growth phase dependent and increases in the stationary phase (Chapter 4.1). Lassek in 2010 [122] found that the archaeal Nop5 protein as a potential interaction partner of the soluble exosome in the stationary phase, by preliminary experiments: The cell free extract from the stationary phase was separated through a sucrose density gradient. The soluble and insoluble exosomes were co-immunoprecipitated with anti-Rrp41 antibodies. The comparison of their composition suggested that in the soluble exosome, DnaG was 'exchanged' by a protein which was then identified by the mass spectrometry analysis as Nop5, a well known subunit of the methylation ribonucleoprotein particle in *S. solfataricus* [122] Figure 4.5.1). In the methylation complex Nop5 is associated with L7Ae and fibrillarin protein [126]. Since only the Nop5 protein was co-purified with the exosome, we assumed Nop5 might have an exosome related function most probably in the stationary phase.

Therefore we wanted to further investigate the reliability of the interaction between the Nop5 and the soluble exosome which might regulate the growth stage dependent changes in the amount of the soluble exosome.

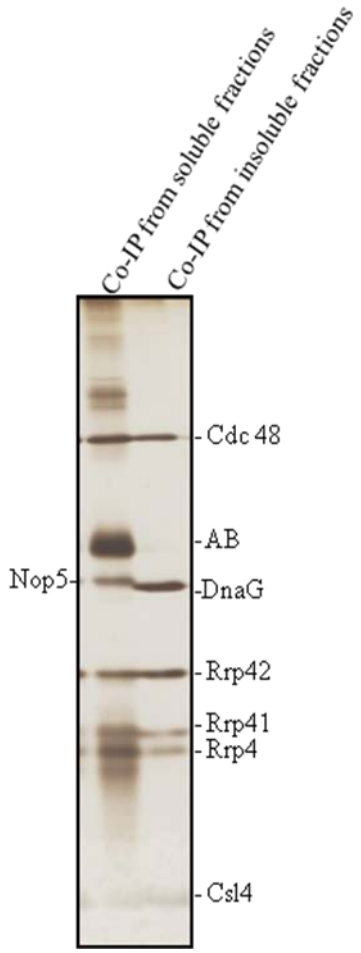

Figure 4.5.1 The Nop5 co-immunoprecipitation with the *S. solfataricus* exosome. The exosome was co-immunoprecipitated using anti-Rrp41 antibodies from the low density fractions of the sucrose density gradient (soluble exosome) and from the high density fractions of the sucrose density gradient (insoluble exosome). The elution fractions were separated on a SDS-PAGE gel, and visualised by silver staining. Nop5 (45 kDa) was identified by the mass spectrometry analysis. The other bands were assigned according to their known migration behaviour [95]. Adopted from [122].

4.5.1. Nop5 as a potential interaction partner of the exosome

To analyse further the interaction between the Nop5 and the archeal exosome, antibodies were raised against a recombinant, His-tagged Nop5 protein expressed and purified from *E. coli* (Lassek and Hou unpublished data). In an attempt to confirm the association of Nop5 with the soluble exosome, Co-IP with anti-Nop5 antibodies was performed with S100 fraction from stationary phase cells. This led to the purification of the methylation complex (Figure 4.5.2A, lane1). The methylation complex consists of Nop5 (45 kDa), fibrillarin (27.5

kDa) and L7ae (13.5 kDa) proteins [126]. The major bands were identified by mass spectrometry analysis. None of the exosomal subunits were among them, although the mobility of the several bands in SDS-PAGE gel was similar to the mobility of the exosomal subunits in the elution fraction of a Co-IP with anti-Rrp41 antibodies (Figure 4.5.2A, compare lane 1 and 2). Although it was expected that the soluble exosome of the stationary phase will contain Nop5, only DnaG was identified by mass spectrometry analysis, in the complex fished by anti-Rrp41 antibodies (Figure 4.5.2A lane 2). In this case, we assumed that the major part of the Nop5 protein in the cells was with the methylation complex and a minor part might interact with the exosome. Furthermore the Nop5 which interacted with the exosome might get hindered by the DnaG because both the proteins run at the same position in the SDS-PAGE gel.

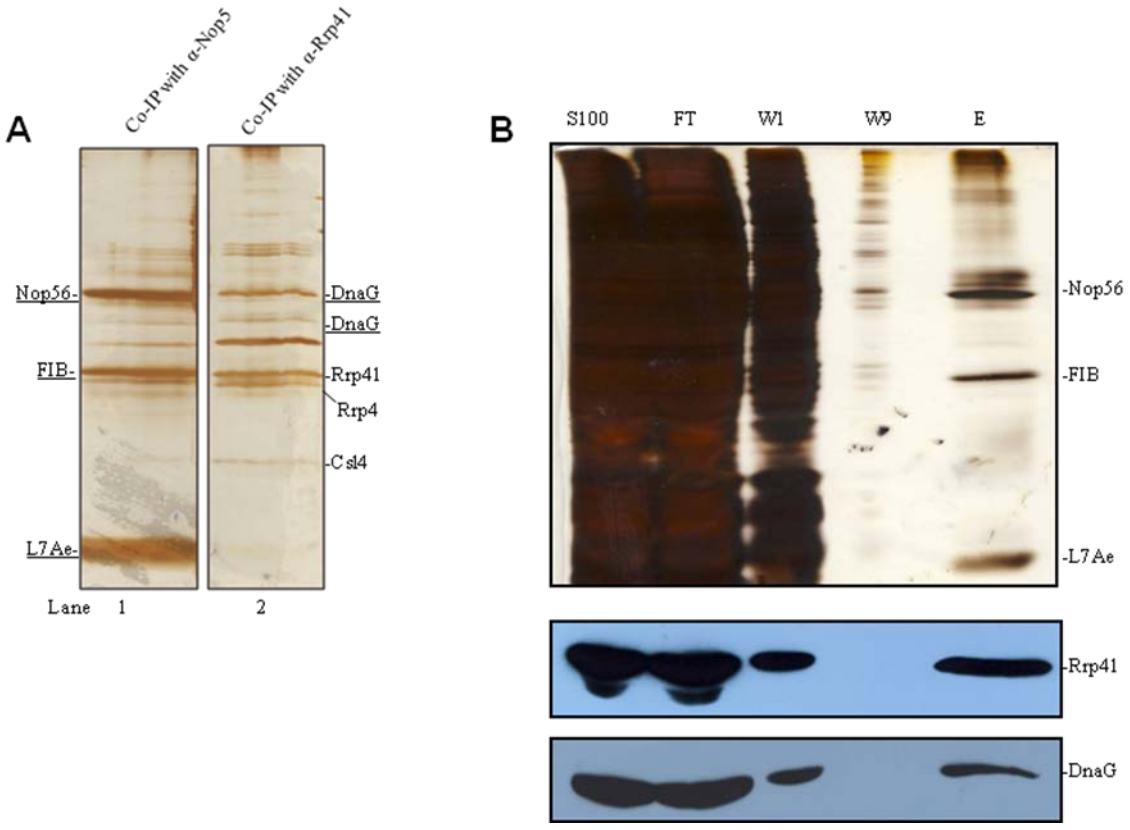

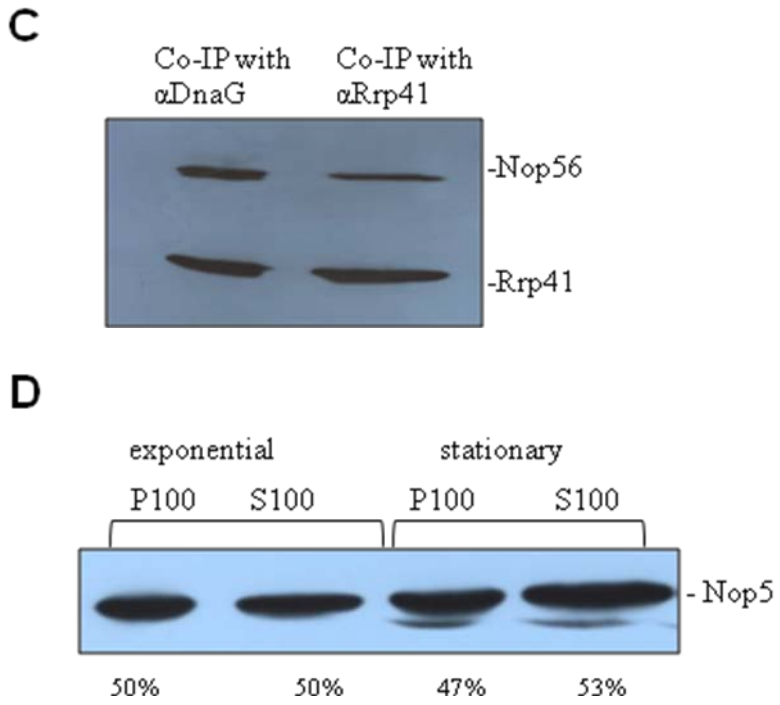

Figure 4.5.2 Analysis of Nop5 as a potential interaction partner of the *S. solfolobus* soluble exosome. A) and B) Co-IP experiments with S100 fractions from stationary phase cells. A) Co-IP was performed with anti-Nop5 antibodies and anti-Rrp41 antibodies. The elution fractions were analysed on a SDS-PAGE gel and visualised by silver staining. Indicated are the bands representing proteins indentified by the mass spectrometry (underlined) or the exosomal subunits with known migration in the gel (full gel in Appendix 4) B) Co-IP with anti-Nop5 antibodies was performed. Input (S100), flow through (FT), the first and the last washing fractions (W1, W9) and the elution fraction (E) were analysed in a silver stained SDS-PAGE gel and by western blotting with anti-Rrp41 and anti-DnaG antibodies. C) The elution fractions of the Co-IP (from S100 fraction) with anti-DnaG and anti-Rrp41 were analysed by SDS-PAGE and Western blot. The proteins which were hybridized are shown in the right side of the panel. D) Relative amounts of Nop5 in S100 and P100 was quantified. The S100 and P100 fractions of cells in exponential and stationary phase were subjected to Western blot hybridization with antibodies specific for Nop5. The relative amounts are given in percentages below the panel.

Furthermore, we detected Rrp41 and DnaG by Western blot hybridization in the elution fractions of the Co-IP done with anti-Nop5 antibodies (Figure 4.5.2B). This result suggested that exosome was co-immunoprecipitated with the Nop5 protein in the methylation complex.

To rule out the fact that the there is no proper protein-protein interaction but via an RNA molecule, (since the exosome and the methylation complex are performing on RNA), we conducted an RNase treatment, before the elution of the Co-IP with anti-DnaG and anti-Rrp41 antibodies. The elution fractions were separated in a 12% SDS-PAGE and Western blot was done by hybridising with Nop5 and Rrp41 antibodies (Figure 4.5.2C). This further

suggested that the Nop5 protein in the methylation complex is co-purified with the exosome. Quantitative analysis of Nop5 in the S100 and P100 fractions in both growth phases was performed to see whether there is any change of the proportion of the protein in the soluble and the insoluble fractions. Nop5 was present in equal amounts in S100 and P100 in both growth phases (Figure 4.5.2D).

However we found in the control experiments that His-tagged DnaG protein stick to the anti-Nop5 antibodies, after an incubation of the protein with anti-Nop5 antibodies covalently bound to protein A Sepharose beads. For this reason, unfortunately, the possibility exist that not only the methylation complex but also the exosome was co-immunoprecipitated together with the methylation complex. When the experiment was done vice verse (incubation of His-tagged Nop5 protein with anti-DnaG antibodies covalently bound to protein A-Sepharose beads) a band was visible by the silver staining in the elution fraction which was in the size of the Nop5 protein. Further, anti- Nop5 and anti-DnaG antibodies gave unspecific signals to His-tagged DnaG and His-tagged Nop5 proteins respectively in Western blot experiments (data not shown).

To check whether the unspecific signals occur due to the His-tag (both anti-DnaG and anti-Nop5 antibodies were raised against the His-tagged protein), the tag was cleaved by thrombin enzyme as the manufacturer specified. After the cleavage, the separation between the cleaved proteins and the His-tagged protein were performed by a Ni-NTA chromatography. The His-tagged proteins should bind to the Ni-NTA beads. However we could detect His-tagged proteins even in the flow through. Therefore, the experiment was not successful.

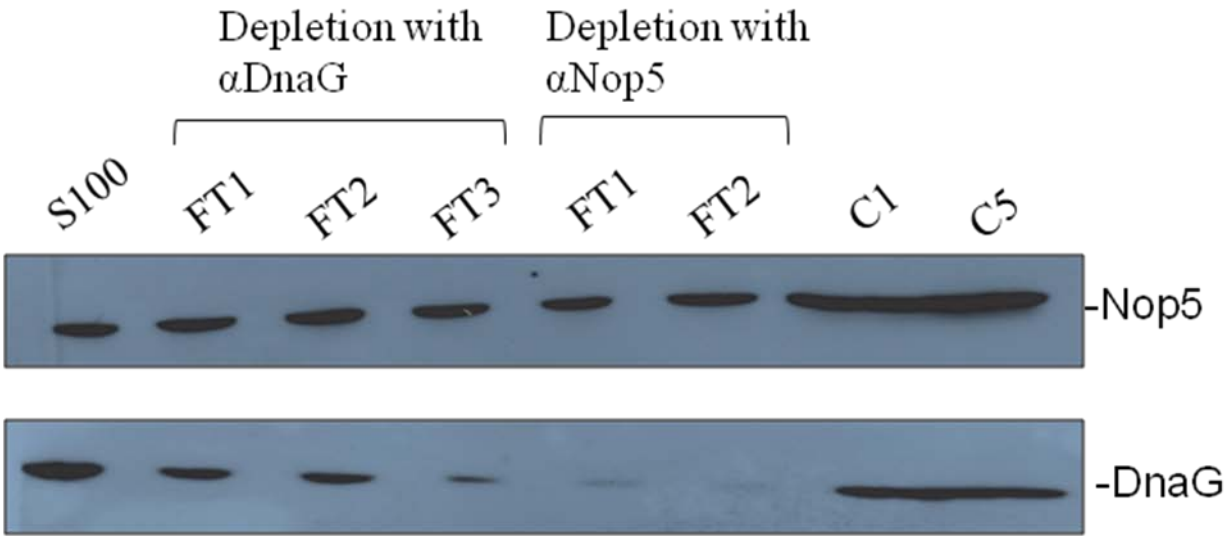

Figure 4.5.3 The soluble exosome was depleted with anti-DnaG antibodies and co-immunoprecipitated with anti-Rrp41 antibodies. The S100 fraction from the exponential stage was subjected to three rounds of Co-IP with anti-DnaG antibodies and then the residual exosome was co-immunoprecipitated with anti-Rrp41 antibodies. The flow through fractions were analyzed by Western blot, the detected proteins were indicated in the right side of the panel .C, control lanes, the S100 fraction was subjected to the same incubation and centrifugation steps without beads.

In the attempt of depleting the DnaG containing exosome from the soluble fraction we observed decrease of the DnaG signal in the flow through, in the sequential Co-IP rounds with anti-DnaG-antibody. However when the Western blot was performed by hybridizing with Nop5 antibodies, the signal for Nop5 was constant (4.5.3).

5. Discussion

5.1. Heterogeneous complexes of the RNA exosome in *Sulfolobus solfataricus*

We found that the soluble and the insoluble exosomes of *S. solfataricus* which co-sediments in different fractions of the sucrose density gradients have different compositions. Though it is known that the majority of the exosomes co-sediments with the membrane fractions in the sucrose density gradient, it was not possible to reproduce that result repeatedly. The typical RNA sedimentation pattern in the sucrose density gradient was changed when the cell free extract was treated with RNases. The peaks corresponding to the 30S and 50S ribosomal subunits disappeared due to the degradation of the rRNA. The hypothesis that the sedimentation pattern is due to RNA or DNA interactions with the exosome was excluded due to no major changes in the Western blot results. The signal in the low density fractions (hybridization with anti-Rrp41 antibody) under standard conditions was not seen in the Western blots in fractions of the treated cell free extract. It could be because the protein is under the limit of detection. Furthermore the signal which occurs in the low density fractions in the Western blot under standard conditions was not always reproducible. The influence of RNAs on the sedimentation pattern of the exosome in the sucrose density gradient is ruled out though the sedimentation of the 30S and 50S ribosomses and the exosomes are in the same fractions.

The soluble and the insoluble exosomes were both active. The exact functions of these are yet to reveal. We can speculate that the soluble exosome is important for the metabolism of mRNAs and tRNAs present in the soluble fraction (soluble exosome), while the exosome insoluble fractions may be involved in rRNA processing (insoluble exosome).

DnaG is an interaction partner of the archaeal exosome. It was first found as an interaction partner of the *S. solfataricus* exosome [95] and then it was found in other archaeal exosomes [127], [128]. DnaG is a highly conserved protein which is present even in the Archaea lacking exosomes. Here we show that the DnaG protein is an integral part of the exosome. The proportion of the DnaG is lesser in the soluble than the insoluble fractions. It could be that DnaG plays an important role mainly in the overall function of the insoluble exosome. It was found that DnaG has a poly (A) preference [98]. It could be that once the mRNA is released from the ribosome, the adenine stretches of the mRNA is recognised by DnaG and

Rrp4 proteins and are rapidly degraded by the exosome. EF1α was fished with the soluble exosome, using two different sera (Rrp41-specific and DnaG-specific) and different protein fractions (S100 or sucrose density gradient fraction). This strongly suggests a functional interaction between EF1α and the protein complex. The archaeal EF1α is involved in translational elongation and termination, and mRNA surveillance pathways [129]. It could be that once the mRNA is released from the ribosomes it is directed to the exosome via EF1α protein for degradation and/or polyadenylation.

5.2. The importance of the KH domain of Rrp4 protein for the poly (A) preference

The reconstitution of exosome containing truncated variants of the Rrp4 protein and the hexameric ring was not successful at low salt concentration. When the salt concentration was high, hydrophobic interactions are forced, and therefore interactions between proteins binding via hydrophobic forces can be expected. However, it was only possible to reconstitute the ΔKH-Rrp4-exosome. In the crystal structure of the Rrp4-exosome it is shown that the Rrp4 protein anchors to the hexameric ring by the N terminal domain [93, 101, 130]. Therefore as anticipated the variants with the N terminus had more probability to form the complex with the hexamer. However, an interaction between the N terminus polypeptide and the hexameric ring was not observed even at the high salt concentrations. The N terminal domain is a small domain of 65 amino acids. It could be due to the peptide size that the interactions were not strong to form the complex.

S1 and KH of the Rrp4 protein are RNA binding domains. The S1 domains of the RNA binding proteins of the exosomal cap structure make the positively charged central pore where the RNA threads though, to the central channel and to the catalytic sites. The KH and N terminal domains are facing the periphery of the exosome. The size of the S1 pore is determined by all three domains by the electrostatic interactions between the amino acids. It could be due to the lack of KH domain, the size of the central pore changes and it limits the entry of the RNA. This might lead to the lesser degradation efficiency of the ΔKH-Rrp4-exosome in comparison to the hexameric ring and the Rrp4-exosome. In the competition assays, irrespective to the huge amounts of tRNA and MCS RNA, the ΔKH variant was able to degrade or polyadenylate the minor amount of poly (A) RNA. This clearly says that the

KH domain of Rrp4 protein is not important for the poly (A) preference. Here, we revealed that there is no poly (A) preference by the KH domain.

5.3. Heteromeric caps of the exosome

Though heteromeric caps were reconstituted *in vitro* [93] the existence of the heteromeric caps *in vivo* was a question. With Co-IP using anti-Rrp4 and anti-Csl4 antibodies, we found that Csl4 and Rrp4 together are present in the *S. solfataricus* exosome. The presence of the heteromeric RNA binding caps probably ensures its interaction with different transcripts. It is important to note that, in comparison to the hexameric ring, the amount of Csl4 fished by the Co-IP with anti-Csl4 antibodies was more than the amount of Csl4 which was fished with anti-Rrp4 antibodies. However when the Co-IP was done with anti-Rrp4 antibodies, the proportion of Rrp4 in relation to hexameric ring was same as the Co-IP done with anti-Csl4 antibodies (Figure 4.2.4A and B). Since we have ruled out the presence of the monomeric Csl4 in the *S. solfataricus* cells, it could be that there is a mixture of only-Csl4 exosomes and heteromeric caps containing exosomes. Nevertheless the exact stoichiometry between Rrp4 and Csl4 is yet to disclose.

5.4. *Sulfolobus* RNA-exosome under stress conditions

Degradation of RNA plays a central role in RNA metabolism. The rapid decay of mRNA serves a continuous adjustment of the messages to the needs of the cell for distinct proteins [34, 131-133] . Nevertheless stable rRNAs and tRNAs are degraded only under various stress conditions or when an RNA molecule is defective [134]. However in both stable and mRNA degrdation the action of similar ribonucleases (RNases) are required.

Most living beings are faced with a constantly changing environment and multitude of stressors that challenge their survival. The adaptive responses to the stress conditions involve a remodelling of bacterial gene expression and quality control of RNA aimed at adjusting cell physiology to the new environmental demands [135]. As a consequence of the stressed cells, the level of defective RNAs increase and these RNA have a potential to interfere with the function of their normal counterparts. Therefore, it might be expected that they would be repaired or eliminated. In stressed *E. coli* cells RNase R or PNPase are required to degrade

the fragments of rRNA during the quality control of rRNA metabolism and polyadenlation of tRNA and degradation of defected tRNA [42, 47, 136].

The Eukaryotic exosome has been shown to be involved in quality control processes that result in degradation of defective tRNA and rRNA. Furthermore the exosome is also a vital component in mRNA degradation and post transcriptional gene regulation [91, 137]. Very little is known about the role of the archeal exosome *in vivo*. It is interesting to find out whether the archaeal exosome plays a role in degradation of RNA in stress conditions.

We show that the proportion of the soluble exosome increase considerably in the stationary phase and the total amount of the exosomal subunits remain constant during the growth curve, except the RNA binding protein Csl4. These findings advocate that different growth conditions have a direct impact on the *S. solfataricus* exosome.

It is known that ribosomes in *E. coli* are degraded under certain physiological conditions [18, 134]. Usually such degradation is associated with conditions in which nutrient sources are lacking, such as starvation [138, 139], which enable the bacterium to gain access to the large store of potential nutrients that are present in ribosomes. In the growing cells the rRNA is most likely be protected by ribosomal proteins, incorporation in the ribosomes. Though the synthesis of rRNA and ribosomal proteins is closely coordinated in different growth rates [140] once the coordination is disrupted the unprotected rRNA molecules become subject to extensive degradation. Furthermore, during the transition from exponential to stationary phase, a large number of mRNAs are involved in altering gene expression to facilitate cell adaptation and survival in a changing environment lacking optimal nutrients.

5.4.1. Archeal exosome as a cold stress protein

We found that the total amount of the exosome after the cold stress for 30 min, increases when compared to the amount of the exosome before stress. Nevertheless we did not observe any major difference of the exosomal amount after pH low, pH high, and heat stress suggesting that the exosome is hardly affected by these stresses.

Temperature is one of the most pervasive challenges faced by any organism. In *E. coli* there is growth arrest after cold stress. Upon temperature downshift, *E. coli* cells rapidly but transiently produce a selective set of proteins called cold stress proteins (CSPs), which are considered to be essential for cellular adaptation to low temperature [117].

There are massive changes in RNA stability during the cold stress response. Such changes may reflect alterations in the degradation machinery, as the changes in the amounts of both the PNPase and RNase R in *E. coli* [141]. RNase R and PNPase are the only cold stress ribonucleases described so far. RNase R is a cold stress protein that is induced seven- to eightfold by cold stress and its expression is tightly regulated by temperature. The increase of RNase R levels is mainly a result of the stabilization of the *rnr* transcripts. The transient stability of the *rnr* transcripts is shown to be regulated by PNPase at the end of the acclimation phase. Studies with an *rnr* mutant revealed a cold-stress phenotype showing that RNase R contributes to growth at low temperatures [120, 142, 143].

In this chapter we introduce the *S.solfolobus* exososme as a new cold stress protein. The increase in Sso- exosome levels under cold stress conditions raises the question about the physiological role of this exoribonuclease at low temperature. The possible reason could be that the exosome degrades stable RNAs which are produced and are unprotected during the acclimation phase. In the acclimation phase after the cold stress, the cellular protein synthesis is blocked most probably in the translation initiation step except for the cold stress proteins [117, 142]. In this phase, most probably, the portion of rRNA molecules that cannot be correctly assembled into ribosomes is focus to degradation as accumulation of the non-correctly assembled rRNA may lead to cell growth arrest or lost of viability [42]. Thus, quality control of stable RNA metabolism would appear to be an important function for cell survival.

Moreover, it is known that some *E. coli* mRNAs can contain secondary structures [144] and [145], which are considered to become more stable at low temperature. These stable mRNA structures inhibit translation initiation and pause the translational elongation steps. They are considered to be more deleterious at low temperatures. Hence such mRNAs should be eliminated. The archeal exosome possibly plays an important role for processing/degradation of RNA molecules containing secondary structures at low temperature. The role of the exosome may be especially important under stress conditions such as cold stress, when the stabilization of secondary structures of nucleic acids leading to reduced efficiency of mRNA translation and transcription. This also could be a possible explanation for the increment of the soluble exosome after the cold stress. Rapid production of exosomes in a short time period as 30 min, in comparison to the doubling time of *S. solfotaricus*, could be lethal for the cells. We speculate that there could be a certain percentage of exosomes which are active in

the cytoplasm, whereas the rest of the total production in the stress conditions may store in the non soluble fractions. We suppose that the exosomes are stored at the membrane where DnaG and Cls4 proteins are more and when situation demands, exosomes move to the cytoplasmic fractions by changing the composition of the exosome. (DnaG and Cls4 proteins are less).

It was known that DnaG and Csl4 were not detected by Western blot analysis in the S100 fraction [110]. Consistent to those results DnaG and Csl4 were not detected in any of the stress conditions in S100 fractions.

5.4.2. The role of archaeal exosome in stationary phase

We have demonstrated that the solubility of the exosome increases significantly from the exponential phase to the stationary phase though the total content of the exosome do not change throughout the life cycle (except Csl4). The presence of Csl4 proteins independently from the exosome complex in the stationary phase is doubtful. If there are independent Csl4 proteins it should be in the low density fractions of the sucrose density gradients, which we did not observe. Nevertheless we cannot exclude the fact that the Csl4 protein could interact with another complex in the stationary phase which will drag Csl4 to the high density fractions of the sucrose density gradients.

Regardless of whether we can fully distinguish the exact purpose of the increment of the soluble exosome we can speculate that it is important in the metabolism of tRNAs, rRNAs and turnover of mRNAs present in the soluble fractions in the stationary phase. Our research group found that the exosomes are membrane associated [110]. It might be that the exosomes are stored at the membrane and when circumstances demands exosomes move to the cytoplasmic fractions.

To analyse these facts, we decided to further investigate the non soluble exosome by overexpressing the exosomal proteins *in vivo* also to see the structure by single particle electron microscopy (Chapter 4.4).

In summary, these results strongly suggest that archeal exosome plays an important role under cold stress and in the stationary phase for the survival of the cells. Our findings not only further reveal the involvement of exosome in the regulation of RNAs, but also will lead to a better understanding of the exosome complex as a combatant for the survival of the cell.

5.5. Exosome under SPEM

5.5.1. Reconstituted exosome under SPEM

It was not possible to purify recombinant DnaG from the *E coli* strain BL21 (DE3). We used *E. coli* strain Arctic Express cells to overexpress DnaG, which is designed to increase solubility of recombinant proteins by inducing chaperonin proteins at low growth temperatures.

We could analyse the shape of the Csl4-exosome of *S. solfataricus.* Nevertheless we could not see any difference between the Csl4-exosome and the DnaG–Cls4 exosome. The possible explanation could be that in the purified DnaG-Csl4 exosome, there could be a mixture of DnaG-Csl4 exosomes and Csl4-exosomes and the negatively charged grid preferably attaches the Csl4-exosomes. Furthermore due to the uneven charge distribution of the exosome [93], positively charged Csl4 caps bind to the negative grids selectively. Since DnaG protein binds to Csl4, it also could be that the DnaG protein gets hindered in the orientation of binding of the protein complex to the grid.

Electron microscopy is arguably the most powerful tool for spatial imaging of structures. To get images in SPEM with the DnaG-Csl4 exosome, we require firstly a positively charge grid for the binding of the complexes and secondly we need to purify the complexes through a gel filtration column and then concentrating the complexes by Ni-NTA chromatography.

5.5.2. Native exosome under SPEM

The DnaG-His_6 containing overexpressing strain was not able to grow over OD_{600} 0.3-0.4. Other constructs (Rrp4 and Csl4) containing *S. solfataricus* cultures did not grow at all. It seems that the overexpression of exosomal subunits was deleterious for the cells.

Using homologous cloning system, it was possible to produce soluble recombinant DnaG-His_6 proteins in *S. solfataricus*. The protein was purified with the rest of the exosomal proteins using Ni-NTA chromatography and was the expected size of 48kDa (due to the presence of His and Strep-tags) when analysed on SDS-PAGE. Interestingly, a second band of equal intensity was also observed which corresponded in size to the native DnaG, which was approximately 45kDa. Indeed both the bands were identified as DnaG by mass spectrometry analysis and by Western blot analysis. It is possible that due to the oligomeric nature of the native protein (as further proven by the SPEM), an association between the native and recombinant polypeptides has occurred, leading to this co-purification. After the

gel filtration, there were two distinct peaks at 290 kDa and 90 kDa and the major peak was at 90 kDa. The reconstituted Rrp4-exosome usually gives a peak at ~270 kDa in the gel filtration [95]. The free dimeric DnaG proteins give a peak at 90 kDa. In consistence with the result of the silver stained SDS-PAGE gels of the elution fraction of the Ni-NTA chromatography, which visually show that the proportion of DnaG is higher than the rest of the exosomal subunits, the major peak of the gel filtration was also the DnaG protein. It seems that the dimeric DnaG which contain the His-tag does not successfully interact with the exosome though it is yet insoluble.

The concentration of the native exosome was too low to analyse the complex under SPEM. Nevertheless we were able to find out the shape of archeal DnaG as a double lobed protein with a central pore. Our findings are consistent with the crystal structure of *E. coli* DnaG primase. It was found that the crystal structure of the *E. coli* DnaG has a 'groove' in the centre and it is a crescent shaped protein [124].

Following the RNases treatment there were no interaction partners fished with the native exosome, except an RNA chaperone Hfq [Bacillus coagulans 2-6]. This was not reproducible and furthermore this was not identified from *Sulfolobus spp.* Therefore we strongly suggest that it is due to a contamination.

The nucleic acids which were co-purified from the elution fractions of Ni-NTA chromatography were RNA molecules. After the RNase treatment the concentration of the nucleic acids was drastically decreased and following the DNase treatment the nucleic acid concentration was relatively constant. Nevertheless, the control experiment of the PCR had a band which clearly indicates that after the DNase treatment the total DNA is not completely digested, and there is DNA contamination.

The structural mechanism of exosomes in the diverse RNA processing and degradation pathways is still poorly understood. For instance, it is unclear how and why exosomes degrade some RNA substrates in a processive manner but only trim some ribosomal RNA substrates. By finding the shape of the archaeal native DnaG protein and reconstituted Csl4-exosome by SPEM, we believe that we made a considerable progress and have taken to the next level of solving the mystery of the structural mechanism of the exosome.

5.6. Nop5 as an interaction partner of the archaeal exosome

We observed differences in the composition of the soluble and insoluble exosome. So far, little is known about direct protein interaction partners of the archeal nine subunit exosome other than DnaG [95] and EF1α (Chapter 4.1). The co-immunoprecipitation of the Nop5 with the soluble exosome led us to analyse further regarding this interaction between the exosome and protein.

The Co-IP with anti-Nop5 antibody fished the methylation complex. The mass spectrometry analysis suggested that there are no exosomal subunits fished with the methylation complex. However, the strong signals in the Western blot analysis, by hybridizing with anti-Rrp41 and anti-DnaG antibodies, state that the exosome was co-purified along with the methylation complex. For the mass spectrometry analysis, there should be a certain amount of protein on the gel. It could be that the amount of exosome fished with the methylation complex by the Co-IP with anti-Nop5 antibody was not sufficient for the mass spectrometry analysis but it was sufficient to give a signal in the Western blot. Another reason could be that Nop5 antibody was raised as a polyclonal antibody and polyclonal antibodies are not absolutely specific.

The fact that the two complexes have an interaction via RNA molecules was ruled out because after the RNase treatment also the Nop5 antibodies was able to fish out the exosome and DnaG antibodies could co-precipitate the methylation complex.

In the control Western blot analysis anti-Nop5 antibody gave a signal for His-tagged DnaG protein and anti-DnaG antibody gave a signal for His-tagged Nop5 protein. It is important to note that these are polyclonal antibodies and the antibodies are raised against the protein with the His-tag. It could be that the cross signals occur due to recognition of the His-tag by the antibody. Since the attempt to cleave the His-tag was failed, it is better to have the Strep-tagged Nop5 recombinant protein and check for the specificity.

Nop5 is an abundant protein in the *S. solfataricus* cell in the soluble and in the insoluble fractions (Figure 4.5.2D). However, in the depletion assays (to deplete the DnaG containing exosomes from the S100 fraction), we could see the decrease of the DnaG signal in the flow through, in the sequential Co-IP rounds with anti-DnaG-antibody (Figure 4.5.3). If anti-DnaG antibody gives an unspecific signal with Nop5, we should not observe the decrease of the DnaG signal because of the high abundance of the Nop5 protein in the cell.

Nop5 as an interaction partner of the exosome, was first identified in the S100 fraction [122]. Furthermore, we assumed that Nop5 is exchanged to DnaG from S100 fraction to P100 fraction. DnaG is an integral part of the exosome and the ‘exchange’ assumption is ruled out. Therefore further experiments should be done to test whether Nop5 is present in insoluble fractions as well.

It was not possible to reconstitute the Nop5 containing exosome (Hou, unpublished data), therefore the project was stopped. Nevertheless, it could be that Nop5 is interacting with the exosome via a chaperone, or the complete methylation complex is needed for the interaction.

The interaction between Nop5 and the RNA-exosome is not yet clear. Further experiments should be conducted to confirm the interaction between the Nop5 and the exosome.

6. Summary

RNA processing and degradation are essential processes in the cell. The exosome of *S. solfatarticus* is able to degrade and polyadenylate RNA and is localized at the periphery of the cell. The in vitro reconstituted *S. solfolobus* exosome is built of a hexameric ring, containing Rrp41 (the catalytically active subunit) and Rrp42 to which a trimeric cap of RNA binding proteins Rrp4 or Csl4 is bound. Rrp4 confers poly (A) specificity to the exosome. The archaeal DnaG protein which is homologues to the bacterial primase, and an Archaea specific exosomal subunit, directly binds to Csl4 protein in the exosome.

The majority of Rrp41 and DnaG is detectable in the insoluble fraction and is localized at the cell periphery. In this study, it was found that the soluble and insoluble exosomes have different compositions. The soluble exosome contains less DnaG and less Csl4 than the insoluble exosome which co-sediments with ribosomal subunits in sucrose density gradients. However, after the RNase treatment the rRNA was completely degraded but the exosome sedimentation pattern was not changed. Furthermore potential interaction partners such as EF1α and Nop5 were found in the soluble exosome. The soluble and the insoluble exosomes were both active. However, different compositions of the exosome in the cell and thereby the localization could apparently be a common system in prokaryotes to separate biochemical processes in cells without compartmentalization.

In this work Csl4 was co-immunoprecipitated with the exosome using anti-Rrp4 antibodies and vice versa. This finding clearly says that heteromeric RNA-binding caps are present *in vivo*. The presence of the heteromeric RNA binding cap probably ensures its interaction with different transcripts and probably different interaction partners. To understand the mechanism for poly (A) specificity of Rrp4, an exosome with an RNA-binding cap composed of truncated Rrp4 lacking the KH domain was reconstituted and analyzed. The deletion of the KH domain decreased the degradation activity, but the poly (A) specificity was retained. This finding says that the KH domain of the RNA binding Rrp4 protein is not responsible for the poly (A) specificity.

It was further found that the proportion of soluble exosome increases in the stationary phase. Moreover the exosome amount increases under the cold stress conditions. The amount of exosome in pH high, pH low and heat stress was constant. These results strongly suggest that

archeal exosome plays an important role under cold stress and in the stationary phase for the survival of the cells.

Homologous cloning system was used to express recombinant His-tagged exosomal proteins in *S. solfataricus.* It was possible to clone the genes *rrp4, csl4* and *dnaG,* as well as the *dnaG* parts encoding the N terminal and the C terminal portions of the protein, in to the pMJ0503 vector. However it was possible to transform and express only the full length DnaG-His_6 in *S. solfataricus* M16. Overexpression was achieved in the stationary phase and the exosome containing DnaG-His_6 and the native DnaG was isolated by Ni-NTA chromatography. For the first time, the native DnaG which was directly isolated from *S. solfataricus* was observed as a dimer with 2 lobes and a central pore using SPEM. The structure of the protein may help to solve many functions delusions.

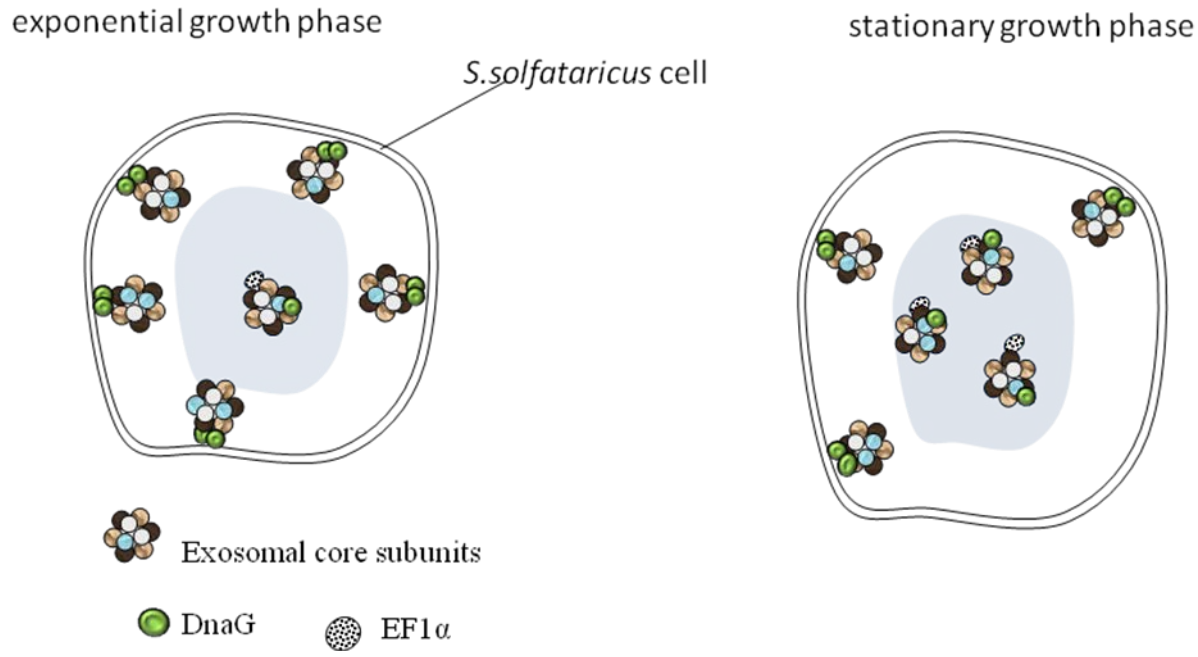

Figure 6.1 Current model of the composition and the distribution of the exosome in *S. solfataricus*. Distribution of the exosomes of different composition in the cell at different growth phases: more soluble exosome is present in the stationary phase than in the exponential phase. Furthermore, the insoluble exosome contain more DnaG and less DnaG is present in the soluble exosome. Proteins such as EF1α, Nop5 interact with the soluble exosome. The model also says that there are heterotrimeric caps in the exosome.

7. List of abbreviations

A	Adenine
Ap	Ampicillin
APS	Ammonium peroxodisulfate
ATP	Adenosine triphosphate
BSA	Bovines-Serum-Albumin
bp	Base pairs
C	Cytosine
°C	Celsius
cDNA	Copy-DNA
Ci	Curie
cpm	Radioactive disintegrations per minute (*counts per minute*)
DNA	Deoxyribonucleic acid
dNTP	Deoxyribonucleoside triphosphate
ddH_2O	Double-distilled water
ds	Double strands
EDTA	Ethylenediaminetetraacetic
et al.	And others
fmol	Femtomol
G	Guanine
g	Grame
g	Gravity
h	Hour

HEPES	4 - (2-hydroxyethyl)-1-piperazine ethanesulphonate
IPTG	isopropylthiogalactoside
k	Kilo
kb	Kilobases (pairs)
kDa	Kilo Dalton
Km	Kanamycin
l	Liter
M	Molar
m	Milli
µ	Micro
mA	Milliamperes
min	Minute
mRNA	Messenger RNA
MW	Molecular weight
Ni-NTA	Ni-NTA-Agarose
nt	Nucleotide
n	Nano
OD	Optical density
PAA	Polyacrylamide
PBS	phosphate buffered saline
PAGE	Polyacrylamide gel electrophoresis
pmol	Pikomol
PPi	pyrophosphate
RNase	Ribonuclease
RNA	Ribonucleic acid
rpm	Revolutions per minute

rRNA	Ribosomal RNA
RT	Room temperature
SDS	Sodium dodecyl sulfate
sec	Seconds
Sm	Streptomycin
snRNAs	Small nuclear RNAs
snoRNAs	Small nucleolar RNAs
ss	Single stranded
T	Thymine
Taq	*Thermus aquaticus*
TAE	Tris-Acetate- EDTA buffer
TBE	Tris-Borate-EDTA buffer
TEMED	N, N, N ', N'-tetramethylethylenediamine
Tris	Tris (hydroxymethyl) aminomethane
tRNA	Transfer RNA
U	Unit (for enzymes)
U	Uracil
UDP	Uridine-5'-diphosphate
UMP	Uridine-5'-monophosphate
UV	Ultraviolet
V	Volt
v/v	Volume /volume ratio
W	Watt
w/v	Weight / volume ratio

8. Appendix

Figure No.	Accession	Name	Mascot Score	Peptides identified	Covered sequence [%]
4.1.2A	gi|15897164	elongation factor 1-alpha [*Sulfolobus solfataricus* P2]	70.6	8	22.06896552
4.1.2A	gi|284173389	DNA primase [*Sulfolobus solfataricus* 98/2]	162	16	41.04477612
4.1.4A	gi|15897164	elongation factor 1-alpha [*Sulfolobus solfataricus* P2]	92	9	23.67816092
4.1.4A	gi|284173389	DNA primase [*Sulfolobus solfataricus* 98/2]	186	15	47.26368159
4.1.4B	gi|261600946	TIP49 domain protein [*Sulfolobus solfataricus* 98/2]	102	13	38.9380531
4.1.4B	gi|284173389	DNA primase [*Sulfolobus solfataricus* 98/2]	272	25	70.64676617
4.2.4A	gi|15897237	exosome complex RNA-binding protein Csl4 [*Sulfolobus solfataricus* P2]	149	12	57.14285714
4.2.4A (left)	gi|284174963	exosome complex RNA-binding protein Rrp4 [*Sulfolobus solfataricus* 98/2]	174	10	44.93927126
4.2.4A (left)	gi|15897237	exosome complex RNA-binding protein Csl4 [*Sulfolobus solfataricus* P2]	254	17	80.42328042
4.2.4A (right)	gi|284174963	exosome complex RNA-binding protein Rrp4 [*Sulfolobus solfataricus* 98/2]	142	13	48.58299595
4.2.4A (right)	gi|15897237	exosome complex RNA-binding protein Csl4 [*Sulfolobus solfataricus* P2]	78.3	8	44.97354497
4.2.4B(left)	gi|284174963	exosome complex RNA-binding protein Rrp4 [*Sulfolobus solfataricus* 98/2]	123	8	36.03238866
4.2.4B (left)	gi|15897237	exosome complex RNA-binding protein Csl4 [*Sulfolobus solfataricus* P2]	183	15	63.49206349

4.2.4B (right)	gi|284174963	exosome complex RNA-binding protein Rrp4 [*Sulfolobus solfataricus* 98/2]	76.6	7	29.55465587
4.2.4B (right)	gi|15897237	exosome complex RNA-binding protein Csl4 [*Sulfolobus solfataricus* P2]	70.3	5	33.33333333
4.4.4E	gi|284173389	DNA primase [Sulfolobus solfataricus 98/2]	199.0	17	49.8
4.4.4E	gi|284173389	DNA primase [Sulfolobus solfataricus 98/2]	195.0	21	56.5
4.4.4E	gi|299689088	Chain A, Crystal Structure Of The S. Solfataricus Archaeal Exosome	73.1	8	30.3
4.4.4E	gi|284174963	exosome complex RNA-binding protein Rrp4 [Sulfolobus solfataricus 98/2]	89.4	7	32.8
4.4.4E	gi|336113906	RNA chaperone Hfq [Bacillus coagulans 2-6]	74.6	4	53.9
4.5.2A	gi|284173389	DNA primase [Sulfolobus solfataricus 98/2]	250	18	52.4
4.5.2A	gi|284173389	DNA primase [Sulfolobus solfataricus 98/2]	235	19	57.21

Appendix 1. Identification of protein bands by mass spectrometry

A

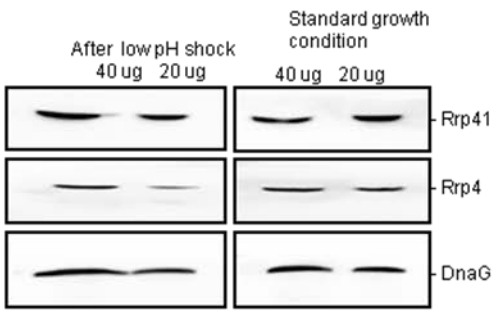

	After low pH shock		Standard growth condition	
	40ug	20 ug	40 ug	20 ug
Rrp41	101	51	96	70
Rrp4	45	30	50	36
DnaG	130	70	145	80

B

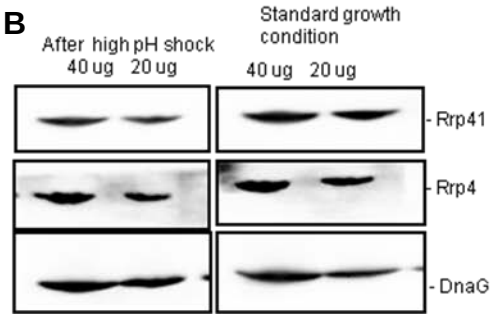

	After high pH shock		Standard growth condition	
	40ug	20 ug	40 ug	20 ug
Rrp41	188	85	200	121
Rrp4	222	80	192	93
DnaG	238	136	210	127

C

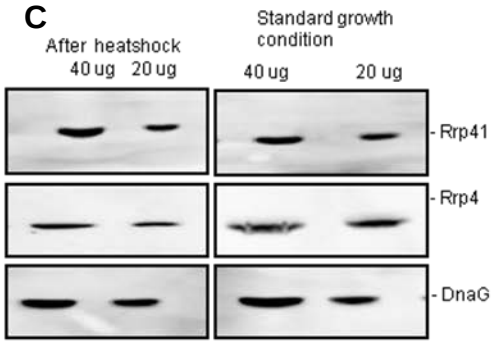

	After heat shock		Standard growth condition	
	40ug	20 ug	40 ug	20 ug
Rrp41	79	44	68	33
Rrp4	93	59	101	60
DnaG	198	89	213	80

Appendix 2. Detection of exosomal subunits in *S. solfataricus* cell-free extract before and after stress by Western blot analysis. The comparison of the Western blot analysis of changes in the amount of the total protein of the exosomal subunits under A) pH low, B) pH high and C) heat shock conditions. Equal weight (µg) amounts of protein were separated in 12% SDS-PAGE, blotted and hybridized with sera directed against the exosomal subunits indicated on the right side of the panels. Quantification of the of signals are measured and indicated on the tables on the right side. The chemiluminescent signals in the Western blot was detected by a digital imaging system in fusion X4 machine and signal intensities were quantified by the fusion X4 software. The intensities are divided by 1000 and rounded to the nearest decimal point.

A

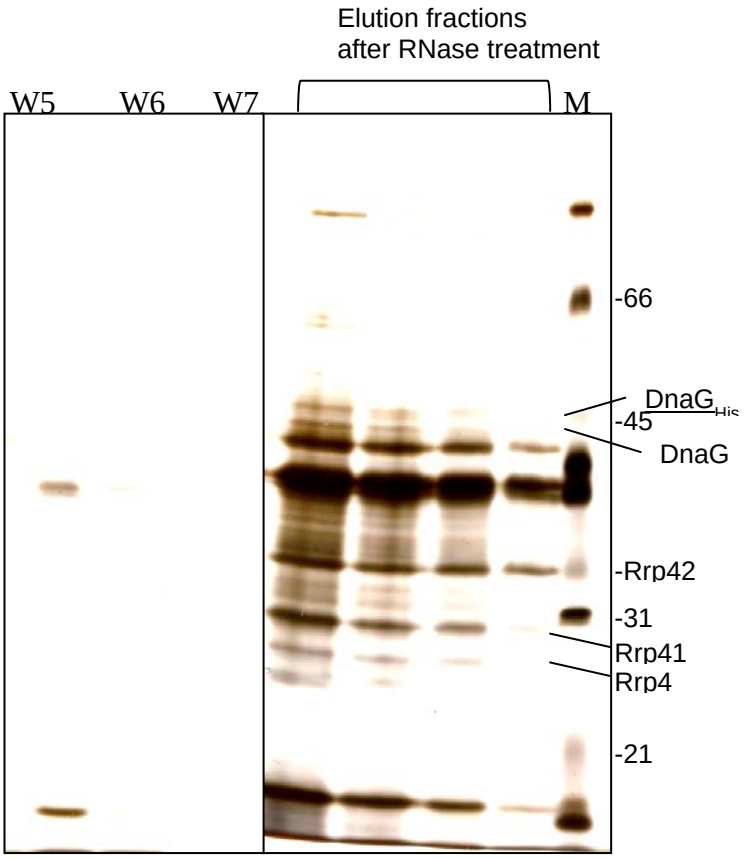
Elution fractions
after RNase treatment
W5
W6
W7
M
-66
DnaG$_{His}$
-45
DnaG
-Rrp42
-31
Rrp41
Rrp4
-21

B

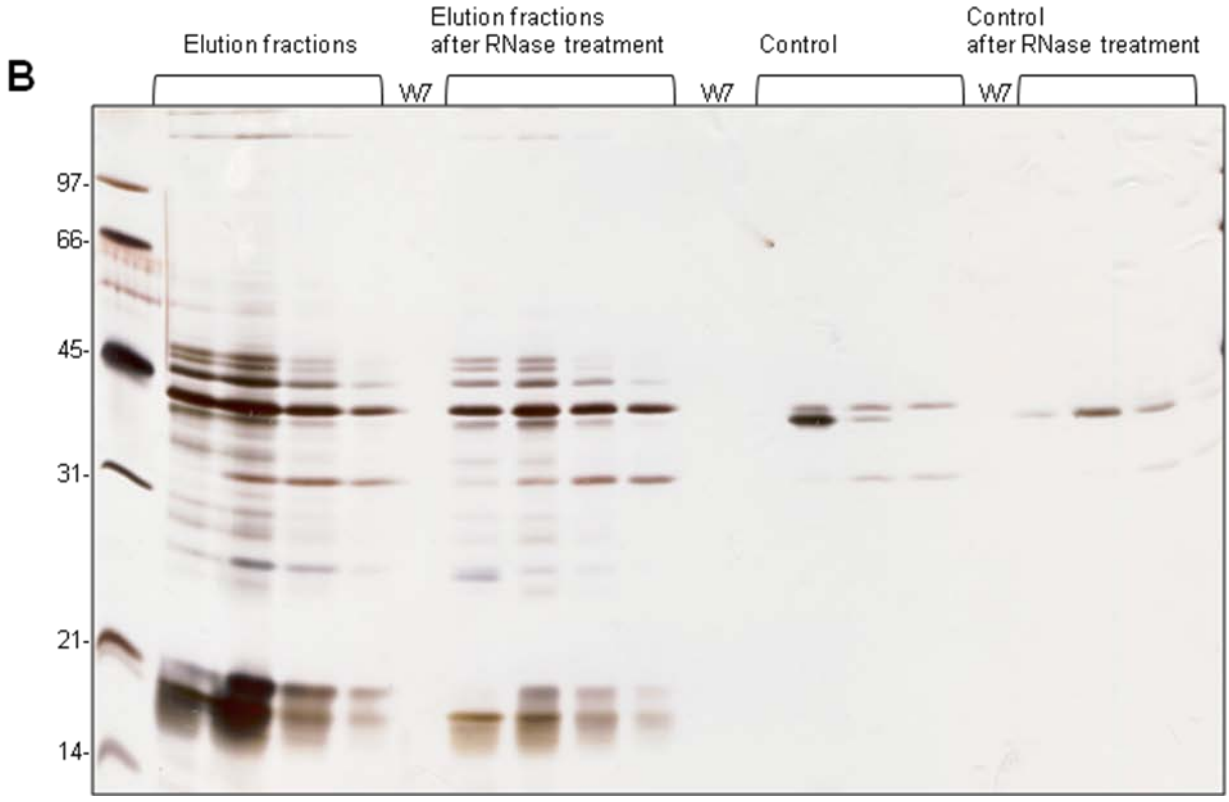
Elution fractions
Elution fractions
after RNase treatment
Control
Control
after RNase treatment
W7
W7
W7
97-
66-
45-
31-
21-
14-

Appendix 3 . A and B: Repetition experiments of purification of the exosome by Ni –NTA chromatography directly from *S. solfataricus*. The elution fractions were separated in a 12% SDS-PAGE gel and silver stained. W5,W6 washing fractions, W7 last washing fraction, M, maker in kDa. The last washing fraction did not contain any proteins.

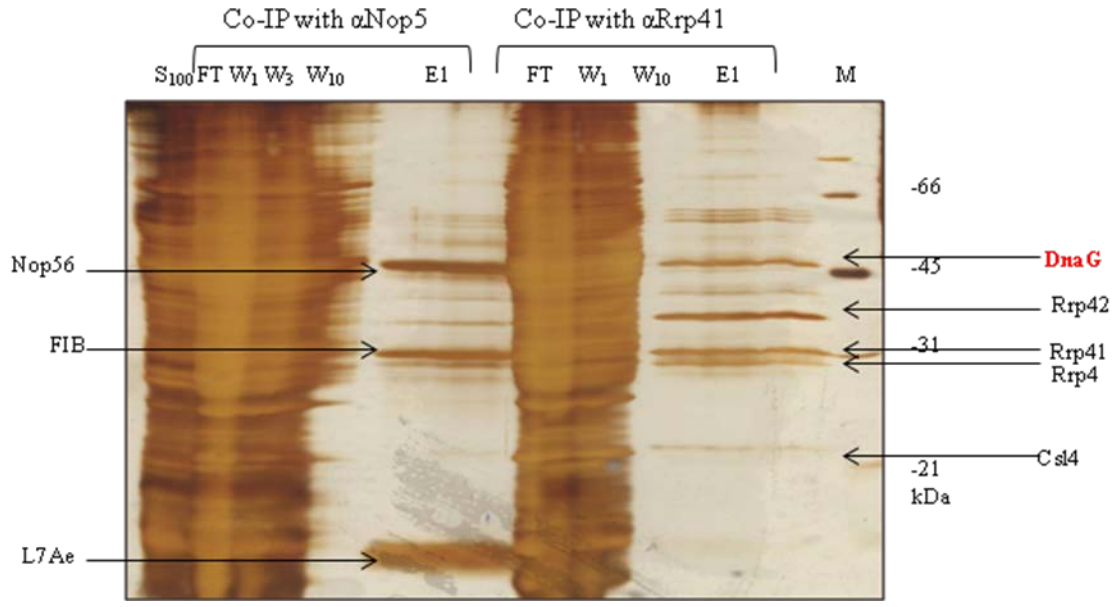

Appendix 4. Co-IP of the Nop5 protein from the S100 fraction of the stationary phase S. solfataricus cells by anti-Nop5 antibodies and anti-Rrp41 antibodies. The silver stained gel with the input (S100), the flow through (FT) and the washing fractions, W1, first washing fraction, W3 washing fractions, W10 last washing fraction, E, elution fraction, M, maker in kDa.

9. Acknowledgement

- I would like to thank everyone who helped me to make this project a success....
- I'd like to give special thanks, beginning with Prof Dr. Gabrile Klug for selecting me to her team and for the support throughout the doctoral program.
- I'd also like to give a heartfelt, special thanks to PD. Dr. Elena Evguenieva-Hackenburg for her remarkable motivation, encouragement and guidance.
- My gratitude is also extended to Prof. Thomas Walz (University of Harvard, Boston, USA) and Dr. Janet Vonck (University of Frankfurt MPI, Germany) for accepting me for the lab rotation, helping and guiding me in SPEM.
- Thanks you Dr. Sonja-Verena Albers and Dr. Benjamin Meyer helping me in *in vivo* cloning.
- Thanks a lot Prof. G. Lochnit for the mass spectrometry analysis of the protein bands.
- Thank you Dr. Verena Roppelt... one of the first friendly faces to greet me when I began this doctoral program and has always been a tremendous help no matter the task or circumstance.
- Thank you my all my lab mates, including Julia, Kathrin and Linlin and all the mates from the Klug's group for the wonderful times we had, in the lab and out of the lab.
- Special thanks for my dearest friend Dhanushka, who encouraged me though out my doctoral program.
- Last, but certainly not least, I must acknowledge with tremendous and deep thanks to my family... for always being there for me...

10. Literature

1. Woese, C.R., O. Kandler, and M.L. Wheelis, *Towards a natural system of organisms: proposal for the domains Archaea, Bacteria, and Eucarya.* Proc Natl Acad Sci U S A, 1990. **87**(12): p. 4576-9.
2. Woese, C.R. and G.E. Fox, *The concept of cellular evolution.* J Mol Evol, 1977. **10**(1): p. 1-6.
3. Huber, H., et al., *A new phylum of Archaea represented by a nanosized hyperthermophilic symbiont.* Nature, 2002. **417**(6884): p. 63-7.
4. Pikuta, E.V., R.B. Hoover, and J. Tang, *Microbial extremophiles at the limits of life.* Critical Reviews in Microbiology, 2007. **33**(3): p. 183-209.
5. Madigan M.T, M.J.M., *Brock Biology of Microorganisms* 11 ed. 2006.
6. Edgell, D.R. and W.F. Doolittle, *Archaea and the origin(s) of DNA replication proteins.* Cell, 1997. **89**(7): p. 995-998.
7. Bell, S.D. and S.P. Jackson, *Transcription and translation in Archaea: A mosaic of eukaryal and bacterial features.* Trends in Microbiology, 1998. **6**(6): p. 222-228.
8. Bell, S.D. and S.P. Jackson, *Transcription in Archaea.* Cold Spring Harbor Symposia on Quantitative Biology, 1998. **63**: p. 41-51.
9. Stetter, K.O., *Hyperthermophiles in the history of life.* Philosophical Transactions of the Royal Society B-Biological Sciences, 2006. **361**(1474): p. 1837-1842.
10. Derosa, M., A. Gambacorta, and J.D. Bulock, *Extremely Thermophilic Acidophilic Bacteria Convergent with Sulfolobus-Acidocaldarius.* Journal of General Microbiology, 1975. **86**(Jan): p. 156-164.
11. Zillig, W., et al., *The Sulfolobus-Caldariella Group - Taxonomy on the Basis of the Structure of DNA-Dependent Rna-Polymerases.* Archives of Microbiology, 1980. **125**(3): p. 259-269.
12. She, Q., et al., *The complete genome of the crenarchaeon Sulfolobus solfataricus P2.* Proc Natl Acad Sci U S A, 2001. **98**(14): p. 7835-40.
13. Grogan, D.W., *Phenotypic characterization of the archaebacterial genus Sulfolobus: comparison of five wild-type strains.* J Bacteriol, 1989. **171**(12): p. 6710-9.
14. Moll, R. and G. Schafer, *Chemiosmotic-H+ Cycling across the Plasma-Membrane of the Thermoacidophilic Archaebacterium Sulfolobus-Acidocaldarius.* Febs Letters, 1988. **232**(2): p. 359-363.
15. Stetter, K.O., *History of discovery of the first hyperthermophiles.* Extremophiles, 2006. **10**(5): p. 357-362.
16. Lynn Margulis, M.C., *Kingdoms and Domains: An Illustrated Guide to the Phyla of Life on Earth*. 2009: Academic Press.
17. Gruissem, W., et al., *Transcriptional and post-transcriptional control of plastid mRNA levels in higher plants.* Trends Genet, 1988. **4**(9): p. 258-63.
18. Deutscher, M.P., *Degradation of RNA in bacteria: comparison of mRNA and stable RNA.* Nucleic Acids Res, 2006. **34**(2): p. 659-66.
19. Rauhut, R. and G. Klug, *mRNA degradation in bacteria.* FEMS Microbiol Rev, 1999. **23**(3): p. 353-70.
20. Bernstein, J.A., et al., *Global analysis of mRNA decay and abundance in Escherichia coli at single-gene resolution using two-color fluorescent DNA microarrays.* Proc Natl Acad Sci U S A, 2002. **99**(15): p. 9697-702.
21. Viegas, S.C. and C.M. Arraiano, *Regulating the regulators: How ribonucleases dictate the rules in the control of small non-coding RNAs.* RNA Biol, 2008. **5**(4): p. 230-43.

22. Vogel, J. and E.G. Wagner, *Target identification of small noncoding RNAs in bacteria.* Curr Opin Microbiol, 2007. **10**(3): p. 262-70.
23. Regnier, P. and C.M. Arraiano, *Degradation of mRNA in bacteria: emergence of ubiquitous features.* Bioessays, 2000. **22**(3): p. 235-44.
24. Yehudai-Resheff, S. and G. Schuster, *Characterization of the E.coli poly(A) polymerase: nucleotide specificity, RNA-binding affinities and RNA structure dependence.* Nucleic Acids Research, 2000. **28**(5): p. 1139-1144.
25. O'Hara, E.B., et al., *Polyadenylylation helps regulate mRNA decay in Escherichia coli.* Proc Natl Acad Sci U S A, 1995. **92**(6): p. 1807-11.
26. Mohanty, B.K. and S.R. Kushner, *The majority of Escherichia coli mRNAs undergo post-transcriptional modification in exponentially growing cells.* Nucleic Acids Res, 2006. **34**(19): p. 5695-704.
27. Deana, A., H. Celesnik, and J.G. Belasco, *The bacterial enzyme RppH triggers messenger RNA degradation by 5' pyrophosphate removal.* Nature, 2008. **451**(7176): p. 355-8.
28. Mackie, G.A., *Ribonuclease E is a 5 '-end-dependent endonuclease.* Nature, 1998. **395**(6703): p. 720-723.
29. Coburn, G.A. and G.A. Mackie, *Degradation of mRNA in Escherichia coli: an old problem with some new twists.* Prog Nucleic Acid Res Mol Biol, 1999. **62**: p. 55-108.
30. Heck, C., et al., *RNase E enzymes from rhodobacter capsulatus and Escherichia coli differ in context- and sequence-dependent in vivo cleavage within the polycistronic puf mRNA.* J Bacteriol, 1999. **181**(24): p. 7621-5.
31. Feng, Y.A., T.A. Vickers, and S.N. Cohen, *The catalytic domain of RNase E shows inherent 3 ' to 5 ' directionality in cleavage site selection.* Proceedings of the National Academy of Sciences of the United States of America, 2002. **99**(23): p. 14746-14751.
32. Morita, T., K. Maki, and H. Aiba, *RNase E-based ribonucleoprotein complexes: mechanical basis of mRNA destabilization mediated by bacterial noncoding RNAs.* Genes Dev, 2005. **19**(18): p. 2176-86.
33. Laalami, S., et al., *Bacillus subtilis RNase Y activity in vivo analysed by tiling microarrays.* PLoS One. **8**(1): p. e54062.
34. Kushner, S.R., *mRNA decay in Escherichia coli comes of age.* J Bacteriol, 2002. **184**(17): p. 4658-65; discussion 4657.
35. Evguenieva-Hackenberg, E. and G. Klug, *RNase III processing of intervening sequences found in helix 9 of 23S rRNA in the alpha subclass of Proteobacteria.* J Bacteriol, 2000. **182**(17): p. 4719-29.
36. Babitzke, P., et al., *Analysis of Messenger-Rna Decay and Ribosomal-Rna Processing in Escherichia-Coli Multiple Mutants Carrying a Deletion in Rnase-Iii.* Journal of Bacteriology, 1993. **175**(1): p. 229-239.
37. Regnier, P., M. Grunberg-Manago, and C. Portier, *Nucleotide sequence of the pnp gene of Escherichia coli encoding polynucleotide phosphorylase. Homology of the primary structure of the protein with the RNA-binding domain of ribosomal protein S1.* J Biol Chem, 1987. **262**(1): p. 63-8.
38. Symmons, M.F., et al., *Running rings around RNA: a superfamily of phosphate-dependent RNases.* Trends Biochem Sci, 2002. **27**(1): p. 11-8.
39. Stickney, L.M., et al., *Function of the conserved S1 and KH domains in polynucleotide phosphorylase.* J Bacteriol, 2005. **187**(21): p. 7214-21.
40. Cheng, Z.F. and M.P. Deutscher, *Purification and characterization of the Escherichia coli exoribonuclease RNase R. Comparison with RNase II.* J Biol Chem, 2002. **277**(24): p. 21624-9.
41. Chen, C. and M.P. Deutscher, *Elevation of RNase R in response to multiple stress conditions.* J Biol Chem, 2005. **280**(41): p. 34393-6.

42. Cheng, Z.F. and M.P. Deutscher, *Quality control of ribosomal RNA mediated by polynucleotide phosphorylase and RNase R.* Proc Natl Acad Sci U S A, 2003. **100**(11): p. 6388-93.
43. Awano, N., et al., *Escherichia coli RNase R Has Dual Activities, Helicase and RNase.* Journal of Bacteriology, 2010. **192**(5): p. 1344-1352.
44. Cheng, Z.F. and M.P. Deutscher, *An important role for RNase R in mRNA decay.* Mol Cell, 2005. **17**(2): p. 313-8.
45. Marujo, P.E., et al., *RNase II removes the oligo(A) tails that destabilize the rpsO mRNA of Escherichia coli.* Rna-a Publication of the Rna Society, 2000. **6**(8): p. 1185-1193.
46. Cheng, Z.F., et al., *The vacB gene required for virulence in Shigella flexneri and Escherichia coli encodes the exoribonuclease RNase R.* J Biol Chem, 1998. **273**(23): p. 14077-80.
47. Li, Z. and M.P. Deutscher, *RNase E plays an essential role in the maturation of Escherichia coli tRNA precursors.* RNA, 2002. **8**(1): p. 97-109.
48. Mohanty, B.K. and S.R. Kushner, *Analysis of the function of Escherichia coli poly(A) polymerase I in RNA metabolism.* Mol Microbiol, 1999. **34**(5): p. 1094-108.
49. Datta, A.K. and K. Niyogi, *A novel oligoribonuclease of Escherichia coli. II. Mechanism of action.* J Biol Chem, 1975. **250**(18): p. 7313-9.
50. Ghosh, S. and M.P. Deutscher, *Oligoribonuclease is an essential component of the mRNA decay pathway.* Proceedings of the National Academy of Sciences of the United States of America, 1999. **96**(8): p. 4372-4377.
51. Even, S., et al., *Ribonucleases J1 and J2: two novel endoribonucleases in B.subtilis with functional homology to E.coli RNase E.* Nucleic Acids Research, 2005. **33**(7): p. 2141-2152.
52. Mathy, N., et al., *5'-to-3' exoribonuclease activity in bacteria: role of RNase J1 in rRNA maturation and 5' stability of mRNA.* Cell, 2007. **129**(4): p. 681-92.
53. Madhugiri, R. and E. Evguenieva-Hackenberg, *RNase J is involved in the 5 '-end maturation of 16S rRNA and 23S rRNA in Sinorhizobium meliloti.* Febs Letters, 2009. **583**(14): p. 2339-2342.
54. Kaberdin, V.R., D. Singh, and L.C. Sue, *Composition and conservation of the mRNA-degrading machinery in bacteria.* Journal of Biomedical Science, 2011. **18**.
55. Cohen, S.N. and K.J. McDowall, *RNase E: still a wonderfully mysterious enzyme.* Mol Microbiol, 1997. **23**(6): p. 1099-106.
56. Carpousis, A.J., *The RNA degradosome of Escherichia coli: an mRNA-degrading machine assembled on RNase E.* Annu Rev Microbiol, 2007. **61**: p. 71-87.
57. Khemici, V. and A.J. Carpousis, *The RNA degradosome and poly(A) polymerase of Escherichia coli are required in vivo for the degradation of small mRNA decay intermediates containing REP-stabilizers.* Mol Microbiol, 2004. **51**(3): p. 777-90.
58. Liou, G.G., et al., *DEAD box RhlB RNA helicase physically associates with exoribonuclease PNPase to degrade double-stranded RNA independent of the degradosome-assembling region of RNase E.* J Biol Chem, 2002. **277**(43): p. 41157-62.
59. Py, B., et al., *A DEAD-box RNA helicase in the Escherichia coli RNA degradosome.* Nature, 1996. **381**(6578): p. 169-172.
60. Khemici, V., et al., *The RNase E of Escherichia coli is a membrane-binding protein.* Molecular Microbiology, 2008. **70**(4): p. 799-813.
61. Taghbalout, A. and L. Rothfield, *RNaseE and RNA helicase B play central roles in the cytoskeletal organization of the RNA degradosome.* J Biol Chem, 2008. **283**(20): p. 13850-5.
62. Lewis, P.J., S.D. Thaker, and J. Errington, *Compartmentalization of transcription and translation in Bacillus subtilis.* Embo Journal, 2000. **19**(4): p. 710-718.
63. Konarska, M.M., R.A. Padgett, and P.A. Sharp, *Recognition of cap structure in splicing in vitro of mRNA precursors.* Cell, 1984. **38**(3): p. 731-6.
64. Edery, I. and N. Sonenberg, *Cap-dependent RNA splicing in a HeLa nuclear extract.* Proc Natl Acad Sci U S A, 1985. **82**(22): p. 7590-4.

65. Wang, Z.R. and M. Kiledjian, *Functional link between the mammalian exosome and mRNA decapping.* Cell, 2001. **107**(6): p. 751-762.
66. Haracska, L., et al., *Trf4 and Trf5 proteins of Saccharomyces cerevisiae exhibit poly(A) RNA polymerase activity but no DNA polymerase activity.* Mol Cell Biol, 2005. **25**(22): p. 10183-9.
67. LaCava, J., et al., *RNA degradation by the exosome is promoted by a nuclear polyade nylation complex.* Cell, 2005. **121**(5): p. 713-724.
68. Raghavan, A. and P.R. Bohjanen, *Microarray-based analyses of mRNA decay in the regulation of mammalian gene expression.* Brief Funct Genomic Proteomic, 2004. **3**(2): p. 112-24.
69. Tucker, M., et al., *The transcription factor associated Ccr4 and Caf1 proteins are components of the major cytoplasmic mRNA deadenylase in Saccharomyces cerevisiae.* Cell, 2001. **104**(3): p. 377-386.
70. Tucker, M., et al., *Ccr4p is the catalytic subunit of a Ccr4p/Pop2p/Notp mRNA deadenylase complex in Saccharomyces cerevisiae.* Embo Journal, 2002. **21**(6): p. 1427-1436.
71. Decker, C.J. and R. Parker, *A turnover pathway for both stable and unstable mRNAs in yeast: evidence for a requirement for deadenylation.* Genes Dev, 1993. **7**(8): p. 1632-43.
72. Mitchell, P., et al., *The exosome: a conserved eukaryotic RNA processing complex containing multiple 3'-->5' exoribonucleases.* Cell, 1997. **91**(4): p. 457-66.
73. Allmang, C., et al., *Degradation of ribosomal RNA precursors by the exosome.* Nucleic Acids Research, 2000. **28**(8): p. 1684-1691.
74. Hilleren, P. and R. Parker, *mRNA surveillance in eukaryotes: Kinetic proofreading of proper translation termination as assessed by mRNP domain organization?* Rna-a Publication of the Rna Society, 1999. **5**(6): p. 711-719.
75. Hilleren, P. and R. Parker, *Mechanisms of mRNA surveillance in eukaryotes.* Annual Review of Genetics, 1999. **33**: p. 229-260.
76. Makino, D.L., M. Baumgartner, and E. Conti, *Crystal structure of an RNA-bound 11-subunit eukaryotic exosome complex.* Nature, 2013. **495**(7439): p. 70-75.
77. Wasmuth, E.V. and C.D. Lima, *Exo- and endoribonucleolytic activities of yeast cytoplasmic and nuclear RNA exosomes are dependent on the noncatalytic core and central channel.* Mol Cell. **48**(1): p. 133-44.
78. Dziembowski, A., et al., *A single subunit, Dis3, is essentially responsible for yeast exosome core activity.* Nature Structural & Molecular Biology, 2007. **14**(1): p. 15-22.
79. Anderson, J.S.J. and R. Parker, *The 3 ' to 5 ' degradation of yeast mRNAs is a general mechanism for mRNA turnover that requires the SKI2 DEVH box protein and 3 ' to 5 ' exonucleases of the exosome complex.* Embo Journal, 1998. **17**(5): p. 1497-1506.
80. Stead, J.A., et al., *The PMC2NT domain of the catalytic exosome subunit Rrp6p provides the interface for binding with its cofactor Rrp47p, a nucleic acid-binding protein.* Nucleic Acids Res, 2007. **35**(16): p. 5556-67.
81. Allmang, C., et al., *Functions of the exosome in rRNA, snoRNA and snRNA synthesis.* EMBO J, 1999. **18**(19): p. 5399-410.
82. Hilleren, P., et al., *Quality control of mRNA 3 '-end processing is linked to the nuclear exosome.* Nature, 2001. **413**(6855): p. 538-542.
83. Woese, C.R. and G.E. Fox, *Phylogenetic structure of the prokaryotic domain: the primary kingdoms.* Proc Natl Acad Sci U S A, 1977. **74**(11): p. 5088-90.
84. Hasenohrl, D., et al., *Translation initiation factor a/eIF2(-gamma) counteracts 5' to 3' mRNA decay in the archaeon Sulfolobus solfataricus.* Proc Natl Acad Sci U S A, 2008. **105**(6): p. 2146-50.
85. Andersson, A.F., et al., *Global analysis of mRNA stability in the archaeon Sulfolobus.* Genome Biology, 2006. **7**(10).
86. Portnoy, V., et al., *RNA polyadenylation in Archaea: not observed in Haloferax while the exosome polynucleotidylates RNA in Sulfolobus.* EMBO Rep, 2005. **6**(12): p. 1188-93.

87. Levy, S., et al., *Distinct activities of several RNase J proteins in methanogenic archaea.* Rna Biology, 2011. **8**(6): p. 1073-1083.
88. Roppelt, V., G. Klug, and E. Evguenieva-Hackenberg, *The evolutionarily conserved subunits Rrp4 and Csl4 confer different substrate specificities to the archaeal exosome.* FEBS Lett. **584**(13): p. 2931-6.
89. Kletzin, A., *Metabolism of inorganic sulfur compounds in Archaea in Archaea : evolution, physiology, and molecular biology*. 2007, Malden, Mass: Blackwell Publications.
90. **Kletzin, A.**, *Chapter 2: General Characteristics and Important Model Organisms in Archaea : evolution, physiology, and molecular biology*. 2007, Washington, DC ASM Press
91. Koonin, E.V., Y.I. Wolf, and L. Aravind, *Prediction of the archaeal exosome and its connections with the proteasome and the translation and transcription machineries by a comparative-genomic approach.* Genome Res, 2001. **11**(2): p. 240-52.
92. Evguenieva-Hackenberg, E., et al., *An exosome-like complex in Sulfolobus solfataricus.* EMBO Rep, 2003. **4**(9): p. 889-93.
93. Buttner, K., K. Wenig, and K.P. Hopfner, *Structural framework for the mechanism of archaeal exosomes in RNA processing.* Mol Cell, 2005. **20**(3): p. 461-71.
94. Ramos, C.R., et al., *The Pyrococcus exosome complex: structural and functional characterization.* J Biol Chem, 2006. **281**(10): p. 6751-9.
95. Walter, P., et al., *Characterization of native and reconstituted exosome complexes from the hyperthermophilic archaeon Sulfolobus solfataricus.* Mol Microbiol, 2006. **62**(4): p. 1076-89.
96. Thoms, S., *Cdc48 can distinguish between native and non-native proteins in the absence of cofactors.* Febs Letters, 2002. **520**(1-3): p. 107-110.
97. Ruggero, D., A. Ciammaruconi, and P. Londei, *The chaperonin of the archaeon Sulfolobus solfataricus is an RNA-binding protein that participates in ribosomal RNA processing.* Embo Journal, 1998. **17**(12): p. 3471-3477.
98. Hou, L., G. Klug, and E. Evguenieva-Hackenberg, *The archaeal DnaG protein needs Csl4 for binding to the exosome and enhances its interaction with adenine-rich RNAs.* RNA Biol. **10**(3).
99. Zuo, Z., et al., *Characterization of a functional DnaG-type primase in archaea: implications for a dual-primase system.* J Mol Biol. **397**(3): p. 664-76.
100. Evguenieva-Hackenberg, E., *The archaeal exosome.* Adv Exp Med Biol. **702**: p. 29-38.
101. Lorentzen, E., et al., *The archaeal exosome core is a hexameric ring structure with three catalytic subunits.* Nat Struct Mol Biol, 2005. **12**(7): p. 575-81.
102. Ng, C.L., et al., *Structure of the Methanothermobacter thermautotrophicus exosome RNase PH ring.* Acta Crystallographica Section D-Biological Crystallography, 2010. **66**: p. 522-528.
103. Lorentzen, E. and E. Conti, *Structural basis of 3' end RNA recognition and exoribonucleolytic cleavage by an exosome RNase PH core.* Mol Cell, 2005. **20**(3): p. 473-81.
104. Navarro, M.V.A.S., et al., *Insights into the mechanism of progressive RNA degradation by the archaeal exosome.* Journal of Biological Chemistry, 2008. **283**(20): p. 14120-14131.
105. Evguenieva-Hackenberg, E., et al., *Rrp4 and Csl4 are needed for efficient degradation but not for polyadenylation of synthetic and natural RNA by the archaeal exosome.* Biochemistry, 2008. **47**(50): p. 13158-68.
106. Luz, J.S., et al., *Identification of archaeal proteins that affect the exosome function in vitro.* Bmc Biochemistry, 2010. **11**.
107. DeVendittis, E. and V. Bocchini, *Protein-encoding genes in the sulfothermophilic archaea Sulfolobus and Pyrococcus.* Gene, 1996. **176**(1-2): p. 27-33.
108. Anderson, J.R., et al., *Sequence-specific RNA binding mediated by the RNase PH domain of components of the exosome.* RNA, 2006. **12**(10): p. 1810-6.
109. van Hoof, A., P. Lennertz, and R. Parker, *Yeast exosome mutants accumulate 3'-extended polyadenylated forms of U4 small nuclear RNA and small nucleolar RNAs.* Mol Cell Biol, 2000. **20**(2): p. 441-52.

110. Roppelt, V., et al., *The archaeal exosome localizes to the membrane.* FEBS Lett. **584**(13): p. 2791-5.
111. Albers, S.V., et al., *Production of recombinant and tagged proteins in the hyperthermophilic archaeon Sulfolobus solfataricus.* Appl Environ Microbiol, 2006. **72**(1): p. 102-11.
112. Porath, J., et al., *Metal chelate affinity chromatography, a new approach to protein fractionation.* Nature, 1975. **258**(5536): p. 598-9.
113. Bradford, M.M., *A rapid and sensitive method for the quantitation of microgram quantities of protein utilizing the principle of protein-dye binding.* Anal Biochem, 1976. **72**: p. 248-54.
114. Shi, Z., et al., *Crystal structure of Escherichia coli PNPase: central channel residues are involved in processive RNA degradation.* RNA, 2008. **14**(11): p. 2361-71.
115. Yehudai-Resheff, S., et al., *Domain analysis of the chloroplast polynucleotide phosphorylase reveals discrete functions in RNA degradation, polyadenylation, and sequence homology with exosome proteins.* Plant Cell, 2003. **15**(9): p. 2003-19.
116. Walter, P., *Aufkarung von struktur und funktion des archaealen Exosoms durch charakterisierung nativer und rekonstituierter proteinkomplexe aus Solfalobus solfataricus*. 2008.
117. Jones, P.G., R.A. VanBogelen, and F.C. Neidhardt, *Induction of proteins in response to low temperature in Escherichia coli.* J Bacteriol, 1987. **169**(5): p. 2092-5.
118. Beran, R.K. and R.W. Simons, *Cold-temperature induction of Escherichia coli polynucleotide phosphorylase occurs by reversal of its autoregulation.* Mol Microbiol, 2001. **39**(1): p. 112-25.
119. Zangrossi, S., et al., *Transcriptional and post-transcriptional control of polynucleotide phosphorylase during cold acclimation in Escherichia coli.* Mol Microbiol, 2000. **36**(6): p. 1470-80.
120. Yamanaka, K. and M. Inouye, *Selective mRNA degradation by polynucleotide phosphorylase in cold shock adaptation in Escherichia coli.* J Bacteriol, 2001. **183**(9): p. 2808-16.
121. Prud'homme-Genereux, A., et al., *Physical and functional interactions among RNase E, polynucleotide phosphorylase and the cold-shock protein, CsdA: evidence for a 'cold shock degradosome'.* Mol Microbiol, 2004. **54**(5): p. 1409-21.
122. Lassek, C., *Master thesis*. 2011.
123. Hahn, J., *Master thesis*. 2012
124. Keck, J.L., et al., *Structure of the RNA polymerase domain of E. coli primase.* Science, 2000. **287**(5462): p. 2482-6.
125. Null, M. 2010.
126. Omer, A.D., et al., *In vitro reconstitution and activity of a C/D box methylation guide ribonucleoprotein complex.* Proc Natl Acad Sci U S A, 2002. **99**(8): p. 5289-94.
127. Farhoud, M.H., et al., *Protein complexes in the archaeon Methanothermobacter thermautotrophicus analyzed by blue native/SDS-PAGE and mass spectrometry.* Mol Cell Proteomics, 2005. **4**(11): p. 1653-63.
128. Li, Z., et al., *Affinity purification of an archaeal DNA replication protein network.* MBio. **1**(5).
129. Kobayashi, K., et al., *Structural basis for mRNA surveillance by archaeal Pelota and GTP-bound EF1alpha complex.* Proc Natl Acad Sci U S A. **107**(41): p. 17575-9.
130. Lu, C., F. Ding, and A. Ke, *Crystal structure of the S. solfataricus archaeal exosome reveals conformational flexibility in the RNA-binding ring.* PLoS One. **5**(1): p. e8739.
131. Jain, C., *Degradation of mRNA in Escherichia coli.* IUBMB Life, 2002. **54**(6): p. 315-21.
132. Condon, C., *RNA processing and degradation in Bacillus subtilis.* Microbiol Mol Biol Rev, 2003. **67**(2): p. 157-74, table of contents.
133. Baker, K.E. and C. Condon, *Under the Tucson sun: a meeting in the desert on mRNA decay.* RNA, 2004. **10**(11): p. 1680-91.

134. Deutscher, M.P., *Degradation of stable RNA in bacteria.* J Biol Chem, 2003. **278**(46): p. 45041-4.
135. Eriksson, S., R. Hurme, and M. Rhen, *Low-temperature sensors in bacteria.* Philos Trans R Soc Lond B Biol Sci, 2002. **357**(1423): p. 887-93.
136. Cohen, L. and R. Kaplan, *Accumulation of nucleotides by starved Escherichia coli cells as a probe for the involvement of ribonucleases in ribonucleic acid degradation.* J Bacteriol, 1977. **129**(2): p. 651-7.
137. Anantharaman, V., E.V. Koonin, and L. Aravind, *Comparative genomics and evolution of proteins involved in RNA metabolism.* Nucleic Acids Res, 2002. **30**(7): p. 1427-64.
138. Jacobson, A. and D. Gillespie, *Metabolic events occurring during recovery from prolonged glucose starvation in Escherichia coli.* J Bacteriol, 1968. **95**(3): p. 1030-9.
139. Schlessinger, D. and F. Ben-Hamida, *Turnover of protein in Escherichia coli starving for nitrogen.* Biochim Biophys Acta, 1966. **119**(1): p. 171-82.
140. Gausing, K., *Regulation of ribosome production in Escherichia coli: synthesis and stability of ribosomal RNA and of ribosomal protein messenger RNA at different growth rates.* J Mol Biol, 1977. **115**(3): p. 335-54.
141. Cairrao, F., et al., *Cold shock induction of RNase R and its role in the maturation of the quality control mediator SsrA/tmRNA.* Mol Microbiol, 2003. **50**(4): p. 1349-60.
142. Yamanaka, K., *Cold shock response in Escherichia coli.* J Mol Microbiol Biotechnol, 1999. **1**(2): p. 193-202.
143. Liang, W. and M.P. Deutscher, *Transfer-messenger RNA-SmpB protein regulates ribonuclease R turnover by promoting binding of HslUV and Lon proteases.* J Biol Chem. **287**(40): p. 33472-9.
144. Gold, L., G. Stormo, and R. Saunders, *Escherichia coli translational initiation factor IF3: a unique case of translational regulation.* Proc Natl Acad Sci U S A, 1984. **81**(22): p. 7061-5.
145. Landick, R. and C. Yanofsky, *Isolation and structural analysis of the Escherichia coli trp leader paused transcription complex.* J Mol Biol, 1987. **196**(2): p. 363-77.